



INSTYTUT INFORMATYKI TEORETYCZNEJ I STOSOWANEJ
POLSKIEJ AKADEMII NAUK

UKŁADY OTWARTE
W INFORMATYCE KWANTOWEJ

ROZPRAWA DOKTORSKA

mgr inż. Łukasz PAWELA
Promotor: dr hab. inż. Piotr GAWRON

Gliwice, Styczeń 2017



INSTITUTE OF THEORETICAL AND APPLIED INFORMATICS,
POLISH ACADEMY OF SCIENCES

OPEN SYSTEMS IN QUANTUM INFORMATICS

DOCTORAL DISSERTATION

mgr inż. Łukasz PAWELA
Supervisor: dr hab. inż. Piotr GAWRON

Gliwice, January 2017

1. When a distinguished but elderly scientist states that something is possible, he is almost certainly right. When he states that something is impossible, he is very probably wrong.
2. The only way of discovering the limits of the possible is to venture a little way past them into the impossible.
3. Any sufficiently advanced technology is indistinguishable from magic.

Arthur C. Clarke,

Hazards of Prophecy: The Failure of Imagination in the collection *Profiles of the Future: An Enquiry into the Limits of the Possible* (1962, rev. 1973), pp. 14, 21, 36

Contents

List of publications included in this dissertation	ix
List of other publications	xi
Streszczenie w języku polskim	xiii
Abstract in English	xv
1 Introduction to quantum information	1
1.1 Mathematical preliminaries	4
1.1.1 Hilbert spaces, <i>kets</i> and <i>bras</i>	4
1.1.2 Linear operators	5
1.1.3 Schatten norms of operators	6
1.1.4 Tensor products	6
1.1.5 Classes of operators	7
1.2 Quantum mechanics	8
1.2.1 Quantum states	8
1.2.2 State transformations	9
1.2.3 Partial trace	11
1.2.4 Quantum channel representations	12
1.2.5 Markovian approximation	13
1.2.6 Quantum measurements	14
1.2.7 Quantum state and channel distances	15
1.3 Quantum channel engineering	16
1.4 Open systems in quantum informatics	17
1.4.1 Decoherence effects in the quantum qubit flip game using Markovian approximation	17
1.4.2 Various methods of optimizing control pulses for quantum systems with decoherence	18
1.4.3 Quantum control with spectral constraints	19

1.4.4	Quantum control robust with respect to coupling with an external environment	20
1.4.5	Quantifying channels output similarity with applica- tions to quantum control	22
2	Decoherence effects in the quantum qubit flip game using Markovian approximation	29
3	Various methods of optimizing control pulses for quantum systems with decoherence	49
4	Quantum control with spectral constraints	69
5	Quantum control robust with respect to coupling with an external environment	83
6	Quantifying channels output similarity with applications to quantum control	95

List of publications included in this dissertation

1. P. Gawron, D. Kurzyk, and Ł. Pawela, “Decoherence effects in the quantum qubit flip game using Markovian approximation,” *Quantum Information Processing*, vol. 13, pp. 665–682, 2014.
2. Ł. Pawela and P. Sadowski, “Various methods of optimizing control pulses for quantum systems with decoherence,” *Quantum Information Processing*, vol. 15, no. 5, pp. 1937–1953, 2016.
3. Ł. Pawela and Z. Puchała, “Quantum control with spectral constraints,” *Quantum Information Processing*, vol. 13, pp. 227–237, 2014.
4. Ł. Pawela and Z. Puchała, “Quantum control robust with respect to coupling with an external environment,” *Quantum Information Processing*, vol. 14, no. 2, pp. 437–446, 2015.
5. Ł. Pawela and Z. Puchała, “Quantifying channels output similarity with applications to quantum control,” *Quantum Information Processing*, vol. 15, no. 4, pp. 1455–1468, 2016.

x *LIST OF PUBLICATIONS INCLUDED IN THIS DISSERTATION*

List of other publications

Published work

1. T. Błachowicz, A. Ehrmann née Tillmanns, P. Stebliński, and Ł. Pawela, “Magnetization reversal in magnetic half-balls influenced by shape perturbations,” *Journal of Applied Physics*, vol. 108, no. 12, p. 123906, 2010.
2. P. Kościelniak, J. Mazur, J. Henek, M. Kwoka, Ł. Pawela, and J. Szuber, “XPS and AFM studies of surface chemistry and morphology of In_2O_3 ultrathin films deposited by rheotaxial growth and vacuum oxidation,” *Thin Solid Films*, vol. 520, no. 3, pp. 927–931, 2011.
3. Ł. Pawela, “Control parameters for the quantum deutsch algorithm,” *Theoretical and Applied Informatics*, vol. 23, no. 3-4, p. 193, 2011.
4. Ł. Pawela and J. Sładkowski, “Quantum prisoner’s dilemma game on hypergraph networks,” *Physica A*, vol. 392, no. 4, pp. 910–917, 2013.
5. Ł. Pawela and J. Sładkowski, “Cooperative quantum Parrondo’s games,” *Physica D*, vol. 256, pp. 51–57, 2013.
6. Ł. Pawela, P. Gawron, Z. Puchała, and J. Sładkowski, “Enhancing pseudo-telepathy in the magic square game,” *PLOS ONE*, vol. 8, no. 6, p. e64694, 2013.
7. R. Winiarczyk, P. Gawron, J. A. Miszczak, Ł. Pawela, and Z. Puchała, “Analysis of patent activity in the field of quantum information processing,” *International Journal of Quantum Information*, vol. 11, no. 1, p. 135007, 2013.
8. J. A. Miszczak, Ł. Pawela, and J. Sładkowski, “General model for an entanglement-enhanced composed quantum game on a two-dimensional lattice,” *Fluctuation and Noise Letters*, vol. 13, no. 02, p. 1450012, 2014.
9. Ł. Pawela, P. Gawron, J. A. Miszczak, and P. Sadowski, “Generalized open quantum walks on Apollonian networks,” *PLOS ONE*, vol. 10, no. 7, p. e0130967, 2015.

10. C. F. Dunkl, P. Gawron, Ł. Pawela, Z. Puchała, and K. Życzkowski, “Real numerical shadow and generalized B-splines,” *Linear Algebra and its Applications*, vol. 479, pp. 12–51, 2015.
11. P. Gawron, Ł. Pawela, Z. Puchała, J. Szklarski, and K. Życzkowski, “Wybory samorządowe 2014 w poszukiwaniu anomalii statystycznych,” *Electoral Studies*, vol. 30, no. 3, pp. 534–545, 2015.
12. P. Sadowski and Ł. Pawela, “Central limit theorem for reducible and irreducible open quantum walks,” *Quantum Information Processing*, vol. 15, no. 7, pp. 2725–2743, 2016.
13. P. Gawron and Ł. Pawela, “Relativistic quantum pseudo-telepathy,” *Acta Physica Polonica B*, vol. 47, no. 4, p. 1147, 2016.
14. Z. Puchała, Ł. Pawela, and K. Życzkowski, “Distinguishability of generic quantum states,” *Physical Review A*, vol. 93, no. 6, p. 062112, 2016.
15. A. Chia, A. Górecka, K. C. Tan, Ł. Pawela, P. Kurzyński, T. Paterek, and D. Kaszlikowski, “Coherent chemical kinetics as quantum walks I: Reaction operators for radical pairs,” *Physical Review E*, vol. 93, p. 032407, 2016.
16. Ł. Pawela, “Quantum games on evolving random networks,” *Physica A*, vol. 458, pp. 179–188, 2016.

Preprints

1. K. Domino, A. Glos, M. Ostaszewski, Ł. Pawela, and P. Sadowski, “Properties of quantum stochastic walks from the Hurst exponent,” *arXiv preprint arXiv:1611.01349*, 2016, submitted to Quantum Information & Computation.
2. I. Nechita, Z. Puchała, Ł. Pawela, and K. Życzkowski, “Almost all quantum channels are equidistant,” *arXiv preprint arXiv:1612.00401*, 2016, submitted to Communications in Mathematical Physics.
3. K. Domino, P. Gawron, and Ł. Pawela, “The tensor network representation of high order cumulant and algorithm for their calculation,” *arXiv preprint arXiv:1701.05420*, 2017, submitted to SIAM Journal on Scientific Computing.

Streszczenie w języku polskim

Informatyka kwantowa jest dziedziną nauki badającą możliwość wykorzystania zasobów kwantowych do przechowywania, przetwarzania i przesyłania informacji. Jako stosunkowo nowa gałąź informatyki wciąż dynamicznie się rozwija i obecnie obejmuje wiele interesujących podobszarów badawczych. Do niedawna jej zakres badań ograniczony był głównie do prac teoretycznych, obecnie jednak duże nadzieje wiążą się z powstającymi komputerami kwantowymi. Choć obecnie, w roku 2017, dysponujemy kilkoma działającymi prototypami oraz jednym komercyjnie dostępnym komputerem kwantowym, to wszystkie te konstrukcje posiadają ograniczenia. Rozważania teoretyczne pozwalają jednak przypuszczać, że wielkoskalowe komputery kwantowe będą w stanie rozwiązać problemy takie jak np. rozkład liczb na czynniki pierwsze z wykorzystaniem algorytmu Shora zdedykowanie szybciej niż komputery klasyczne. Pomimo tych postępów istnieje ciągle wiele otwartych pytań w tej dziedzinie.

Celem niniejszej dysertacji jest omówienie i zbadanie zagadnienia inżynierii kanałów kwantowych opisujących działanie otwartych układów kwantowych. W tym celu będziemy koncentrować się na poprawnym wyborze i adaptacji modeli już istniejących w informatyce kwantowej. Chcemy bowiem pokazać, że pozwoli to na uzyskanie efektów bliskich optymalnym dla badanego zagadnienia.

Głównym obiektem badań w tej pracy są układy modelowane równaniem Goriniego-Kossakowskiego-Sudarshana-Lindblada. Kanał kwantowy w tych układach tworzymy poprzez oddziaływanie na ich część przedziałami stałymi funkcjami sterującymi. Będziemy badać rozmaite ograniczenia, które można nałożyć na wyżej wspomniane funkcje. Pierwszym z nich będzie z góry ustalona liczba okresów funkcji sterujących. Kolejnym – ograniczenie na spektrum tych funkcji. Na koniec przejdziemy do badania optymalizacji tych funkcji z minimalną normą L_1 .

Oprócz wyżej wymienionych ograniczeń zbadamy możliwość wykonania operacji unitarnej w kwantowym układzie otwartym. W tym celu dodać mamy do rozważanego układu dodatkowy system, na który aplikujemy funkcje sterujące a następnie pokazujemy, że po odrzuceniu tego dodatkowego układu uzyskujemy kanał kwantowy będący blisko kanału unitarnego. Na koniec wprowadzamy nową funkcję dla procedury optymalizacji. Bazuje ona na funkcji nadwierności stanów kwantowych, stąd jej nazwa – nadwiorność kanałów kwantowych. Ma ona tę zaletę, że jest łatwo obliczalna dla szerskiej klasy kanałów kwantowych i pozwala nam przedstawić szereg wyników analitycznych.

W Rozdziale 1 zamieszczono krótkie wprowadzenie do matematycznego

języka informatyki kwantowej. Ostatnia część tego rozdziału zawiera krótki opis pięciu publikacji stanowiących podstawę niniejszej dysertacji oraz dokładny opis mojego wkładu w powstanie każdej z nich.

Pozostała część dysertacji zawiera pięć opublikowanych artykułów naukowych dotyczących tematu inżynierii kanałów kwantowych. Pierwszy z nich, zaprezentowany w Rozdziale 2, dotyczy zagadnienia oszukiwania w grze kwantowej. Dokładniej mówiąc, badamy przypadek, w którym gracze posiadają niesymetryczną informację dotyczącą gry. W rozważanej przez nas sytuacji jeden z graczy myśli, że gra odbywa się na qubicie izolowanym od środowiska, podczas gdy drugi wie, że układ jest sprzężony ze środowiskiem.

Następnie w Rozdziale 3 badamy możliwość wykonania operacji unitarnej na otwartym układzie kwantowym. W tym celu dodajemy do układu dodatkowy system i wykonujemy na nim funkcje sterujące. W ten sposób pokazujemy, że po odrzuceniu dodatkowego systemu otrzymamy operację unitarną. Warunkiem otrzymania poprawnej operacji jest, aby sprzężenie ze środowiskiem było na tym samym poziomie co sprzężenie między układami.

W Rozdziale 4 skupimy się na przypadku ograniczeń na częstotliwości pojawiające się w transformacie Fouriera tych funkcji. Uzyskane w ten sposób funkcje sterujące, po zaaplikowaniu filtra dolnoprzepustowego, pozwalają uzyskać wyższą wierność operacji kwantowej, niż w przypadku, gdy przy optymalizacji nie uwzględniono tego ograniczenia.

Praca przedstawiona w Rozdziale 5 skupia się na sprzężeniu ze środowiskiem – doprecyzowując, badamy przypadek, w którym funkcje sterujące powodują sprzężenie ze środowiskiem. Celem jest sprawdzenie, czy istnieje możliwość optymalizacji funkcji kontrolnych z minimalną normą L_1 w taki sposób, by zmniejszyć sprzężenie ze środowiskiem.

W Rozdziale 6 badamy funkcje celu wykorzystywane w inżynierii kanałów kwantowych. Aby porównać wyjścia dwóch kanałów kwantowych, wykorzystujemy funkcję nadwierności stanów kwantowych. W wyniku tej operacji otrzymujemy nową funkcję celu – nadwiorność kanałów.

Podsumowując, w niniejszej dysertacji zbadaliśmy zagadnienia znajdowania funkcji sterujących dla otwartych układów kwantowych. Wyniki zaprezentowane w Rozdziałach 2–6 pokazują, że poprawny wybór i adaptacja modeli informatyki kwantowej pozwala na efektywną inżynierię kanałów kwantowych w otwartych układach kwantowych.

Abstract in English

Quantum information theory is a branch of science which utilizes quantum mechanical resource for storing, processing and sending information. In the recent years this field has expanded into a plethora of subfields. Up until recently, most of the research was theoretical. Working quantum devices were far on the horizon. Now, in 2017, the development of actual quantum computers is still in its early stages. There are some working prototypes constructed and one commercially available quantum computer. Nonetheless, they all have their limitations. However, theoretical work lets us expect that, if constructed, large-scale quantum computers would be able to solve some important problems quicker than any classical computer. These include integer factorization using the Shor's algorithm. Despite this, there still remain some open questions in this field.

The purpose of this dissertation is to discuss and analyze the problem of engineering quantum channels acting in open quantum systems. We aim at proper selection and adaption of models of quantum informatics systems and argue that their proper selection and adaption will allow for efficient engineering of quantum channels.

In this work we focus on systems modeled by the Gorini-Kossakowski-Sudarshan-Lindblad master equation. The quantum channel is implemented with external manipulation of a part of the quantum system under consideration via piecewise constant control functions. We study various constraints imposed on these control functions. The first one is an arbitrary set number of time steps. Next, we study the possibility of finding these functions with limited spectrum. Then we move to studying the optimization of these functions with minimal L_1 norm. Aside from the restricted control function case, we study the possibility of engineering a unitary operation on an open quantum system. To achieve this, we add an ancilla to the system, which at the same time is the target of the control functions. We show, that after discarding the ancillary system, we achieve an operation which is close to a unitary one. Finally, we introduce a new figure of merit for the optimization procedure. This figure is based on the superfidelity of quantum states and we call it channel superfidelity. It has the advantage of being easily computable for a large family of quantum channels and allows us to present a number of analytical results.

Chapter 1 gives a brief introduction to the mathematical language of quantum informatics. The final part of this chapter provides a brief description of the five papers constituting this dissertation and details my personal contribution to their development.

Subsequent chapters consist of five published papers on the subject of

quantum channel engineering. The first of them, presented in Chapter 2, touches upon the subject of cheating in a quantum game. Speaking precisely, we are interested in the case when players have asymmetric information regarding the game. In our setting one of the players thinks the game is played on an isolated qubit, while the other is aware that, in fact, the system is coupled to an environment.

Next, in Chapter 3 we study the possibility of implementing a unitary mapping on an open quantum system. To achieve this, we add a small ancillary system to the main setup and apply the control functions on the ancilla only. We show that this allows us to achieve the desired unitary operation, given the coupling to the environment is on the same level as the coupling between the systems under consideration.

In Chapter 4 we present a scheme for optimizing control functions with restriction on their frequency spectrum. This allows us to find control functions which, after applying a low-pass filter, achieve higher fidelity of the operation compared to the case when these restriction were not taken into account in the optimization process.

The work presented in Chapter 5 studies the coupling with an external environment. The focus of the study is on the case when the application of the control functions results in a coupling with the environment. Hence, the focus is the minimization of the L_1 norm of the control functions.

In Chapter 6 we focus on figures of merit used in quantum channel engineering. We use the notion of superfidelity to compare the output of two quantum channels. The result is a new, easily computable figure of merit: channel superfidelity.

Summarizing, in this work we analyzed the problem of finding control functions for open quantum systems. Results, which are presented in Chapters 2–6 show that proper selection and adaptation of models of quantum informatics allows us to efficiently engineer quantum channels in open quantum systems.

Chapter 1

Introduction to quantum information

Quantum mechanics is the crown jewel of the twentieth century science. The theory was fathered by Max Planck, who used the concept of finite portions of energy, *quanta*, to explain the ultraviolet catastrophe in the theory of black body radiation [1]. Planck himself insisted, that his approach was merely a convenient mathematical trick, rather than an element of reality. Nonetheless, one of the fundamental constants, h , is named after the father of quantum theory. As the theory developed, it ultimately allowed us to construct fast and energy-efficient *classical* computing devices

Quantum information science studies the application of quantum mechanics to processing, storing and transmitting information. The main trends of research involving theoretical aspects of quantum computing are: quantum information theory, quantum computation, quantum cryptography, quantum communication and quantum games. The origins of the field date back to the first decades of the twentieth century, when the bases of quantum mechanics were formulated. The beginnings of quantum information theory can be traced back to von Neumann [2], but the first established research in this area was conducted by Holevo [3] and Ingarden [4].

In the last two decades of the twentieth century, the groundwork for quantum computing was laid. First in the eighties, Bennett and Brassard [5], then seven years later Ekert [6] discovered quantum key distribution (QKD) protocols. These research achievements gave rise to the whole new field of quantum cryptography. The Feynman's idea of quantum simulators [7] and Deutsch's work [8] on the universal quantum computer, followed by the discovery of the first quantum algorithms by Shor [9] and Grover [10] in the nineties of the twentieth century created the whole new field of research on quantum computing and quantum algorithms.

All of the above is possible due to very counterintuitive behavior of quantum systems. This is reflected in the equations governing their dynamics. In the simplest case, the dynamics of a quantum system is governed by the von Neumann equation

$$\frac{\partial \rho(t)}{\partial t} = -i[H, \rho(t)], \quad (1.1)$$

which yields a *unitary* evolution of the system

$$\rho(t) = \exp(-iHt)\rho(0)\exp(iHt), \quad (1.2)$$

for some Hermitian H and some initial quantum state $\rho(0)$. Unfortunately, this model describes only the quantum system, neglecting the unavoidable interaction with a surrounding environment. The description of this case requires us to extend the formalism.

Quantum systems need to be considered as open systems. The reasons are twofold. First, this is due to the fact that, any realistic system is coupled in some way to an uncontrollable environment whose influence is non-negligible. Thus, the theory of open quantum systems plays a major role in quantum information processing. Secondly, even if we could describe complex systems using an accurate microscopic description, at the end, we would get an intractable amount of information about the system, most of which would be useless to us. Thus again, we need to apply a simpler description of open system dynamics [11].

The construction and usage of quantum computers is a complicated process. We need several layers of knowledge in order to construct such devices. First of all, we need algorithms that will give us a significant advantage over their classical counterparts. In the past two decades a number of such algorithms has been discovered, let us mention here Shor's [9] and Grover's [10] work as the most famous examples. Another building block we need are quantum programming languages. Currently, there exist a number of quantum programming languages like QML [12] and QCL [13] and more recent projects including Quipper [14] and LIQUi|⟩ [15]. Moving forward, we need computational models, like the quantum circuit model [16]. The next layer is quantum error correction, which currently is a blooming field of study [17].

Having all of the above layers is not enough, as they all will fail without a good understanding of the physical structure of the quantum computer. The main focus of this work is the proper selection and adaption of models of quantum informatics systems. This will allow for efficient engineering of quantum channels on real-life systems. The transition from algorithm to physical implementation is particularly tricky, as due to the unavoidable noise in the system, the algorithm's speedup might be lost. In Figs 1.1 and 1.2 we schematically show where the work presented here fits.

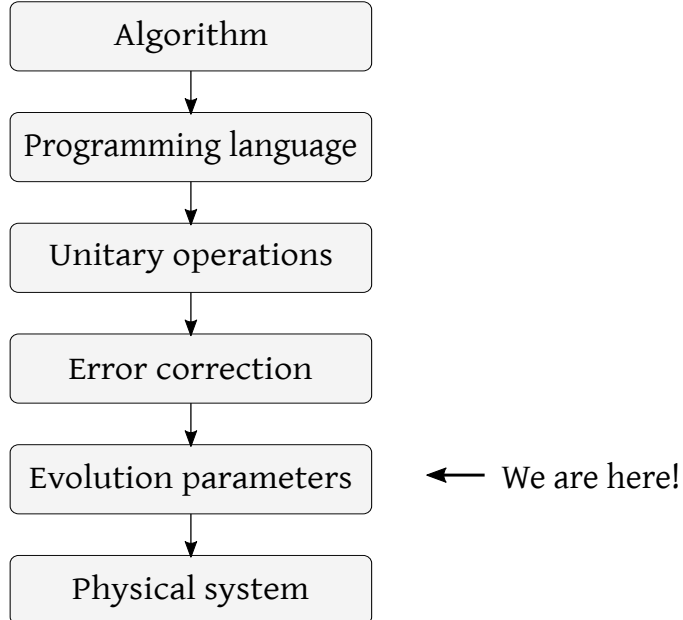


Figure 1.1: All the layers required for actual quantum computation.

The main thesis of this dissertation is
“Proper selection and adaptation of models of quantum informatics systems allows for efficient quantum channel engineering”.

The main original results of this work are as follows:

- Numerically engineering control functions for a specific noise model.
- Showing that adding an ancilla to a system under decoherence, may allow us to achieve better fidelity of a unitary operation on the smaller system.
- Proposing an optimization scheme for finding control functions with spectral constraints.
- Studying the control functions in a setting in which the applications of the function causes a coupling to the environment.
- Introducing a new figure of merit for optimizing operations in open quantum systems.

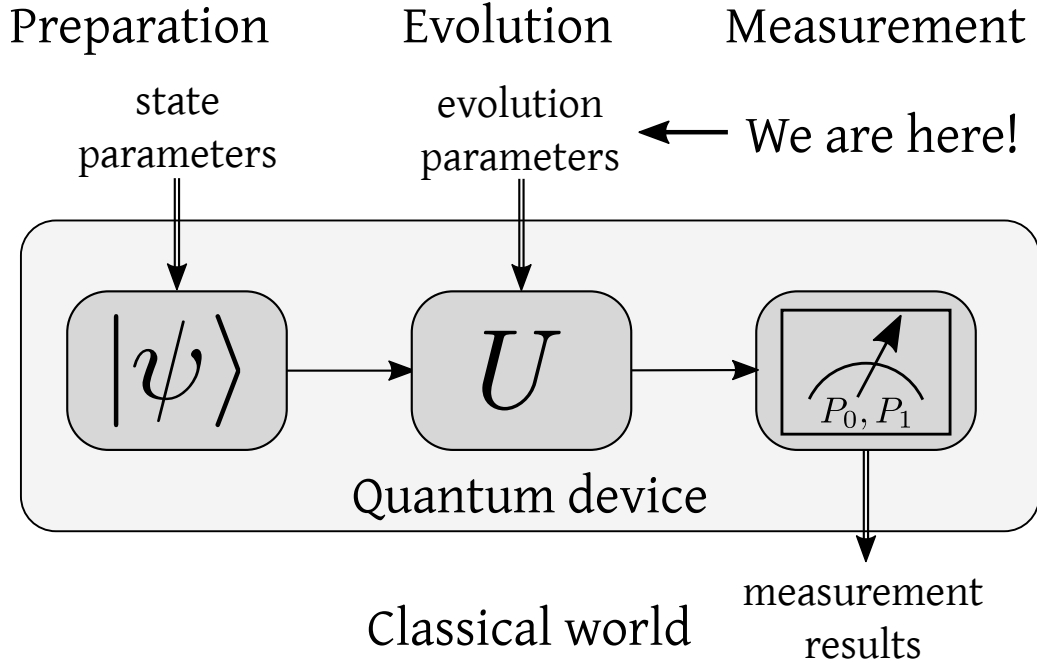


Figure 1.2: A schematic overview of a quantum computation procedure, showing where the results of this dissertation come into play. Figure reproduced with permission from [18].

1.1 Mathematical preliminaries

In this section we will introduce the core mathematical concepts used throughout this work. We will start with the definition of a Hilbert space and then move to vectors and operators on these spaces.

1.1.1 Hilbert spaces, *kets* and *bras*

Let \mathcal{X} be a vector space with an inner product $\langle \phi | \psi \rangle$ and the norm defined in terms of the inner product

$$\| |\phi \rangle \| = \sqrt{\langle \phi | \phi \rangle}. \quad (1.3)$$

We call \mathcal{X} a Hilbert space if it is a complete metric space with the metric induced by the norm (1.3).

The inner product satisfies the following properties:

- Conjugate symmetry

$$\langle \phi | \psi \rangle = \overline{\langle \psi | \phi \rangle}, \quad (1.4)$$

where \bar{z} denotes the complex conjugate of z .

- Linearity in the second term. Given $|\psi\rangle = a|\xi_1\rangle + b|\xi_2\rangle$ we have

$$\langle\phi|\psi\rangle = a\langle\phi|\xi_1\rangle + b\langle\phi|\xi_2\rangle. \quad (1.5)$$

- Non-negativity

$$\langle\phi|\phi\rangle \geq 0, \quad (1.6)$$

where the equality holds iff $|\phi\rangle = 0$.

We will focus on finite-dimensional Hilbert spaces and denote them by \mathcal{X} , \mathcal{Y} , \mathcal{Z} . Their dimensions will be denoted by $\dim(\mathcal{X})$. As we limit ourselves to the finite dimensional case, hereafter we will use the names Hilbert space and complex Euclidean space interchangeably. When we need to state the dimension of the Hilbert space explicitly, we will write \mathbb{C}^N for some finite dimension N . We will denote vectors in this space using the Dirac's bra-ket notation. Therefore, we will write $|\phi\rangle \in \mathcal{X}$ for a vector $|\phi\rangle$ and call $|\phi\rangle$ a *ket*. The corresponding dual vector will be denoted by $\langle\phi|$, i.e. $\langle\phi| = (\langle\phi|)^\dagger$, and called a *bra*. The \cdot^\dagger denotes the Hermitian conjugation of a vector, i.e. the transposition and the complex conjugation of all elements. The elements of a vector $|\phi\rangle$ will be denoted by ϕ_i . Usually, we will use a special orthonormal basis for the space \mathcal{X} , called the computational basis. The vectors forming this particular basis will be denoted by $|0\rangle, |1\rangle, \dots, |\dim(\mathcal{X}) - 1\rangle$. We assign an explicit representation to these vectors: $|i\rangle$ is a vector with the i^{th} index equal to one and others equal to zero.

1.1.2 Linear operators

Given Hilbert spaces \mathcal{X} and \mathcal{Y} we introduce the notion of a *linear operator* as a mapping of the form

$$A : \mathcal{X} \rightarrow \mathcal{Y}. \quad (1.7)$$

We will denote the set of all such operators as $L(\mathcal{X}, \mathcal{Y})$. For compactness we will put $L(\mathcal{X}) := L(\mathcal{X}, \mathcal{X})$. The identity operator on the space \mathcal{X} will be denoted as $\mathbb{1}_{\mathcal{X}}$.

Note that the set $L(\mathcal{X}, \mathcal{Y})$ forms a vector space. Given some operators $A, B \in L(\mathcal{X}, \mathcal{Y})$, we define the operator $(A + B) \in L(\mathcal{X}, \mathcal{Y})$ as the unique operator satisfying the equation

$$(A + B)|\phi\rangle = A|\phi\rangle + B|\phi\rangle, \quad (1.8)$$

for all $|\phi\rangle \in \mathcal{X}$. We define the operator $\alpha A \in L(\mathcal{X}, \mathcal{Y})$ as the unique operator such that

$$(\alpha A)|\phi\rangle = \alpha(A|\phi\rangle), \quad (1.9)$$

for all $|\phi\rangle \in \mathcal{X}$.

The kernel of an operator $A \in L(\mathcal{X}, \mathcal{Y})$ is the subspace of \mathcal{X} given by

$$\ker(A) = \{|\phi\rangle \in \mathcal{X} : A|\phi\rangle = 0\}. \quad (1.10)$$

The image of A is a subspace of \mathcal{Y} defined as

$$\text{im}(A) = \{A|\phi\rangle : |\phi\rangle \in \mathcal{X}\}. \quad (1.11)$$

The rank of A is the dimension of the subspace $\text{im}(A)$, *i.e.* $\text{rank}(A) = \dim(\text{im}(A))$. Hence, for every $A \in L(\mathcal{X}, \mathcal{Y})$ it holds that $\dim(\ker(A)) + \text{rank}(A) = \dim(\mathcal{X})$.

Given two operators $A, B \in L(\mathcal{X})$, their commutator, $AB - BA$, will be denoted by $[A, B]$. Their anticommutator, $AB + BA$ will be denoted by $\{A, B\}$.

1.1.3 Schatten norms of operators

Definition 1 For any $A \in L(\mathcal{X}, \mathcal{Y})$ and any real number $p \geq 1$, we define the Schatten p -norm of A as

$$\|A\|_p = [\text{Tr}((A^\dagger A)^{p/2})]^{1/p}. \quad (1.12)$$

We also define

$$\|A\|_\infty = \max \{\|A|\phi\rangle\| : |\phi\rangle \in \mathcal{X}, \langle\phi|\phi\rangle = 1\}, \quad (1.13)$$

which coincides with $\lim_{p \rightarrow \infty} \|A\|_p$.

1.1.4 Tensor products

We further introduce the notion of the *tensor product* of complex Euclidean spaces. Given spaces \mathcal{X}, \mathcal{Y} , the tensor product is their complex Euclidean space

$$\mathcal{X} \otimes \mathcal{Y} = \mathbb{C}^{\dim(\mathcal{X}) \cdot \dim(\mathcal{Y})}. \quad (1.14)$$

In the case of vectors $|\phi\rangle \in \mathbb{C}^{N_1}$, $|\psi\rangle \in \mathbb{C}^{N_2}$ we define $|\phi\rangle \otimes |\psi\rangle$ as:

$$|\phi\rangle \otimes |\psi\rangle = \begin{pmatrix} \phi_1|\psi\rangle \\ \vdots \\ \phi_{N_1}|\psi\rangle \end{pmatrix}. \quad (1.15)$$

Instead of writing $|\phi\rangle \otimes |\psi\rangle$ we will write $|\phi\rangle|\psi\rangle$ or even shorter $|\phi\psi\rangle$. The elementary vectors $|\phi\psi\rangle$ span the entire space $\mathcal{X} \otimes \mathcal{Y}$, but not every vector from this space can be written in such a form.

Now, we introduce the notion of the tensor product of linear operators.

Definition 2 Given linear operators $A \in L(\mathcal{X}_1, \mathcal{Y}_1)$, $B \in L(\mathcal{X}_2, \mathcal{Y}_2)$ the tensor product $A \otimes B \in L(\mathcal{X}_1 \otimes \mathcal{X}_2, \mathcal{Y}_1 \otimes \mathcal{Y}_2)$ is defined as the unique operator that satisfies

$$(A \otimes B)|\phi\psi\rangle = (A|\phi\rangle) \otimes (B|\psi\rangle), \quad (1.16)$$

for all choices of $|\phi\psi\rangle \in \mathcal{X}_1 \otimes \mathcal{X}_2$. As vectors $|\phi\psi\rangle$ span the entire space $\mathcal{X}_1 \otimes \mathcal{X}_2$, such a unique operator must exist.

Next, we will define a reshaping operation, which preserves the lexicographical order and its inverse.

Definition 3 We define the linear mapping

$$\text{res} : L(\mathcal{X}, \mathcal{Y}) \rightarrow \mathcal{Y} \otimes \mathcal{X} \quad (1.17)$$

for dyadic operators $|\psi\rangle\langle\phi|$, $|\psi\rangle \in \mathcal{X}$, $|\phi\rangle \in \mathcal{Y}$ as

$$\text{res}(|\psi\rangle\langle\phi|) = |\psi\rangle\overline{|\phi\rangle} \quad (1.18)$$

and uniquely extend the definition to the whole space $L(\mathcal{X}, \mathcal{Y})$ by linearity.

Definition 4 We define the linear mapping

$$\text{unres} : \mathcal{Y} \otimes \mathcal{X} \rightarrow L(\mathcal{X}, \mathcal{Y}) \quad (1.19)$$

as the transformation which satisfies

$$\forall A \in L(\mathcal{X}, \mathcal{Y}) \quad \text{unres}(\text{res}(A)) = A. \quad (1.20)$$

Remark 5 For every choice of Hilbert spaces \mathcal{X}_1 , \mathcal{X}_2 , \mathcal{Y}_1 , \mathcal{Y}_2 and every choice of operators $A \in L(\mathcal{X}_1, \mathcal{Y}_1)$, $B \in L(\mathcal{X}_2, \mathcal{Y}_2)$, $X \in L(\mathcal{X}_2, \mathcal{X}_1)$ it holds that:

$$(A \otimes B)\text{res}(X) = \text{res}(AXB^T). \quad (1.21)$$

1.1.5 Classes of operators

We call an operator $A \in L(\mathcal{X})$ *normal* if it commutes with its Hermitian conjugate, i.e. $[A, A^\dagger] = 0$. An operator is *Hermitian* if $A = A^\dagger$. We call an operator A *positive semidefinite* and write $A \geq 0$, if $\langle\phi|A|\phi\rangle \geq 0$ for every $|\phi\rangle \in \mathcal{X}$. An operator $U \in L(\mathcal{X})$ is unitary if it preserves the norm of vectors, that is, given $|\psi\rangle = U|\phi\rangle$, we have $|\langle\psi|\psi\rangle| = |\langle\phi|\phi\rangle|$. We will denote the set of all unitary operators by $U(\mathcal{X})$. The set of all unitary operators with unit determinant will be denoted by $SU(\mathcal{X})$.

1.2 Quantum mechanics

1.2.1 Quantum states

Definition 6 We call an operator $\rho \in L(\mathcal{X})$ a density operator iff $\rho \geq 0$ and $\text{Tr}\rho = 1$. We denote the set of all density operators on \mathcal{X} by $\Omega_{\mathcal{X}}$.

Definition 7 A quantum state $\rho \in L(\mathcal{X})$ is called pure iff $\text{rank}(\rho) = 1$.

From this it follows that a pure quantum state is a rank one projection $\rho = |\phi\rangle\langle\phi|$.

Given two quantum systems, one in state $\rho \in \Omega_{\mathcal{X}}$ and another in state $\sigma \in \Omega_{\mathcal{Y}}$, the state of the joint system composed of the previous two is given by the tensor product $\rho \otimes \sigma \in \Omega_{\mathcal{X} \otimes \mathcal{Y}}$. States of this form are called *product states*. If a state $\xi \in \Omega_{\mathcal{X} \otimes \mathcal{Y}}$ can be written as a convex combination of product states, it is called a *separable state*. On the other hand, if a $\xi \in \Omega_{\mathcal{X} \otimes \mathcal{Y}}$ cannot be written as a convex combination of product states, it is called an *entangled state*.

A two-dimensional quantum system is called a quantum bit, or a qubit for short. Its state is described by $\rho \in \Omega_{\mathbb{C}^2}$. If the state ρ is pure i.e. $\rho = |\phi\rangle\langle\phi|$ then the vector $|\phi\rangle$ may be written as

$$|\phi\rangle = e^{i\gamma} \left(\cos\left(\frac{\theta}{2}\right) |0\rangle + e^{i\varphi} \sin\left(\frac{\theta}{2}\right) |1\rangle \right), \quad 0 \leq \theta \leq \pi, \quad 0 \leq \varphi \leq 2\pi, \quad (1.22)$$

$$0 \leq \gamma \leq 2\pi.$$

In quantum information science we are not concerned with the global phase, $e^{i\gamma}$, as it has no physical meaning and we omit this factor entirely. Indeed, note that the mapping $|\phi\rangle \mapsto |\phi\rangle\langle\phi|$ results in the cancellation of this global phase. In such a case Eq. (1.22) specifies a point on the unit sphere in \mathbb{R}^3 , called the Bloch Sphere. It is shown in Fig. 1.3.

Pure states are localized on the Bloch Sphere. All density operators which are not pure states are convex combinations of them. Hence, in the case of $\mathcal{X} = \mathbb{C}^2$ they are inside the Bloch Sphere, forming the Bloch Ball. The state located in the center of the Bloch Ball is called the maximally mixed state. It is given by $\Omega_{\mathbb{C}^2} \ni \rho_* = \mathbb{1}_{\mathbb{C}^2}/2$.

Based on the discussion above we note that the mapping from the Bloch Ball in \mathbb{R}^3 to the space of quantum states $\Omega_{\mathbb{C}^2}$ is a bijection. It is explicitly given by

$$\rho = \frac{1}{2}(\mathbb{1} + r \cdot \boldsymbol{\sigma}), \quad (1.23)$$

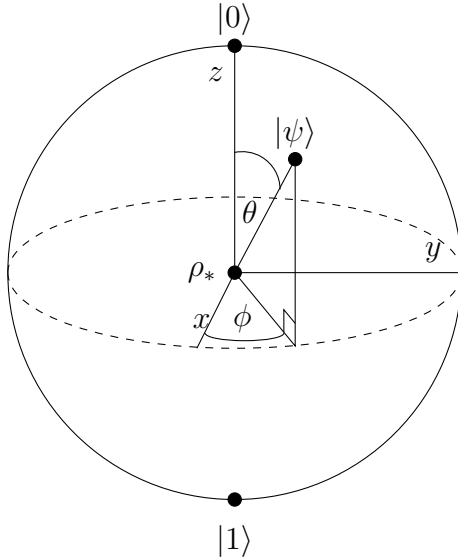


Figure 1.3: A schematic representation of the Bloch Sphere. The angles θ and φ correspond to the values in Eq. (1.22). The symbol ρ_* denotes the maximally mixed state.

where $r \in \mathbb{R}^3$ and $\|r\|_2 = 1$, $\boldsymbol{\sigma} = [\sigma_x, \sigma_y, \sigma_z]$. Here σ_i are called the Pauli matrices, which are given by

$$\sigma_x = \begin{pmatrix} 0 & 1 \\ 1 & 0 \end{pmatrix}, \quad \sigma_y = \begin{pmatrix} 0 & i \\ -i & 0 \end{pmatrix}, \quad \sigma_z = \begin{pmatrix} 1 & 0 \\ 0 & -1 \end{pmatrix}. \quad (1.24)$$

1.2.2 State transformations

A simple state transformation is given by a unitary operator $U \in \mathrm{U}(\mathcal{X})$. For every such operator and every $|\phi\rangle \in \mathcal{X}$ we have $\|U|\phi\rangle\|_2 = \||\phi\rangle\|_2$. From this, we get the following properties of a unitary state transformation:

1. it maps pure states to pure states,
2. it maps mixed states to mixed states,
3. it is reversible.

However, in the case of open systems, we need a wider class of possible state transformations, called *quantum channels* [19]. These are operations that map density operators to density operators and represent general transformations of quantum system. In the next paragraphs, we will formally introduce these mathematical objects.

Definition 8 A superoperator is a linear mapping acting on linear operators $L(\mathcal{X})$ and transforming them into operators on another finite dimensional Hilbert space \mathcal{Y} . Thus

$$\Phi : L(\mathcal{X}) \rightarrow L(\mathcal{Y}). \quad (1.25)$$

We will denote the set of all such mappings as $M(\mathcal{X}, \mathcal{Y})$. We will write $M(\mathcal{X}) := M(\mathcal{X}, \mathcal{X})$.

The identity mapping on the space $L(\mathcal{X})$ will be denoted by $\mathbb{1}_{L(\mathcal{X})}$. The composition of $\Phi, \Psi \in M(\mathcal{X})$ will be denoted $(\Phi \circ \Psi)(\rho) := \Phi(\Psi(\rho))$.

This definition is too broad to represent a general quantum operation, since we need to assure that all of the states are positive semidefinite.

In order to properly define a quantum channel, we shall introduce the definition of the tensor product of superoperators.

Definition 9 Given superoperators

$$\Phi_1 \in M(\mathcal{X}_1, \mathcal{Y}_1), \Phi_2 \in M(\mathcal{X}_2, \mathcal{Y}_2), \quad (1.26)$$

we define the product superoperator

$$\Phi_1 \otimes \Phi_2 \in M(\mathcal{X}_1 \otimes \mathcal{X}_2, \mathcal{Y}_1 \otimes \mathcal{Y}_2) \quad (1.27)$$

to be the unique linear mapping that satisfies the following equation

$$(\Phi_1 \otimes \Phi_2)(A_1 \otimes A_2) = \Phi_1(A_1) \otimes \Phi_2(A_2), \quad (1.28)$$

for all operators $A_1 \in L(\mathcal{X}_1)$, $A_2 \in L(\mathcal{X}_2)$. The extension to the whole space $\mathcal{X}_1 \otimes \mathcal{X}_2$, including the operators not in a tensor product form follows from linearity.

Next, we introduce a class of superoperators that map positive operators to positive operators, which we will simply call positive superoperators.

Definition 10 A superoperator $\Phi \in M(\mathcal{X}, \mathcal{Y})$ is called positive iff for every $A \in L(\mathcal{X})$, $A \geq 0$, we have $\Phi(A) \geq 0$.

Now we have all the building blocks needed to define quantum channels.

Definition 11 A quantum channel is a superoperator $\Phi \in M(\mathcal{X}, \mathcal{Y})$ that satisfies the following restrictions:

1. Φ is trace-preserving, i.e. $\forall A \in L(\mathcal{X}) \quad \text{Tr}(\Phi(A)) = \text{Tr}(A)$,

2. Φ is completely positive, that is for every finite-dimensional Hilbert space \mathcal{Z} the product of Φ and $\mathbb{1}_{L(\mathcal{Z})}$ is a positive operator, i.e.

$$\forall \mathcal{Z} \quad \forall A \in L(\mathcal{X} \otimes \mathcal{Z}) \quad A \geq 0 \Rightarrow (\Phi \otimes \mathbb{1}_{L(\mathcal{Z})})(A) \geq 0. \quad (1.29)$$

We will denote the set of all quantum channels $\Phi : L(\mathcal{X}) \rightarrow L(\mathcal{Y})$ as $C(\mathcal{X}, \mathcal{Y})$. For brevity, the set of channels mapping $L(\mathcal{X})$ to itself will be denoted by $C(\mathcal{X}) := C(\mathcal{X}, \mathcal{X})$.

One may ask, why quantum channels need to be completely positive, not only positive mappings. This is easy to explain. Let us consider a quantum system in some state $\rho \in \Omega_{\mathcal{X} \otimes \mathcal{Y}}$. If we have only access to one part of the system ρ and we wish to perform some operation Φ on it, we get the state $\xi = (\Phi \otimes \mathbb{1}_{L(\mathcal{Y})})(\rho)$. As ξ still describes a quantum system, this operator must be positive. Hence, we need Φ to be completely positive.

Definition 12 Given a superoperator $\Phi \in M(\mathcal{X}, \mathcal{Y})$, for every $A \in L(\mathcal{X})$ and $B \in L(\mathcal{Y})$ we define the conjugate superoperator $\Phi^\dagger \in M(\mathcal{Y}, \mathcal{X})$ as the unique mapping satisfying

$$\text{Tr}(\Phi(A)B) = \text{Tr}(A\Phi^\dagger(B)). \quad (1.30)$$

Note, that the conjugate of a quantum channel is completely positive, but is not necessarily trace-preserving.

1.2.3 Partial trace

At this point, one may ask a question: what happens if we have a composite system, say consisting of two qubits, and we discard one of them? What is the resulting state of the subsystem? These questions are answered using the *partial trace* mapping.

First, let us recall that trace is a mapping $\text{Tr} : L(\mathcal{X}) \rightarrow \mathbb{C}$, given by:

$$\text{Tr} : A \mapsto \sum_{i=1}^{\dim(\mathcal{X})} \langle e_i | A | e_i \rangle, \quad (1.31)$$

where $\{|e_i\rangle\}$ forms an orthonormal basis of \mathcal{X} . Following this, we may introduce the *partial trace* as a mapping $\text{Tr}_{\mathcal{X}} : L(\mathcal{X} \otimes \mathcal{Y}) \rightarrow L(\mathcal{Y})$, which for product operators $A \otimes B$, $A \in L(\mathcal{X})$, $B \in L(\mathcal{Y})$, is given by:

$$\text{Tr}_{\mathcal{X}} : A \otimes B \mapsto B \text{Tr}(A). \quad (1.32)$$

As this is a linear map, it may be uniquely extended to the case of operators which are not in a tensor product form. An alternative method of expressing the partial trace is:

$$\text{Tr}_{\mathcal{X}} : \text{L}(\mathcal{X} \otimes \mathcal{Y}) \ni A \mapsto \sum_{i=1}^{\dim(\mathcal{X})} (\langle e_i | \otimes \mathbb{1}_{\mathcal{Y}}) A (|e_i\rangle \otimes \mathbb{1}_{\mathcal{Y}}). \quad (1.33)$$

Note that the partial trace operator is a quantum channel.

1.2.4 Quantum channel representations

In this section we discuss different representations of quantum channels and the relationships between them. Let us describe in detail three specific representations, which reveal interesting and non-trivial properties of quantum channels.

Natural representation

Definition 13 *Given $\Phi \in \text{M}(\mathcal{X}, \mathcal{Y})$, the natural representation of this map is the uniquely determined operator $S(\Phi) \in \text{L}(\mathcal{X} \otimes \mathcal{X}, \mathcal{Y} \otimes \mathcal{Y})$ satisfying*

$$S(\Phi)\text{res}(A) = \text{res}(\Phi(A)), \quad (1.34)$$

for all $A \in \text{L}(\mathcal{X})$.

Note that $S : \text{M}(\mathcal{X}, \mathcal{Y}) \rightarrow \text{L}(\mathcal{X} \otimes \mathcal{X}, \mathcal{Y} \otimes \mathcal{Y})$ is a linear bijection.

This representation is called natural, because it gives the action of the superoperator Φ as a matrix-vector multiplication, which is the natural way of thinking about linear operations. Unfortunately, this representation has a downside, as it has no connection to the properties of complete positivity and trace preservation.

Kraus representation

Definition 14 *The Kraus representation of $\Phi \in \text{M}(\mathcal{X}, \mathcal{Y})$ is given by the sets of operators $\{K_i : K_i \in \text{L}(\mathcal{X}, \mathcal{Y})\}$ and $\{L_i : L_i \in \text{L}(\mathcal{X}, \mathcal{Y})\}$*

$$\Phi(A) = \sum_{i=1}^r K_i A L_i^\dagger, \quad (1.35)$$

where r is the rank of the superoperator Φ .

If Φ is completely positive, we have [16]

$$\Phi(A) = \sum_{i=1}^r K_i A K_i^\dagger. \quad (1.36)$$

Additionally, if Φ is trace-preserving the Kraus operators fulfill

$$\sum_{i=1}^r K_i^\dagger K_i = \mathbb{1}_{\mathcal{X}}. \quad (1.37)$$

Choi-Jamiołkowski representation

Definition 15 Given $\Phi \in M(\mathcal{X}, \mathcal{Y})$ we define a mapping $J : M(\mathcal{X}, \mathcal{Y}) \rightarrow L(\mathcal{Y} \otimes \mathcal{X})$ as

$$J(\Phi) = (\Phi \otimes \mathbb{1}_{L(\mathcal{X})})(\text{res}(\mathbb{1}_{\mathcal{X}})\text{res}(\mathbb{1}_{\mathcal{X}})^\dagger). \quad (1.38)$$

The operator $J(\Phi)$ is called the *Choi operator* [20].

We can equivalently define $J(\Phi)$ as

$$J(\Phi) = \sum_{i,j=0}^{\dim(\mathcal{X})-1} \Phi(|i\rangle\langle j|) \otimes |i\rangle\langle j|. \quad (1.39)$$

Note that the Choi-Jamiołkowski representation, is also linear bijection, as was the case with the natural representation. There are, however, fundamental differences between the two representations. The action of a superoperator in the Choi representation is given by:

$$\Phi(A) = \text{Tr}_{\mathcal{X}}(J(\Phi)(\mathbb{1}_{\mathcal{Y}} \otimes A^T)), \quad (1.40)$$

which implies the most profound properties of the Choi representation. Firstly, Φ is completely positive iff $J(\Phi) \geq 0$. Secondly Φ is trace preserving iff $\text{Tr}_{\mathcal{Y}} J(\Phi) = \mathbb{1}_{\mathcal{X}}$. Finally, if $J(\Phi)$ is Hermitian, then Φ is Hermiticity preserving.

If $J(\Phi) \geq 0$, then the corresponding quantum state $\rho_\Phi = \frac{1}{\dim(\mathcal{Y} \otimes \mathcal{X})} J(\Phi)$ is called the *Jamiołkowski state* [21].

1.2.5 Markovian approximation

A large class of physical phenomena may be described by approximate evolutions which fulfill the semigroup property. A quantum dynamical semigroup is a family of quantum channels $\{\Phi_t, t \geq 0\}$ such that

$$(\Phi_s \circ \Phi_t)(\rho) = \Phi_{s+t}(\rho), \quad (1.41)$$

and $\text{Tr}[\Phi_t(\rho)A]$ is a continuous function of t for any ρ and A . There exists a linear map \mathcal{L} , called a generator of the semigroup, such that

$$\dot{\rho} = \mathcal{L}\rho. \quad (1.42)$$

Hence, we get $\Phi_t = e^{t\mathcal{L}}$. In the case of complex Euclidean spaces, the linear map \mathcal{L} is given by

$$\mathcal{L}\rho = -i[H, \rho(t)] + \sum_k \gamma_k L_k \rho L_k^\dagger - \frac{1}{2} \{L_k^\dagger L_k, \rho(t)\}, \quad (1.43)$$

where $\{A, B\}$ denotes the anticommutator, H is a Hermitian operator (the Hamiltonian of the system) and L_k are dissipation operators which describe the interaction with the environment. Furthermore, we have $L_i L_j = 0$ for $i \neq j$ and $\text{Tr} L_i = 0$ for all i .

Thus we arrive at the following equation for the evolution of the quantum system

$$\dot{\rho} = -i[H, \rho(t)] + \sum_k \gamma_k L_k \rho L_k^\dagger - \frac{1}{2} \{L_k^\dagger L_k, \rho(t)\}, \quad (1.44)$$

which is called the Gorini-Kossakowski-Sudarshan-Lindblad (GKSL) master equation [22, 23].

1.2.6 Quantum measurements

Quantum mechanical measurement is a non-trivial problem. This is mainly due to the fact, that the outcomes are inherently probabilistic. This means, that regardless of the amount of effort and how carefully the measurement procedure is conducted, the possible outcomes will be distributed according to some probability distribution. Secondly, the measurement process changes the state of the system.

Definition 16 Suppose that O is a finite set of measurement outcomes $O = \{o_i\}_{i=1}^N$ and F is the set of measurement operators $F = \{A_i : A_i \in \mathcal{L}(\mathcal{X}, \mathcal{Y})\}_{i=1}^N$ that fulfill the following relation

$$\sum_{i=1}^N A_i^\dagger A_i = \mathbb{1}_Y \quad (1.45)$$

Then, an arbitrary mapping $\mu : O \rightarrow F$ is called a quantum measurement. Probability p_i of measuring the outcome o_i in the state ρ is given by $p_i = \text{Tr}(A_i \rho A_i^\dagger)$. Given the measurement outcome o_i , the quantum state after the measurement μ is given by $\rho_{o_i} = \frac{A_i \rho A_i^\dagger}{p_i}$.

1.2.7 Quantum state and channel distances

In this section we discuss the common distances between quantum states and channels.

Trace distance

Given two quantum states $\rho, \sigma \in \Omega_{\mathcal{X}}$, their trace distance is

$$D(\rho, \sigma) = \frac{1}{2} \|\rho - \sigma\|_1. \quad (1.46)$$

This distance is a metric on the space of quantum states. The trace distance is a generalization of the Kolmogorov distance of classical probability distributions.

Fidelity

Fidelity is a measure of distance of quantum states. It is an example of a distance measure which is not a metric on the space of quantum states. The fidelity of two quantum states $\rho, \sigma \in \Omega_{\mathcal{X}}$ is given by

$$F(\rho, \sigma) = \|\sqrt{\rho}\sqrt{\sigma}\|_1. \quad (1.47)$$

Superfidelity

Superfidelity is an upper bound on the fidelity of two quantum states $\rho, \sigma \in \Omega_{\mathcal{X}}$. It is defined by

$$G(\rho, \sigma) = \text{Tr}\rho\sigma + \sqrt{1 - \text{Tr}\rho^2}\sqrt{1 - \text{Tr}\sigma^2}. \quad (1.48)$$

Diamond norm

In order to introduce the diamond norm, we first introduce the notion of the induced trace norm. Given $\Phi \in M(\mathcal{X}, \mathcal{Y})$ we define its induced trace norm as

$$\|\Phi\|_1 = \max \{\|\Phi(X)\|_1 : X \in L(\mathcal{X}), \|X\|_1 \leq 1\}. \quad (1.49)$$

The diamond norm of Φ is defined as

$$\|\Phi\|_{\diamond} = \|\Phi \otimes \mathbb{1}_{L(\mathcal{X})}\|_1. \quad (1.50)$$

One important property of the diamond norm is that for Hermiticity-preserving $\Phi \in M(\mathcal{X}, \mathcal{Y})$ we obtain

$$\|\Phi\|_{\diamond} = \max \left\{ \left\| (\Phi \otimes \mathbb{1}_{L(\mathcal{X})}) (|\psi\rangle\langle\psi|) \right\|_1 : |\psi\rangle \in \mathcal{X} \otimes \mathcal{X}, \langle\psi|\psi\rangle = 1 \right\}. \quad (1.51)$$

1.3 Quantum channel engineering

In this section we introduce a model in which we engineer quantum channels in systems governed by the GKSL equation. We will assume that the control of a quantum system is performed via piecewise constant functions. Then, the Hamiltonian can be written as

$$H(t) = H_0 + H_c(t), \quad (1.52)$$

where H_0 is called the drift Hamiltonian and describes the internal dynamics of the system. The $H_c(t)$ part represents the external control.

The setting on which we will focus is the Heisenberg spin-1/2 chain model of a finite length n , in which the drift Hamiltonian is given by

$$H_0 = J \sum_{i=1}^{n-1} \sigma_x^{(i)} \sigma_x^{(i+1)} + \sigma_y^{(i)} \sigma_y^{(i+1)} + \sigma_z^{(i)} \sigma_z^{(i+1)}, \quad (1.53)$$

where J is the coupling strength and $\sigma_x^{(i)} = \mathbb{1}_{\mathbb{C}^{2^{i-1}}} \otimes \sigma_x \otimes \mathbb{1}_{\mathbb{C}^{2^{n-i}}}$ denotes the operator σ_x acting on site i . Thus this model describes a chain of n interacting qubits.

If we assume that the control is performed only on the k^{th} qubit, then $H_c(t)$ can be written as

$$H_c(t) = b(t) \sigma_z^{(k)} + c(t) \sigma_x^{(k)}, \quad (1.54)$$

where $b(t)$ and $c(t)$ are piecewise constant functions of time t .

Integration of the GKSL in the time intervals $[t_i, t_{i+1}]$ in which $b(t)$ and $c(t)$ are constant gives us a family of quantum channels $\Phi_{\tau_1}, \dots, \Phi_{\tau_n}$, where $\tau_i = t_{i+1} - t_i$. Using the semigroup property we may write $\Phi_T(\rho) = (\Phi_{\tau_n} \circ \dots \circ \Phi_{\tau_1})(\rho)$ for $T = t_n - t_1$.

Our goal is to find such functions that maximize a given figure of merit. In the case of closed quantum systems, that is when all γ_k in Eq. (1.44) are equal to zero, this number can be chosen as

$$F = \frac{1}{2^n} \text{Tr} U_T^\dagger U(T), \quad (1.55)$$

where U_T is the target unitary operation, and $U(T)$ is the unitary implemented by the control functions $b(t)$ and $c(t)$. This number is called the gate fidelity.

In the case of open quantum systems the proper choice of a figure of merit is a complicated task. On the one hand, the diamond norm is a natural way

of quantifying the distance between two quantum channels $\Phi, \Psi \in C(\mathcal{X}, \mathcal{Y})$. On the other hand, this quantity can not be used in realistic applications, due to needed optimizations. Therefore, extending the approach from closed quantum systems, we use the following figure of merit

$$F = \frac{1}{2^{2n}} \Re \text{Tr} S_T^\dagger S(T), \quad (1.56)$$

where S_T and $S(T)$ denote the target channel and the channel implemented by the control functions respectively in their natural representations. As it is not possible to overcome the environmental interaction via coherent control, as a part of this work, we introduced a protocol of adding ancillary qubits to the system to help alleviate this particular problem. This will be discussed in the next section. Furthermore, as a part of this work, we introduced a new possible figure of merit for quantum channel optimization, which is also discussed in the next section.

1.4 Open systems in quantum informatics

One of the major obstacles in the construction of quantum computers and quantum cryptographic systems is the interaction of a quantum system with its surrounding environment. This interaction, or uncontrollable coupling, of a quantum system to the environment occurs spontaneously, and thus is difficult to avoid. This gives rise to errors in the computation and cryptographic schemes. Some of these errors resemble those known from the classical theory, such as the bit flip errors. Generally speaking, my work focused on engineering quantum channels for systems interacting with an environment.

1.4.1 Decoherence effects in the quantum qubit flip game using Markovian approximation

Problem description and results

One of the first commercial uses of the results of quantum information science are random number generators used in on-line casinos and lotteries [24]. The next step may be games with quantum resources. This leads to the question, what happens when one of the parties participating in the game has malicious intentions? Is it possible for the other party to detect attempts of cheating?

We consider a quantum version of the penny flip game. In this case, we treat a qubit as a quantum coin. As in the classical case the game is

divided into three rounds. Starting with Alice, in each round, one player performs a unitary operation on the quantum coin. The rules of the game are constrained by its physical implementation.

Our goal is to study the possible environmental interactions and how it can help each of the players win the game. We show that for a quantum coin strongly coupled to an environment, there is always a way for one of the players to achieve a significant advantage in the game, regardless of the actions of the other one.

In the second part, we attempt to engineer an optimal set of control functions so that the player's winning probability approaches unity. It turns out that in the case of one of the players, Bob in this setup, it is possible to significantly increase his winning probability.

Personal contribution

My main contribution to this work was performing the numerical simulations of the game. This involved proposing a figure of merit for our optimization. Next, I found the appropriate set of equations in the subject literature, which were then solved numerically. The final step was adapting them to our model of the quantum system.

My detailed contribution to this work was:

- creating the simulation software,
- performing the numerical calculations,
- developing the results,
- reviewing the literature on the subject,
- co-editing the paper.

1.4.2 Various methods of optimizing control pulses for quantum systems with decoherence

Problem description and results

Engineering a quantum channel on a quantum system undergoing decoherence is a major issue. There are many known approaches to this problem, like dynamical decoupling [25] or sliding mode control [26]. However, we aim at a simpler approach.

In this work we propose to add an ancillary qubit to the quantum system and apply the control functions $b(t)$ and $c(t)$ on it, and at the end simply discard it. Additionally, as it is difficult to obtain exact analytical formulas for the derivative of the figure of merit with respect to the control functions, we investigate three approaches to calculate it.

In the first approach we simply approximate the value of the derivative. In the second approach, we approximate the evolution of the system and obtain

an exact formula for the derivative in this case. Finally, for comparison we utilize genetic programming.

The results we obtained show that, by adding an ancilla, it is possible to implement a unitary evolution on a system under the Markovian approximation. What we have found is that it is sufficient to apply the control functions to the ancillary qubits. This is caused by the fact that the interaction between the two qubits smooths the impact of the control fields. This is limited to the case when the environment is slower than the frequency of oscillation of the qubits. In other words we require that $\gamma < J$ in Eq. (1.44). As for the optimization method, we shown that approximate gradient-based approach allows us to get the best results in terms of fidelity of the target unitary operation.

Personal contribution

In this work my main contribution was the definition of the entire research problem. I proposed to add an ancillary qubit to the system and apply the control functions to it. Furthermore, I proposed to utilize the three optimization schemes presented in the paper and conducted numerical research for two of them: the approximate gradient and approximate evolution method.

My detailed contribution to this work was:

- defining the research problem,
- co-creating the simulation software,
- performing the numerical calculations,
- developing the results,
- reviewing the literature on the subject,
- co-editing the paper.

1.4.3 Quantum control with spectral constraints

Problem description and results

One of the fundamental issues of the quantum information science is the ability to manipulate the dynamics of a given complex quantum system. A widely used method for manipulating a quantum system is a coherent control strategy, where the manipulation of the quantum states is achieved by applying semi-classical potentials in a fashion that preserves quantum coherence. In the case when a system is controllable it is a point of interest what actions must be performed to control a system most efficiently, bearing in mind limitations imposed by practical restrictions. Various constraints concerning control fields can be imposed in the realistic implementations of quantum control systems. One of the most important is the restriction on the frequency spectrum of acceptable control functions. In this work we presented a general method of obtaining a piecewise-constant controls,

which is robust with respect to low-pass filtering. The above means, that elimination of high-frequencies in a Fourier spectra reduces the fidelity only by a small amount.

We focus our study on the Heisenberg spin chain model not interacting with the environment. Despite this, our approach may be applied to any qubit interaction model. In order to take into account the frequency spectrum of the control function we add a Fourier transform dependent term P , and then introduce a new figure of merit which is a combination of the frequency dependent part and the gate fidelity part

$$F' = (1 - \mu)P - \mu F. \quad (1.57)$$

After obtaining the control functions $b(t)$ and $c(t)$, we run them through a low pass filter and calculate the fidelity of the operation. We compare this to the case of filtering control functions obtained for $\mu = 1$. The control functions optimized with the spectral constraints taken into account achieve orders of magnitude higher fidelity of operation compared to the case when we neglect the frequency constraints.

Personal contribution

In this work my main contribution was the numerical modeling of the studied quantum systems. I was responsible for the proper adaption of known optimization algorithm in order to take into account the frequency spectrum limitation. Another part of my contribution was performing the numerical simulations and developing their results.

My detailed contribution to this work was:

- creating the simulation software,
- performing the numerical calculations,
- developing the results,
- reviewing the literature on the subject,
- co-editing the paper.

1.4.4 Quantum control robust with respect to coupling with an external environment

Problem description and results

In many situations, the interaction of the quantum system with the control functions $b(t)$ and $c(t)$ may cause an undesirable coupling with an environment. In light of this, it is reasonable to look for a scheme of finding the functions $b(t)$ and $c(t)$ which takes this problem into account. There can be various models of such interactions, hence in this work we focus only on one of the possibilities. We model the environment as a single qubit which

gets coupled to the quantum system under consideration and the coupling strength is proportional to the magnitude of the control functions.

Based on the discussion in the previous paragraph, we introduce an additional constraint on the piecewise constant functions $b(t)$ and $c(t)$. We aim to minimize their L_1 norm. To achieve this we introduce a penalty, P , for the L_1 norm and wish to minimize the following function

$$F' = (1 - \mu)P - \mu F, \quad (1.58)$$

where $\mu \in [0, 1]$ and F is the gate fidelity. The main problem with efficient minimization of F' is the fact that it is dependent on the L_1 norm, which in turn depends on the absolute values of the functions $b(t)$ and $c(t)$. This poses a problem in numerical optimizations, as we need an analytical expression for the derivative of F' with respect to $b(t)$ and $c(t)$. In this work we proposed three ways of avoiding this problem. The first one was to use the function $\text{sgn}(x)$ as the derivative of $|x|$. The next approach was to use a fractional derivative

$$\frac{d^\alpha |x|}{dx^\alpha} = \pm \frac{1}{\Gamma(2 - \alpha)} x^{1-\alpha}, \quad (1.59)$$

where $\alpha \in (0, 1)$. Finally, we use a rescaled Fermi-Dirac distribution as an approximation of the derivative

$$\frac{d|x|}{dx} = 2 \left(\frac{-1}{\exp\left(\frac{x}{kT}\right) + 1} + \frac{1}{2} \right). \quad (1.60)$$

Our results show that it is possible to obtain control fields which have minimal energy and still give a high fidelity of the quantum operation. Our method may be used in situations where the interaction with the control field causes additional coupling to the environment. As our method allows one to minimize the number of control pulses, it also minimizes the amount of coupling to the environment. It is important to note that our model differs from other approaches known in the literature. For instance, in the well studied dynamical decoupling [25] approach an additional perturbation on a system is added, which protects the evolution against the effects of the environment influence. In our case the interaction with the environment is related to the control strategy, and it emerges only if the control is applied. Our model allows to optimize high fidelity control pulses for the cases with and without external environment as long as the coupling is induced by the control pulses themselves.

Personal contribution

My main contribution in this work was the introduction of various ways of approximating the derivative of the absolute value. This includes the $\text{sgn}(x)$ function, the fractional derivative approach and the rescaled Fermi-Dirac distribution. Furthermore, I was responsible for adaption of the numerical algorithms, so that they took the L_1 norm constraint into account. The next step was actually performing the numerical simulations and developing their results.

My detailed contribution to this work was:

- co-creating the simulation software,
- performing the numerical calculations,
- proposing the optimization scheme
- developing the results,
- reviewing the literature on the subject,
- co-editing the paper.

1.4.5 Quantifying channels output similarity with applications to quantum control

Problem description and results

One of the problems in optimization of the piecewise constant control functions in open quantum systems is the choice of the figure of merit of the obtained quantum operation. The diamond norm is computationally expensive, while other, fidelity-type figures of merit, operate on non-normal matrices. In this work we approached this problem with the usage of the superfidelity function [27], which is an upper bound on the fidelity of two quantum states.

Our focus in this work was on comparing outputs of two quantum channels $\Phi, \Psi \in C(\mathcal{X})$ in the case of the same input state $\sigma \in \Omega_{\mathcal{X}}$. Using the superfidelity function, we obtain an analytical formula which gives an upper bound on the fidelity of output of two quantum channels, which we call channel superfidelity

$$G_{\text{ch}} = \sum_{i,j} \left| \text{Tr} \sigma K_i^\dagger L_j \right|^2 + \sqrt{1 - \sum_{i,j} \left| \text{Tr} \sigma K_i^\dagger K_j \right|^2} \sqrt{1 - \sum_{i,j} \left| \text{Tr} \sigma L_i^\dagger L_j \right|^2}, \quad (1.61)$$

where $\{K_i\}$ and $\{L_j\}$ are the Kraus representations of the channels Φ and Ψ respectively.

We study the sensitivity of this quantity to errors in the control functions $b(t)$ and $c(t)$. First, we take a spin chain and find some optimal control functions for it. Next, we add Gaussian noise to these functions with mean zero and variance s^2 . We obtain that the channel superfidelity behaves for

a wide range of s as

$$G_{\text{ch}} = 1 - \alpha s^2, \quad (1.62)$$

for some constant α .

Personal contribution

My main contribution to this work includes proving Corollaries 1–3. Another part of the contribution is showing the sensitivity of the channel superfidelity functional to channel and Hamiltonian errors. Finally, my contribution includes performing the numerical simulations depicting the usefulness of the channel superfidelity functional in control function optimization.

My detailed contribution to this work was:

- proving some of the theorems,
- creating the simulation software,
- performing the numerical calculations,
- developing the results,
- reviewing the literature on the subject,
- co-editing the paper.

Bibliography

- [1] M. Planck, “Über das Gesetz der Energieverteilung im Normalspectrum,” *Annalen der physik*, vol. 309, no. 3, pp. 553–563, 1901.
- [2] J. Von Neumann, “Thermodynamik quantenmechanischer Gesamtheiten,” *Göttinger Nachrichten*, vol. 1, no. 11, pp. 273–291, 1927.
- [3] A. S. Holevo, “Information-theoretical aspects of quantum measurement,” *Problemy Peredachi Informatsii*, vol. 9, no. 2, pp. 31–42, 1973.
- [4] R. S. Ingarden, “Quantum information theory,” *Reports on Mathematical Physics*, vol. 10, no. 1, pp. 43–72, 1976.
- [5] C. Bennett and G. Brassard, “Quantum cryptography: Public key distribution and coin tossing,” in *Proceedings of IEEE International Conference on Computers, Systems and Signal Processing*, vol. 175, Bangalore, India, 1984.
- [6] A. Ekert, “Quantum cryptography based on Bell’s theorem,” *Physical review letters*, vol. 67, no. 6, pp. 661–663, 1991.
- [7] R. Feynman, “Simulating physics with computers,” *International journal of theoretical physics*, vol. 21, no. 6, pp. 467–488, 1982.
- [8] D. Deutsch, “Quantum theory, the Church-Turing principle and the universal quantum computer,” *Proceedings of the Royal Society of London. A. Mathematical and Physical Sciences*, vol. 400, no. 1818, pp. 97–117, 1985.
- [9] P. Shor, “Algorithms for quantum computation: discrete logarithms and factoring,” in *Foundations of Computer Science, 1994 Proceedings., 35th Annual Symposium on*, pp. 124–134, IEEE, 1994.
- [10] L. Grover, “A fast quantum mechanical algorithm for database search,” in *Proceedings of the twenty-eighth annual ACM symposium on Theory of computing*, pp. 212–219, ACM, 1996.

- [11] H.-P. Breuer and F. Petruccione, *The theory of open quantum systems*. Oxford University Press, 2002.
- [12] T. Altenkirch and J. Grattage, “A functional quantum programming language,” in *Logic in Computer Science, 2005. LICS 2005. Proceedings. 20th Annual IEEE Symposium on*, pp. 249–258, IEEE, 2005.
- [13] B. Ömer, “A procedural formalism for quantum computing,” Master’s thesis, Technical University of Vienna, 1998.
- [14] A. S. Green, P. L. Lumsdaine, N. J. Ross, P. Selinger, and B. Valiron, “Quipper: a scalable quantum programming language,” in *ACM SIGPLAN Notices*, vol. 48, pp. 333–342, ACM, 2013.
- [15] D. Wecker and K. M. Svore, “LIQUi|>: A software design architecture and domain-specific language for quantum computing,” *arXiv preprint arXiv:1402.4467*, 2014.
- [16] M. A. Nielsen and I. L. Chuang, *Quantum computation and quantum information*. Cambridge university press, 2010.
- [17] D. A. Lidar and T. A. Brun, *Quantum error correction*. Cambridge University Press, 2013.
- [18] P. Gawron, M. Cholewa, and K. Kara, *Rewolucja stanu – fantastyczne wprowadzenie do informatyki kwantowej*. Gliwice: IITiS PAN, 2016.
- [19] I. Bengtsson and K. Życzkowski, *Geometry of quantum states: an introduction to quantum entanglement*. Cambridge University Press, Cambridge, U.K., 2006.
- [20] M.-D. Choi, “Completely positive linear maps on complex matrices,” *Linear algebra and its applications*, vol. 10, no. 3, pp. 285–290, 1975.
- [21] A. Jamiołkowski, “Linear transformations which preserve trace and positive semidefiniteness of operators,” *Reports on Mathematical Physics*, vol. 3, no. 4, pp. 275–278, 1972.
- [22] V. Gorini, A. Kossakowski, and E. C. G. Sudarshan, “Completely positive dynamical semigroups of N -level systems,” *Journal of Mathematical Physics*, vol. 17, no. 5, pp. 821–825, 1976.
- [23] G. Lindblad, “On the generators of quantum dynamical semigroups,” *Communications in Mathematical Physics*, vol. 48, no. 2, pp. 119–130, 1976.

- [24] “Random number generation reference applications.” <http://www.idquantique.com/random-number-generation/rng-reference-applications>. Accessed: 2017-01-20.
- [25] L. Viola, E. Knill, and S. Lloyd, “Dynamical decoupling of open quantum systems,” *Physical Review Letters*, vol. 82, no. 12, p. 2417, 1999.
- [26] D. Dong and I. R. Petersen, “Sliding mode control of quantum systems,” *New Journal of Physics*, vol. 11, no. 10, p. 105033, 2009.
- [27] J. A. Miszczak, Z. Puchała, P. Horodecki, A. Uhlmann, and K. Życzkowski, “Sub-and super-fidelity as bounds for quantum fidelity,” *Quantum Information & Computation*, vol. 9, no. 1, pp. 103–130, 2009.

Chapter 2

Decoherence effects in the
quantum qubit flip game using
Markovian approximation

Decoherence effects in the quantum qubit flip game using Markovian approximation

Piotr Gawron · Dariusz Kurzyk · Łukasz Pawela

Received: 30 July 2013 / Accepted: 31 October 2013 / Published online: 17 November 2013
© The Author(s) 2013. This article is published with open access at Springerlink.com

Abstract We are considering a quantum version of the penny flip game, whose implementation is influenced by the environment that causes decoherence of the system. In order to model the decoherence, we assume Markovian approximation of open quantum system dynamics. We focus our attention on the phase damping, amplitude damping and amplitude raising channels. Our results show that the Pauli strategy is no longer a Nash equilibrium under decoherence. We attempt to optimize the players' control pulses in the aforementioned setup to allow them to achieve higher probability of winning the game compared with the Pauli strategy.

Keywords Lindblad master equation · Decoherence effects · Quantum games · Open quantum systems

1 Introduction

Quantum information experiments can be described as a sequence of three operations: state preparation, evolution and measurement [1]. In most cases, one cannot assume that experiments are conducted perfectly; therefore, imperfections have to be taken into account while modeling them. In this work, we are interested in how the knowledge about imperfect evolution of a quantum system can be exploited by players engaged in a quantum game. We assume that one of the players possesses the knowledge about

P. Gawron · D. Kurzyk (✉) · Ł. Pawela
Institute of Theoretical and Applied Informatics, Polish Academy of Sciences,
Bałycka 5, 44-100 Gliwice, Poland
e-mail: dariusz.kurzyk@polsl.pl

D. Kurzyk
Institute of Mathematics, Silesian University of Technology, Kaszubska 23, 44-100 Gliwice, Poland

imperfections in the system, while the other is ignorant of their existence. We ask a question of how much the player's knowledge about those imperfections can be exploited by him/her for their advantage.

We consider implementation of the quantum version of the penny flip game, which is influenced by the environment that causes decoherence of the system. In order to model the decoherence, we assume Markovian approximation of open quantum system dynamics. This assumption is valid, for example, in the case of two-level atom coupled to the vacuum, undergoing spontaneous emission (amplitude damping). The coherent part of the atom's evolution is described by one-qubit Hamiltonian. Spontaneous emission causes an atom in the excited state to drop down into the ground state, emitting a photon in the process. Similarly, phase damping channel can be considered. This channel causes a continuous decay of coherence without energy dissipation in a quantum system [2].

The paper is organized as follows: in the two following subsections, we discuss related work and present our motivation to undertake this task. In Sect. 2, we recall the penny flip game and its quantum version; in Sect. 3, we present the noise model; in Sect. 4, we discuss the strategies applied in the presence of noise and finally in Sect. 5, we conclude the obtained results.

1.1 Related work

Imperfect realizations of quantum games have been discussed in literature since the beginning of the century. Johnson [3] discusses a three-player quantum game played with a corrupted source of entangled qubits. The author implicitly assumes that the initial state of the game had passed through a bit-flip noisy channel before the game began. The corruption of quantum states in schemes implementing quantum games was studied by various authors, *e.g.*, in [4], the authors study the general treatment of decoherence in two-player, two-strategy quantum games; in [5], the authors perform an analysis of the two-player prisoners' dilemma game; in [6], the multiplayer quantum minority game with decoherence is studied; in [7,8], the authors analyze the influence of the local noisy channels on quantum Magic Squares games, while the quantum Monty Hall problem under decoherence is studied first in [9] and subsequently in [10]. In [11], the authors study the influence of the interaction of qubits forming a spin chain on the qubit flip game. An analysis of trembling hand-perfect equilibria in quantum games was done in [12]. Prisoners' dilemma in the presence of collective dephasing modeled by using the Markovian approximation of open quantum systems dynamics is studied in [13]. Unfortunately, the model applied in this work assumes that decoherence acts only after the initial state has been prepared and ceases to act before unitary strategies are applied. Another interesting approach to quantum games is the study of relativistic quantum games [14,15]. This setup has also been studied in a noisy setup [16].

1.2 Motivation

In the quantum game, theoretic literature decoherence is typically applied to a quantum game in the following way:

1. The entangled state is prepared,
2. It is transferred through a noisy channel,
3. Players' strategies are applied,
4. The resulting state is transferred once again through a noisy channel,
5. The state is disentangled,
6. Quantum local measurements are performed, and the outcomes of the games are calculated.

In some cases, where it is appropriate, steps 4 and 5 are omitted. The problem with the above procedure is that it separates unitary evolution from the decoherent evolution. In Miszczak et al. [11], it was proposed to observe the behavior of the quantum version of the penny flip game under more physically realistic assumptions where decoherence due to coupling with the environment and unitary evolution happen simultaneously. In the papers, the authors study an implementation of the qubit flip game on quantum spin chains. First, a design, expressed in the form of quantum control problem, of the game on the trivial, one-qubit spin chain is proposed. Then the environment in the form of an additional qubit is added, and spin-spin coupling is adjusted, so one of the players, under some assumptions, can not detect that the system is implemented on two qubits rather than on one qubit. In the paper, it is shown that if one of the players posses the knowledge about the spin coupling, he or she can exploit it for augmenting his or hers winning probability.

2 Game as a quantum experiment

In this work, our goal is to follow the work done in [11] and to discuss the quantum penny flip game as a physical experiment consisting in preparation, evolution and measurement of the system. For the purpose of this paper, we assume that preparation and measurement, contrary to noisy evolution of the system are perfect. We investigate the influence of the noise on the players' odds and how the noisiness of the system can be exploited by them. The noise model we use is described by the Lindblad master equation, and the dynamics of the system is expressed in the language of quantum systems control.

2.1 Penny flip game

In order to provide classical background for our problem, let us consider a classical two-player game, consisting in flipping over a coin by the players in three consecutive rounds. As usual, the players are called Alice and Bob. In each round, Alice and Bob performs one of two operations on the coin: flips it over or retains it unchanged.

At the beginning of the game, the coin is turned heads up. During the course of the game the coin is hidden and the players do not know the opponents actions. If after the last round, the coin tails up, then Alice wins, otherwise the winner is Bob.

The game consists of three rounds: Alice performs her action in the first and the third round, while Bob performs his in the second round of the game. Therefore, the set of allowed strategies consists of eight sequences (N, N, N) , (N, N, F) , \dots , (F, F, F) ,

Table 1 Bob's pay-off table for the penny flip game

	NN	FN	NF	FF
N	1	-1	-1	1
F	-1	1	1	-1

where N corresponds to the *non-flipping strategy* and F to the *flipping strategy*. Bob's pay-off table for this game is presented in Table 1. Looking at the pay-off tables, it can be seen that utility function of players in the game is balanced; thus, the penny flip game is a zero-sum game.

A detailed analysis of this game and its asymmetrical quantization can be found in [17]. In this work it was shown that there is no winning strategy for any player in the penny flip game. It was also shown, that if Alice was allowed to extend her set of strategies to quantum strategies she could always win. In Miszczak et al. [11] it was shown that when both players have access to quantum strategies the game becomes fair and it has the Nash equilibrium.

2.2 Qubit flip game

The quantum version of the qubit flip game was studied for the first time by Meyer [18]. In our study, we wish to follow the work done in the aforementioned paper [11]. Hence, we consider a quantum version of the penny flip game. In this case, we treat a qubit as a quantum coin. As in the classical case the game is divided into three rounds. Starting with Alice, in each round, one player performs a unitary operation on the quantum coin. The rules of the game are constrained by its physical implementation. In order to obtain an arbitrary one-qubit unitary operation it is sufficient to use a control Hamiltonian built using only two traceless Pauli operators [19]. Therefore, we assume that in each round each of the players can choose three control parameters $\alpha_1, \alpha_2, \alpha_3$ in order to realize his/hers strategy. The resulting unitary gate is given by the equation:

$$U(\alpha_1, \alpha_2, \alpha_3) = e^{-i\alpha_3\sigma_z\Delta t} e^{-i\alpha_2\sigma_y\Delta t} e^{-i\alpha_1\sigma_z\Delta t}, \quad (1)$$

where Δt is an arbitrarily chosen constant time interval.

Therefore, the system defined above forms a single qubit system driven by time-dependent Hamiltonian $H(t)$, which is a piecewise constant and can be expressed in the following form

$$H(t) = \begin{cases} \alpha_1^{A_1}\sigma_z & \text{for } 0 \leq t < \Delta t, \\ \alpha_2^{A_1}\sigma_y & \text{for } \Delta t \leq t < 2\Delta t, \\ \alpha_3^{A_1}\sigma_z & \text{for } 2\Delta t \leq t < 3\Delta t, \\ \alpha_1^B\sigma_z & \text{for } 3\Delta t \leq t < 4\Delta t, \\ \alpha_2^B\sigma_y & \text{for } 4\Delta t \leq t < 5\Delta t, \\ \alpha_3^B\sigma_z & \text{for } 5\Delta t \leq t < 6\Delta t, \\ \alpha_1^{A_2}\sigma_z & \text{for } 6\Delta t \leq t < 7\Delta t, \\ \alpha_2^{A_2}\sigma_y & \text{for } 7\Delta t \leq t < 8\Delta t, \\ \alpha_3^{A_2}\sigma_z & \text{for } 8\Delta t \leq t \leq 9\Delta t. \end{cases} \quad (2)$$

Control parameters in the Hamiltonian $H(t)$ will be referred to vector $\alpha = (\alpha_1^{A_1}, \alpha_2^{A_1}, \alpha_3^{A_1}, \alpha_1^B, \alpha_2^B, \alpha_3^B, \alpha_1^{A_2}, \alpha_2^{A_2}, \alpha_3^{A_2})$, where $\alpha_i^{A_1}, \alpha_i^{A_2}$ are determined by Alice and α_i^B are selected by Bob.

Suppose that players are allowed to play the game by manipulating the control parameters in the Hamiltonian $H(t)$ representing the coherent part of the dynamics, but they are not aware of the action of the environment on the system. Hence, the time evolution of the system is non-unitary and is described by a master equation, which can be written generally in the *Lindblad* form as

$$\frac{d\rho}{dt} = -i[H(t), \rho] + \sum_j \gamma_j (L_j \rho L_j^\dagger - \frac{1}{2} \{L_j^\dagger L_j, \rho\}), \quad (3)$$

where $H(t)$ is the system Hamiltonian, L_j are the *Lindblad* operators, representing the environment influence on the system [2] and ρ is the state of the system.

For the purpose of this paper we chose three classes of decoherence: *amplitude damping*, *amplitude raising* and *phase damping* which correspond to noisy operators $\sigma_- = |0\rangle\langle 1|$, $\sigma_+ = |1\rangle\langle 0|$ and σ_z , respectively.

Let us suppose that initially the quantum coin is in the state $|0\rangle\langle 0|$. Next, in each round, Alice and Bob perform their sequences of controls on the qubit, where each control pulse is applied according to Eq. (3). After applying all of the nine pulses, we measure the expected value of the σ_z operator. If $\text{tr}(\sigma_z \rho(T)) = -1$ Alice wins, if $\text{tr}(\sigma_z \rho(T)) = 1$ Bob wins. Here, $\rho(T)$ denotes the state of the system at time $T = 9\Delta t$.

Alternatively we can say that the final step of the procedures consists in performing orthogonal measurement $\{O_{\text{tails}} \rightarrow |1\rangle\langle 1|, O_{\text{heads}} \rightarrow |0\rangle\langle 0|\}$ on state $\rho(T)$. The probability of measuring O_{tails} and O_{heads} determines pay-off functions for Alice and Bob, respectively. These probabilities can be obtained from relations $p(\text{tails}) = \langle 1|\rho(T)|1\rangle$ and $p(\text{heads}) = \langle 0|\rho(T)|0\rangle$.

2.3 Nash equilibrium

In this game, pure strategies cannot be in Nash equilibrium [18]. Hence, the players choose mixed strategies, which are better than the pure ones. We assume that Alice and Bob use the *Pauli strategy*, which is mixed and gives Nash equilibrium [11]; therefore, this strategy is a reasonable choice for the players. According to the Pauli strategy, each player chooses one of the four unitary operations $\{\mathbb{1}, i\sigma_x, i\sigma_y, i\sigma_z\}$ with equal probability. Thus, to obtain the Pauli strategy, each player chooses a sequence of control parameters $(\alpha_1^\square, \alpha_2^\square, \alpha_3^\square)$ listed in Table 2. The symbol \square can be substituted by A_1, B, A_2 . It means that in each round, one player performs a unitary operation chosen randomly with a uniform probability distribution from the set $\{\mathbb{1}, i\sigma_x, i\sigma_y, i\sigma_z\}$.

3 Influence of decoherence on the game

In this section, we perform an analytical investigation which shows the influence of decoherence on the game result. In accordance with the Lindblad master equation,

Table 2 Control parameters for realizing the Pauli strategy

	α_1^\square	α_2^\square	α_3^\square
$\mathbb{1}$	0	0	0
$i\sigma_x$	$\frac{\pi}{4}$	$-\frac{\pi}{2}$	$-\frac{\pi}{4}$
$i\sigma_y$	0	$-\frac{\pi}{2}$	0
$i\sigma_z$	$-\frac{\pi}{4}$	0	$-\frac{\pi}{4}$

The left column indicates the resulting gate

the environment influence on the system is represented by Lindblad operators L_j , while the rate of decoherence is described by parameters γ_j . In our game, players use the Pauli strategy; hence, the quantum system evolves depending on the Hamiltonians expressed as $H(t) = \alpha_i^\square \sigma_y$ or $H(t) = \alpha_i^\square \sigma_z$. To simplify the discussion, we consider Hamiltonians represented by diagonal matrices. In our case, $H = \alpha_i^\square \sigma_z$ is diagonal, but Hamiltonian $\alpha_i^\square \sigma_y$ requires diagonalization. Therefore, we will consider solutions of Lindblad equations for the Hamiltonians given by $H_z = \alpha_i^\square \sigma_z$ and $H_y = \alpha_i^\square U^\dagger \sigma_y U = \alpha_i^\square \begin{pmatrix} -1 & 0 \\ 0 & 1 \end{pmatrix}$, where $U = \begin{pmatrix} -\frac{\sqrt{2}}{2} & -\frac{\sqrt{2}}{2} \\ i\frac{\sqrt{2}}{2} & -i\frac{\sqrt{2}}{2} \end{pmatrix}$ is unitary matrix, whose columns are the eigenvectors of σ_y . Thus, we consider the solutions of the Lindblad equation for the Hamiltonian of the form

$$H = \beta_1 |0\rangle\langle 0| + \beta_2 |1\rangle\langle 1|. \quad (4)$$

3.1 Amplitude damping and amplitude raising

First we consider the amplitude damping decoherence, which corresponds to the Lindblad operator σ_- . Thus, the master Eq. (3) is expressed as

$$\frac{d\rho}{dt} = -i[H, \rho(t)] + \gamma(\sigma_- \rho(t) \sigma_+ - \frac{1}{2} \sigma_+ \sigma_- \rho(t) - \frac{1}{2} \rho(t) \sigma_+ \sigma_-), \quad (5)$$

where $\sigma_+ = \sigma_-^\dagger = |1\rangle\langle 0|$. The equation can be rewritten in the following form

$$\frac{d\rho}{dt} = A\rho(t) + \rho(t)A^\dagger + \gamma\sigma_- \rho(t) \sigma_+, \quad (6)$$

where $A = -iH(t) - \frac{1}{2}\gamma\sigma_+\sigma_-$. In solving this equation it is helpful to make a change of variables $\rho(t) = e^{At} \hat{\rho}(t) e^{-A^\dagger t}$. Hence, we obtain

$$\frac{d\hat{\rho}}{dt} = \gamma B(t) \hat{\rho}(t) B^\dagger(t), \quad (7)$$

where $B(t) = e^{-At} \sigma_- e^{At} = e^{-i(\beta_2 - \beta_1)t - \frac{\gamma}{2}t} \sigma_-$. It follows that

$$\frac{d\hat{\rho}}{dt} = \gamma e^{-\gamma t} \sigma_- \hat{\rho}(t) \sigma_+. \quad (8)$$

Due to the fact that $\sigma_- \sigma_- = \sigma_+ \sigma_+ = 0$ and $\sigma_- \frac{d\hat{\rho}}{dt} \sigma_+ = 0$ it is possible to write $\hat{\rho}(t)$ as

$$\hat{\rho}(t) = \hat{\rho}(0) - e^{-\gamma t} \sigma_- \hat{\rho}(0) \sigma_+. \quad (9)$$

Coming back to the original variables we get the expression

$$\rho(t) = e^{At} \rho(0) e^{A^\dagger t} - e^{-\gamma t} \sigma_- \rho(0) \sigma_+. \quad (10)$$

In order to study the asymptotic effects of decoherence on the results of the game, we consider the following limit

$$\lim_{\gamma \rightarrow \infty} e^{At} \rho(0) e^{A^\dagger t} - e^{-\gamma t} \sigma_- \rho(0) \sigma_+ = |0\rangle \langle 0| \rho(0) |0\rangle \langle 0|. \quad (11)$$

Let $\rho(0) = |0\rangle \langle 0|$; thus, the above limit is equal to $|0\rangle \langle 0|$. This result shows that for high values of γ , chances of winning the game by Bob increase to 1 as γ increases. Figure 1 shows an example of the evolution of a quantum system with amplitude damping decoherence for two values of the parameter γ . Figure 1a, b show the player's control pulses. In this case they are the ones implementing the Pauli strategy. Figure 1c, d show the time evolution of the state expressed as the expectation values of the observables σ_x , σ_y and σ_z for both cases. Finally, Fig. 1e, f show the evolution of the qubit's state in the Bloch sphere. This shows how a little amount of noise influences the evolution of the system and changes the probability of winning the game.

The noisy operator σ_+ is related to amplitude raising decoherence, and the solution of the master equation has the following form

$$\rho(t) = e^{At} \rho(0) e^{A^\dagger t} - e^{-\gamma t} \sigma_+ \rho(0) \sigma_-, \quad (12)$$

where $A = -iH(t) - \frac{1}{2}\gamma\sigma_-\sigma_+$. It is easy to check that as $\gamma \rightarrow \infty$ the state $|1\rangle \langle 1|$ is the solution of the above equation, in which case Alice wins.

3.2 Phase damping

Now, we consider the impact of the phase damping decoherence on the outcome of the game. In this case, the Lindblad operator is given by σ_z . Hence, the Lindblad equation has the following form

$$\begin{aligned} \frac{d\rho}{dt} &= -i[H, \rho(t)] + \gamma(\sigma_z \rho(t) \sigma_z - \frac{1}{2} \sigma_z \sigma_z \rho(t) - \frac{1}{2} \rho(t) \sigma_z \sigma_z) \\ &= -i[H, \rho(t)] + \gamma(\sigma_z \rho(t) \sigma_z - \rho(t)). \end{aligned} \quad (13)$$

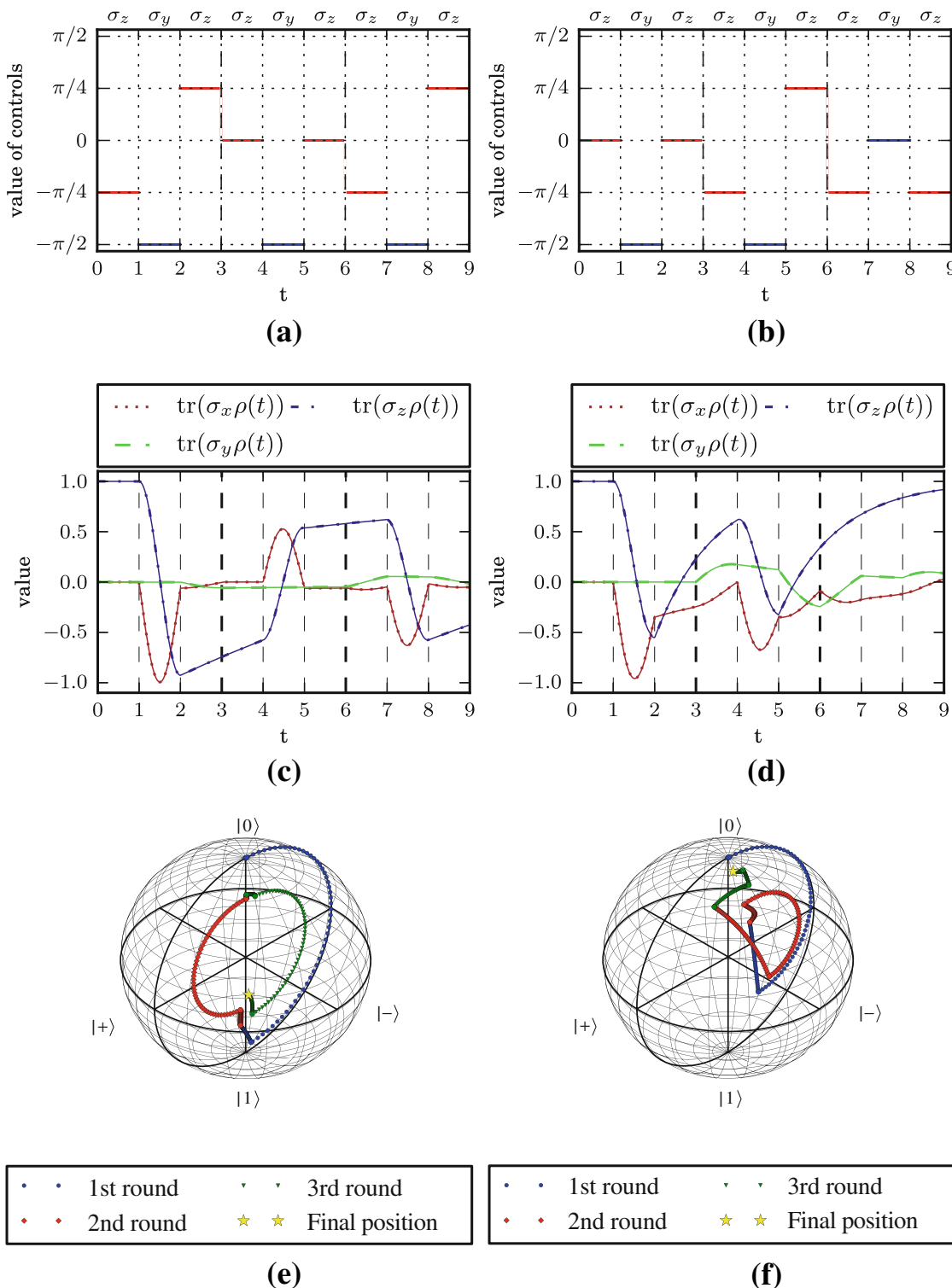


Fig. 1 Example of the time evolution of a quantum system with the amplitude damping decoherence for a sequence of control parameters α and fixed $\gamma = 0.1$ (left side), $\gamma = 0.7$ (right side). **a** Control parameters $\alpha = (-\frac{\pi}{4}, -\frac{\pi}{2}, \frac{\pi}{4}, 0, -\frac{\pi}{2}, 0, -\frac{\pi}{4}, -\frac{\pi}{2}, \frac{\pi}{4})$. **b** Control parameters $\alpha = (0, -\frac{\pi}{2}, 0, -\frac{\pi}{4}, -\frac{\pi}{2}, \frac{\pi}{4}, -\frac{\pi}{4}, 0, -\frac{\pi}{4})$. **c** Mean values of σ_x , σ_y and σ_z . **d** Mean values of σ_x , σ_y and σ_z . **e** Time evolution of a quantum coin. **f** Time evolution of a quantum coin

Next, we make a change of variables $\hat{\rho}(t) = e^{iHt}\rho(t)e^{-iHt}$, which is helpful to solve the equation. We obtain

$$\begin{aligned} \frac{d\hat{\rho}}{dt} &= \frac{de^{iHt}}{dt}\rho(t)e^{-iHt} + e^{iHt}\frac{d\rho}{dt}e^{-iHt} + e^{iHt}\rho(t)\frac{de^{-iHt}}{dt} \\ &= iHe^{iHt}e^{-iHt}\hat{\rho}(t)e^{iHt}e^{-iHt} - ie^{iHt}He^{-iHt}\hat{\rho}(t)e^{iHt}e^{-iHt} \\ &\quad + ie^{iHt}e^{-iHt}\hat{\rho}(t)e^{iHt}He^{-iHt} + \gamma e^{iHt}\sigma_z e^{-iHt}\hat{\rho}(t)e^{iHt}\sigma_z e^{-iHt} \\ &\quad - e^{iHt}e^{-iHt}\hat{\rho}e^{iHt}e^{-iHt} - ie^{iHt}e^{-iHt}\hat{\rho}e^{iHt}e^{-iHt}H \\ &= \gamma(\sigma_z\rho(t)\sigma_z - \rho(t)). \end{aligned} \quad (14)$$

It follows that the solution of the above equation is given by

$$\begin{aligned} \hat{\rho}(t) &= |0\rangle\langle 0|\rho(0)|0\rangle\langle 0| + |1\rangle\langle 1|\rho(0)|1\rangle\langle 1| + \\ &\quad + e^{-2\gamma t}(|0\rangle\langle 0|\rho(0)|1\rangle\langle 1| + |1\rangle\langle 1|\rho(0)|0\rangle\langle 0|). \end{aligned} \quad (15)$$

Coming back to the original variables we get the expression

$$\begin{aligned} \rho(t) &= |0\rangle\langle 0|\rho(0)|0\rangle\langle 0| + |1\rangle\langle 1|\rho(0)|1\rangle\langle 1| + \\ &\quad + e^{-2\gamma t}e^{-iHt}(|0\rangle\langle 0|\rho(0)|1\rangle\langle 1| + |1\rangle\langle 1|\rho(0)|0\rangle\langle 0|)e^{iHt}. \end{aligned} \quad (16)$$

Consider the following limit

$$\lim_{\gamma \rightarrow \infty} \rho(t) = |0\rangle\langle 0|\rho(0)|0\rangle\langle 0| + |1\rangle\langle 1|\rho(0)|1\rangle\langle 1|. \quad (17)$$

The above result is a diagonal matrix dependent on the initial state. For high values of γ , the initial state $\rho(0)$ has a significant impact on the game. If $\rho(0) = |0\rangle\langle 0|$ then $\lim_{\gamma \rightarrow \infty} \rho(t) = |0\rangle\langle 0|$. This kind of decoherence is conducive to Bob. Similarly, if $\rho(0) = |1\rangle\langle 1|$, then Alice wins. The evolution of a quantum system with the phase damping decoherence and fixed Hamiltonian is shown in Fig. 2. Figures 2a,b show the player's control pulses. In this case they are the ones implementing the Pauli strategy. Figure 2c,d show the time evolution of the state expressed as the expectation values of the observables σ_x , σ_y and σ_z for both cases. Finally, Fig. 2e,f show the evolution of the qubit's state in the Bloch sphere. In this case, we can see that a low amount of phase damping noise does not have a significant impact on the outcome of the game. On the other hand, for higher values of γ we can see mainly the effect of the decoherence rather than the effect of player's actions, *i.e.*, the state evolves almost directly toward the maximally mixed state.

4 Optimal strategy for the players

Due to the noisy evolution of the underlying qubit, the strategy given by Table 2 is no longer a Nash equilibrium. We study the possibility of optimizing one player's strategy, while the other one uses the Pauli strategy. It turns out that this optimization

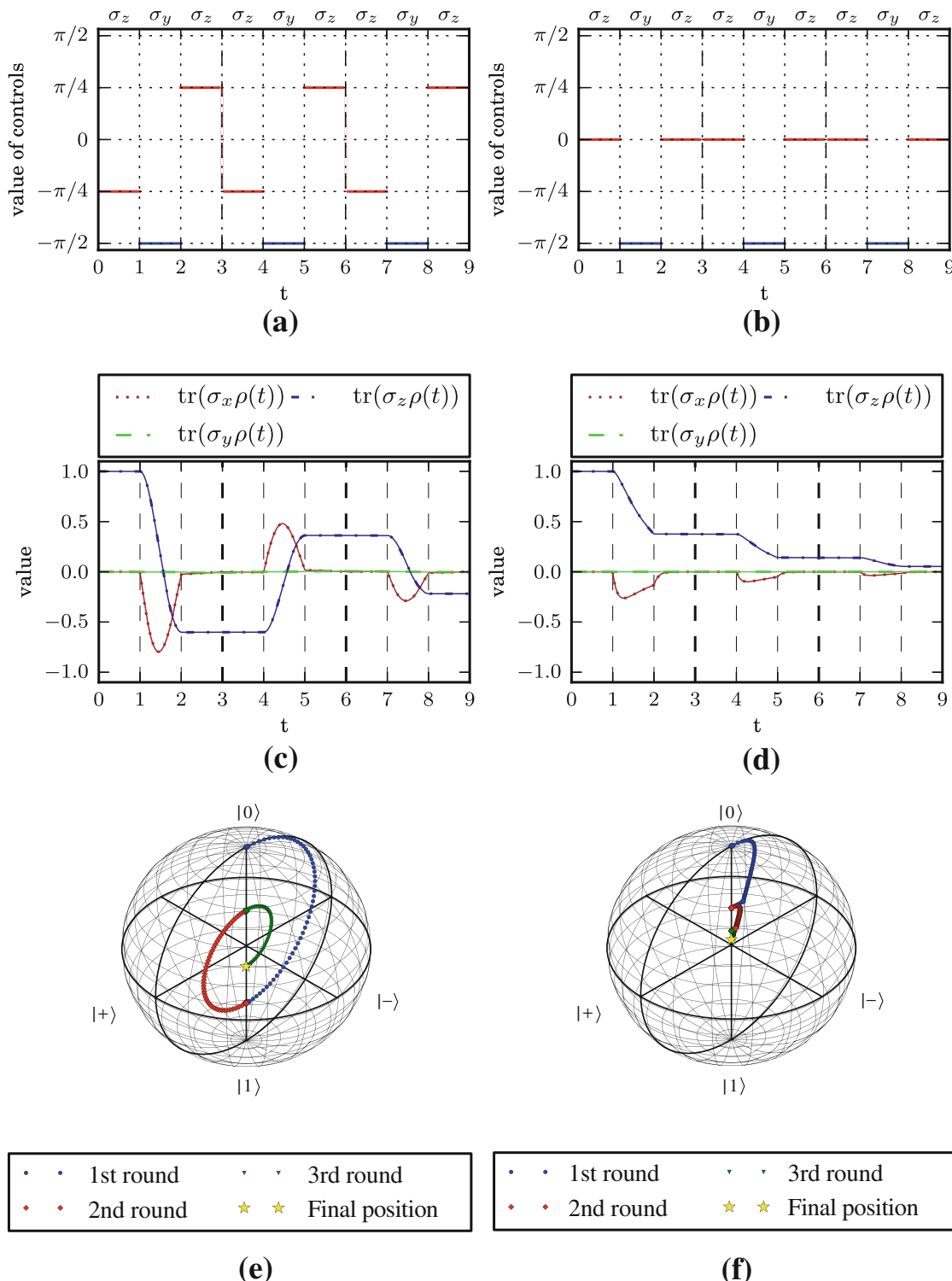


Fig. 2 Example of the time evolution of a quantum system with the phase damping decoherence for fixed $\gamma = 0.5$ (left side), $\gamma = 5$ (right side) and a sequence of control parameters α . **a** Control parameters $\alpha = (-\frac{\pi}{4}, -\frac{\pi}{2}, \frac{\pi}{4}, -\frac{\pi}{4}, -\frac{\pi}{2}, \frac{\pi}{4}, -\frac{\pi}{4}, -\frac{\pi}{2}, \frac{\pi}{4})$. **b** Control parameters $\alpha = (0, -\frac{\pi}{2}, 0, 0, -\frac{\pi}{2}, 0, 0, -\frac{\pi}{2}, 0)$. **c** Mean values of σ_x , σ_y and σ_z . **d** Mean values of σ_x , σ_y and σ_z . **e** Time evolution of a quantum coin. **f** Time evolution of a quantum coin

is not always possible. If the rate of decoherence is high enough, then the players' strategies have little impact on the game outcome. In the low noise scenario, it is possible to optimize the strategy of both players.

In each round, one player performs a series of unitary operations, which are chosen randomly from a uniform distribution. Therefore, the strategy of a player can be seen as a random unitary channel. In this section Φ_{A_1} , Φ_{A_2} denote mixed unitary channels used by Alice who implements the Pauli strategy. Similarly, Φ_B denotes channels used by Bob.

4.1 Optimization method

In order to find optimal strategies for the players, we assume the Hamiltonian in (3) to have the form

$$H = H(\varepsilon(t)), \quad (18)$$

where $\varepsilon(t)$ are the control pulses. As the optimization target, we introduce the cost functional

$$J(\varepsilon) = \text{tr}\{F_0(\rho(T))\}, \quad (19)$$

where $F_0(\rho(T))$ is a functional that is bounded from below and differentiable with respect to $\rho(T)$. A sequence of control pulses that minimizes the functional (19) is said to be *optimal*. In our case we assume that

$$\text{tr}\{F_0(\rho(T))\} = \frac{1}{2} \|\rho(T) - \rho_T\|_F^2, \quad (20)$$

where ρ_T is the target density matrix of the system.

In order to solve this optimization problem, we need to find an analytical formula for the derivative of the cost functional (19) with respect to control pulses $\varepsilon(t)$. Using the Pontryagin principle [20], it is possible to show that we need to solve the following equations to obtain the analytical formula for the derivative

$$\frac{d\rho(t)}{dt} = -i[H(\varepsilon(t)), \rho(t)] - iL_D[\rho(t)], \quad t \in [0, T], \quad (21)$$

$$\frac{d\lambda(t)}{dt} = -i[H(\varepsilon(t)), \lambda(t)] - iL_D^\dagger[\lambda(t)], \quad t \in [0, T], \quad (22)$$

$$L_D[A] = i \sum_j \gamma_j (L_j A L_j^\dagger - \frac{1}{2} \{L_j^\dagger L_j, A\}), \quad (23)$$

$$\rho(0) = \rho_s, \quad (24)$$

$$\lambda(T) = F'_0(\rho(T)), \quad (25)$$

where ρ_s denotes the initial density matrix, $\lambda(t)$ is called the adjoint state and

$$F'_0(\rho(T)) = \rho(T) - \rho_T. \quad (26)$$

The derivation of these equations can be found in [21].

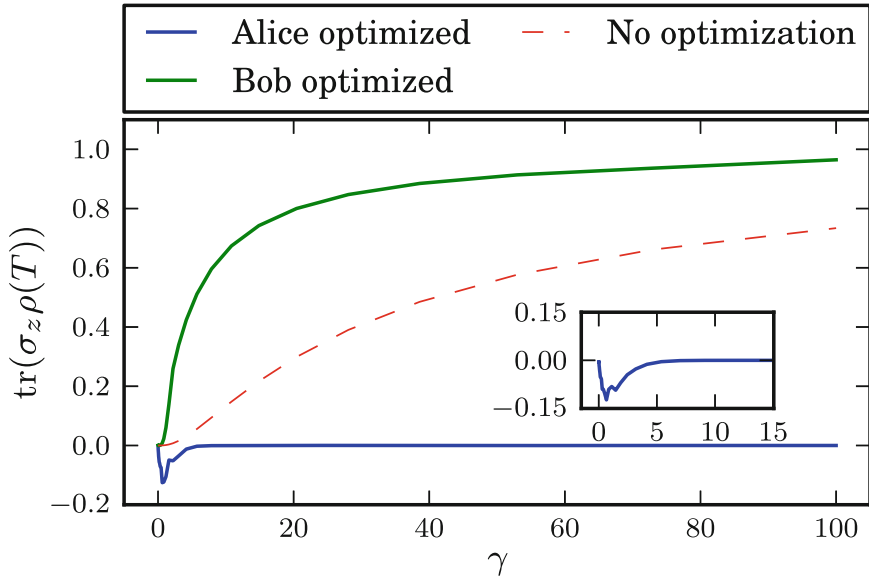


Fig. 3 Mean value of the pay-off for the phase damping channel with and without optimization of the player’s strategies. The *inset* shows the region where Alice is able to increase her probability of winning to exceed $\frac{1}{2}$

In order to optimize the control pulses using a gradient method, we convert the problem from an infinite dimensional (continuous time) to a finite dimensional (discrete time) one. For this purpose, we discretize the time interval $[0, T]$ into M equal sized subintervals Δt_k . Thus, the problem becomes that of finding $\varepsilon = [\varepsilon_1, \dots, \varepsilon_M]^T$ such that

$$J(\varepsilon) = \inf_{\zeta \in \mathbb{R}^M} J(\zeta). \quad (27)$$

The gradient of the cost functional is

$$G = \left[\frac{\partial J}{\partial \varepsilon_1}, \dots, \frac{\partial J}{\partial \varepsilon_M} \right]^T. \quad (28)$$

It can be shown [21] that elements of vector (28) are given by

$$\frac{\partial J}{\partial \varepsilon_k} = \text{tr} \left\{ -i\lambda_k \left[\frac{\partial H(\varepsilon_k)}{\partial \varepsilon_k}, \rho_k \right] \right\} \Delta t_k, \quad (29)$$

where ρ_k and λ_k are solutions of the Lindblad equation and the adjoint system corresponding to time subinterval Δt_k , respectively. To minimize the gradient given in Eq. (28) we use the BFGS algorithm [22].

4.2 Optimization setup

Our goal is to find control strategies for players, which maximize their respective chances of winning the game. We study three noise channels: the amplitude damping,

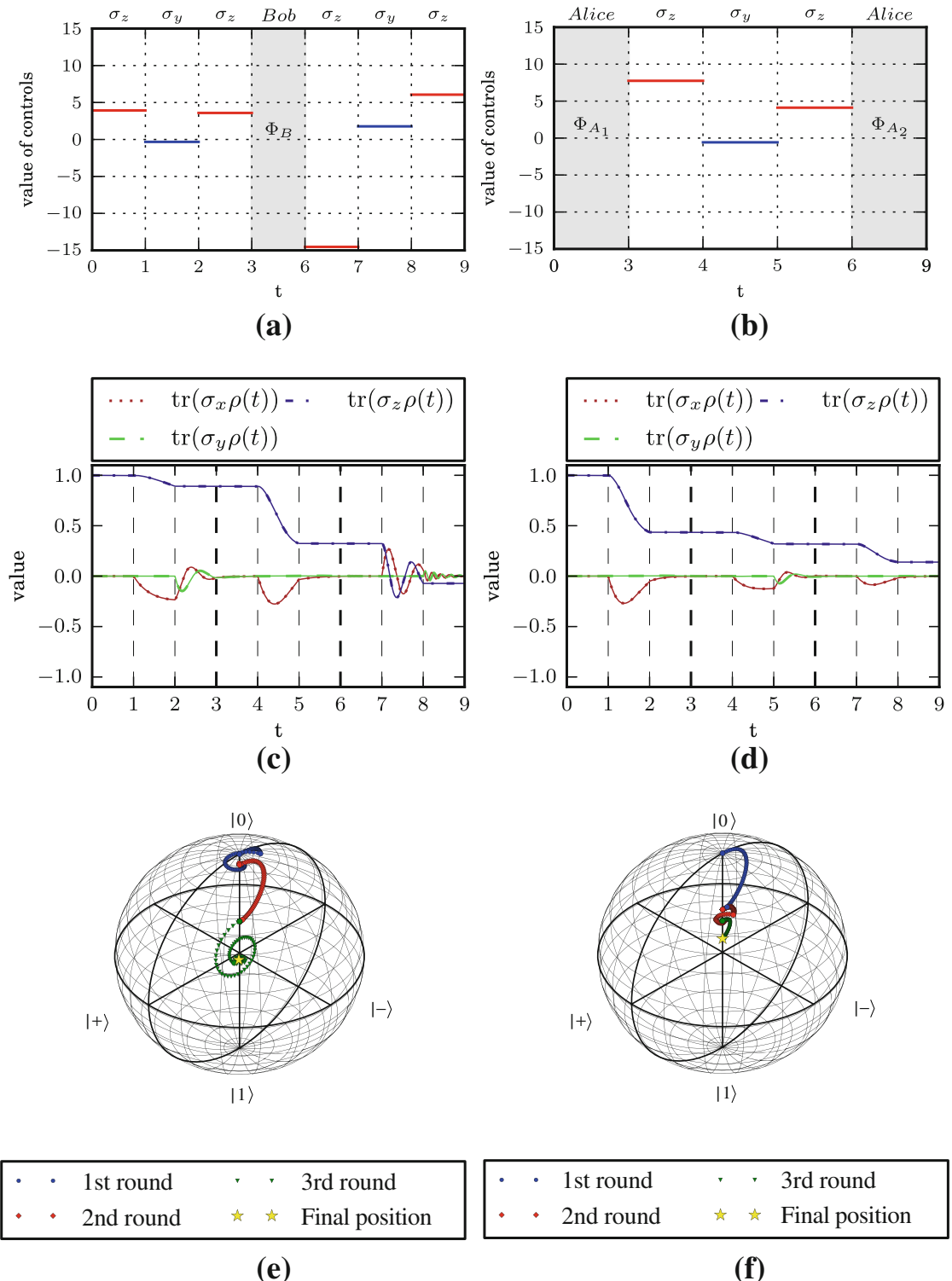


Fig. 4 Game results for the phase damping channel. Optimal Alice's strategy when $\gamma = 1.172$ (left side), and optimal Bob's strategy when $\gamma = 1.610$ (right side). **a** Optimal controls for Alice, **b** Optimal controls for Bob, **c** Mean values of σ_x , σ_y and σ_z , **d** Mean values of σ_x , σ_y and σ_z , **e** Time evolution of a quantum coin, **f** Time evolution of a quantum coin

the phase damping and the amplitude raising channel. They are given by the Lindblad operators σ_- , σ_z and $\sigma_+ = \sigma_-^\dagger$, respectively. In all cases, we assume that one of the players uses the Pauli strategy, while for the other player we try to optimize a control

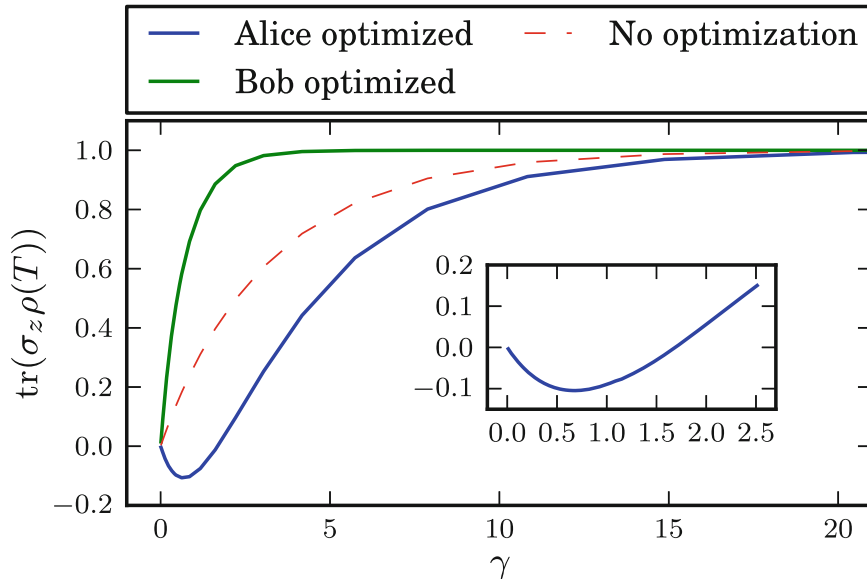


Fig. 5 Mean value of the pay-off for the amplitude damping channel with and without optimization of the player’s strategies. The *inset* shows the region where Alice is able to increase her probability of winning to exceed $\frac{1}{2}$

strategy that maximizes that player’s probability of winning. However, in our setup it is convenient to use the value of the observable σ_z rather than probabilities. Value 0 means that each player has a probability of $\frac{1}{2}$ of winning the game. Values closer to 1 mean higher probability of winning for Bob, while values closer to -1 mean higher probability of winning for Alice.

4.3 Optimization results

4.3.1 Phase damping

The results for the phase damping channel are shown in Fig. 3. As it can be seen, in this case, both players are able to optimize their strategies, and so Alice can optimize her strategy for low values of γ to obtain the probability of winning greater than $\frac{1}{2}$. The region where this occurs is shown in the inset. For high noise values, she is able to achieve the probability of winning equal to $\frac{1}{2}$. In the case of high values of γ , the best strategy for Alice is to drive the state as close as possible to the maximally mixed state on her first move. This state can not be changed neither by Bob’s actions, nor by the phase damping channel. On the other hand, optimization of Bob’s strategy shows that he is able to achieve high probabilities of winning for relatively low values of γ . This is consistent with the limit shown in Eq. (17) as our initial state is $\rho = |0\rangle\langle 0|$. Figure 4 presents optimal game strategies for both players. For Alice we chose $\gamma = 1.172$ which corresponds to her maximal probability of winning the game. In the case of Bob’s strategies we arbitrarily choose the value $\gamma = 1.610$. In these cases the evolution of the qubit is much more complex. This is due to the fact that the players are not restricted to the Pauli strategy.

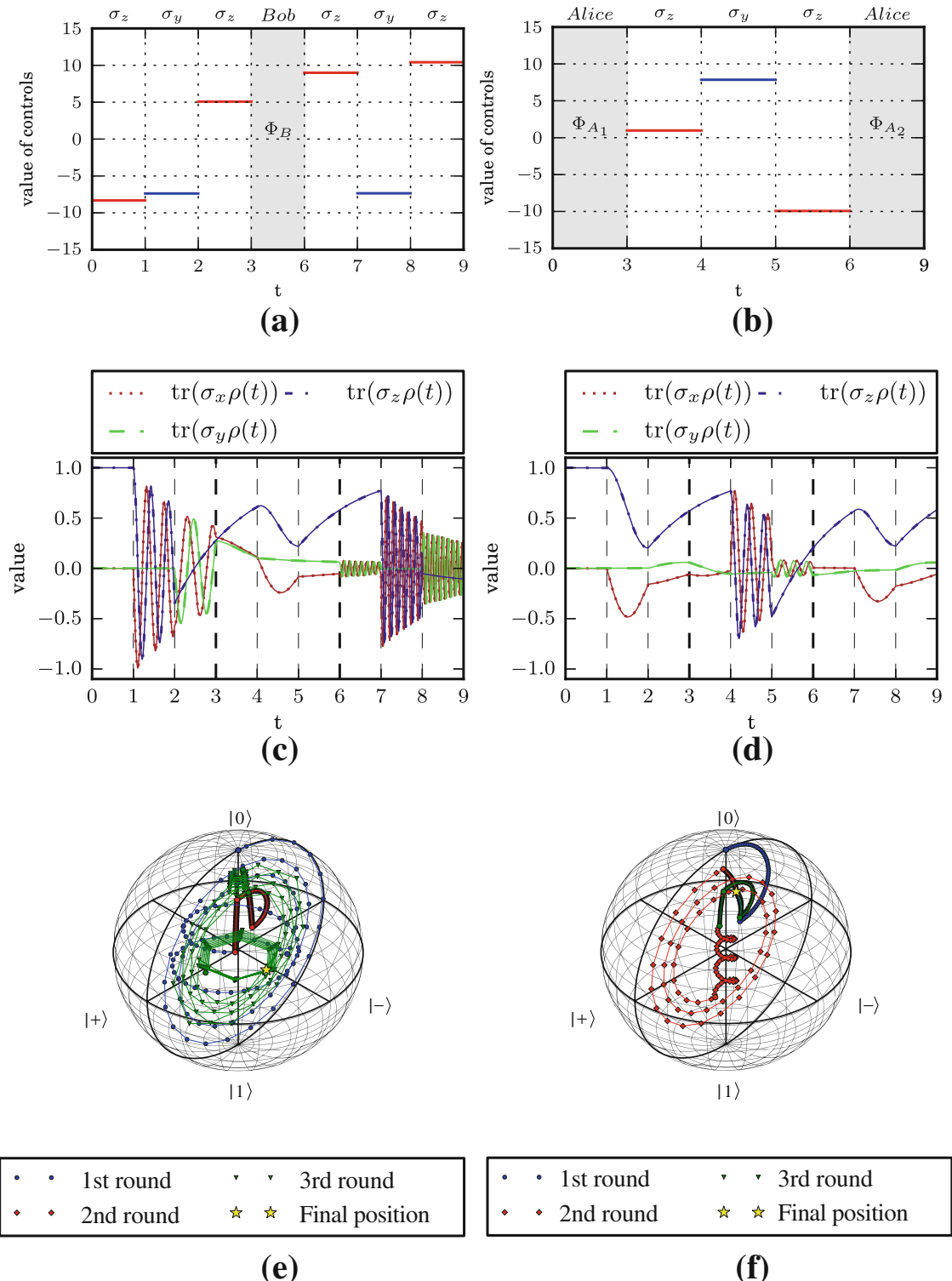


Fig. 6 Game results obtained for the amplitude damping channel with γ equal to 0.621. Optimal Alice's strategy (*left side*), and optimal Bob's strategy (*right side*). **a** Optimal controls for Alice, **b** Optimal controls for Bob, **c** Mean values of σ_x , σ_y and σ_z , **d** Mean values of σ_x , σ_y and σ_z , **e** Time evolution of a quantum coin, **f** Time evolution of a quantum coin

4.3.2 Amplitude damping

Next, we present the results obtained for the amplitude damping channel. They are shown in Fig. 5. Unfortunately, for Alice, for high values of γ Bob always wins. This

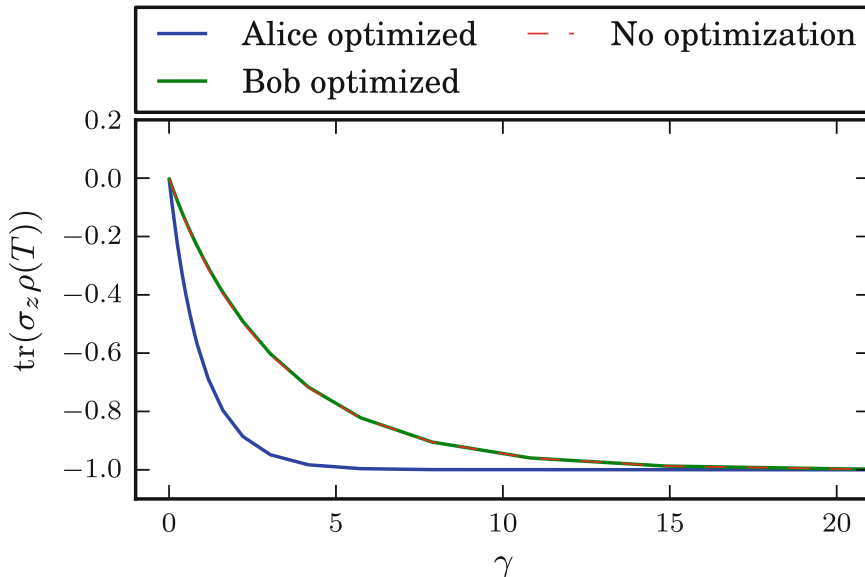


Fig. 7 Mean value of the pay-off for the amplitude raising channel with and without optimization of the player's strategies

is due to the fact that in this case the state quickly decays to state $|0\rangle\langle 0|$. Additionally, Bob is also able to optimize his strategies. He is able to achieve probability of winning equal to 1 for relatively low values of γ . However, for low values of γ , the interaction allows Alice to achieve higher than $\frac{1}{2}$ probability of winning. The region where this happens is magnified in the inset. Interestingly, for very low values of γ , Alice can increase her probability of winning. This is due to the fact that low noise values are sufficient to distort Bob's attempts to perform the Pauli strategy. On the other hand, they are not high enough to drive the system toward state $|0\rangle\langle 0|$. Optimal game results for both players are shown in Fig. 6. For both players, we chose $\gamma = 0.621$ which corresponds to Alice's maximal probability of winning the game. As can be seen, in this case, the evolutions of the observables σ_x , σ_y and σ_z show rapid oscillations. This behavior is turned on by applying control pulses associated with the σ_y Hamiltonian.

4.3.3 Amplitude raising

Finally, we present optimization results for the amplitude raising channel. The optimization results, shown in Fig. 7, indicate that Alice can achieve probability of winning equal to 1 for lower values of γ compared with the unoptimized case. In this case, Bob cannot do any better than in the unoptimized case due to a limited number of available control pulses.

5 Conclusions

We studied the quantum version of the coin flip game under decoherence. To model the interaction with external environment, we used the Markovian approximation in the form of the Lindblad equation. Because of the fact that Pauli strategy is a known Nash equilibrium of the game, therefore, it was natural to investigate this strategy in the presence of noise. Our results show that in the presence of noise, the

Pauli strategy is no longer a Nash equilibrium. One of the players, Bob in our case, is always favoured by amplitude and phase damping noise. If we had considered a game with another initial state *i.e.*, $\rho_0 = |1\rangle\langle 1|$, Alice would have been favoured in this case. Our next step was to check if the players were able to do better than the Pauli strategy. For this, we used the BFGS gradient method to optimize the players' strategies. Our results show that Alice, as well as Bob, are able to increase their respective winning probabilities. Alice can achieve this for all three studied cases, while Bob can only do this for the phase damping and amplitude damping channels.

Acknowledgments The work was supported by the Polish Ministry of Science and Higher Education Grants: P. Gawron under the project number IP2011 014071. D. Kurzyk under the project number N N514 513340. Ł. Pawela under the project number N N516 481840.

Open Access This article is distributed under the terms of the Creative Commons Attribution License which permits any use, distribution, and reproduction in any medium, provided the original author(s) and the source are credited.

References

1. Heinosaari, T., Ziman, M.: *The Mathematical Language of Quantum Theory: From Uncertainty to Entanglement*. Cambridge University Press, Cambridge (2011)
2. Nielsen, M.A., Chuang, I.L.: *Quantum Computation and Quantum Information*. Cambridge University Press, Cambridge (2000)
3. Johnson, N.F.: Playing a quantum game with a corrupted source. *Phys. Rev. A* **63**(2), 20302 (2001)
4. Flitney, A.P., Derek, A.: Quantum games with decoherence. *J. Phys. A Math. Gen.* **38**(2), 449 (2005)
5. Chen, J.-L., Kwek, L., Oh, C.: Noisy quantum game. *Phys. Rev. A* **65**(5), 052320 (2002)
6. Flitney, A.P., Hollenberg, L.C.L.: Multiplayer quantum minority game with decoherence. *Quantum Inf. Comput.* **7**(1), 111–126 (2007)
7. Gawron, P., Miszczak, J.A., Sładkowski, J.: Noise effects in quantum magic squares game. *Int. J. Quantum Inf.* **6**(1), 667–673 (2008)
8. Pawela, Ł., Gawron, P., Puchała, Z., Sładkowski, J.: Enhancing pseudo-telepathy in the magic square game. *PLoS ONE* **8**(6), e64694 (2013)
9. Gawron, P.: Noisy quantum monty hall game. *Fluct. Noise Lett.* **9**(1), 9–18 (2010)
10. Khan, S., Ramzan, M., Khan, M.K.: Quantum monty hall problem under decoherence. *Commun. Theor. Phys.* **54**(1), 47 (2010)
11. Miszczak, J.A., Gawron, P., Puchała, Z.: Qubit flip game on a Heisenberg spin chain. *Quantum Inf. Process.* **11**(6), 1571–1583 (2012)
12. Pakuła, I.: Analysis of trembling hand perfect equilibria in quantum games. *Fluct. Noise Lett.* **8**(01), 23–30 (2008)
13. Nawaz, A.: Prisoners' dilemma in the presence of collective dephasing. *J. Phys. A Math. Theor.* **45**(19), 195304 (2012)
14. Salman, K., Khan, M.K.: Relativistic quantum games in noninertial frames. *J. Phys. A Math. Theor.* **44**(35), 355302 (2011)
15. Goudarzi, H., Beyrami, S.: Effect of uniform acceleration on multiplayer quantum game. *J. Phys. A Math. Theor.* **45**(22), 225301 (2012)
16. Salman, K., Khan, M.K.: Noisy relativistic quantum games in noninertial frames. *Quantum Inf. Process.* **12**(2), 1351–1363 (2013)
17. Piotrowski, E.W., Sładkowski, J.: An invitation to quantum game theory. *Int. J. Theor. Phys.* **42**(5), 1089–1099 (2003)
18. Meyer, D.A.: Quantum strategies. *Phys. Rev. Lett.* **82**(5), 1052 (1999)
19. d'Alessandro, D.: *Introduction to Quantum Control and Dynamics*. CRC press, Boca Raton (2007)
20. Pontryagin, L.S., Boltyanskii, V.G., Gamkrelidze, R.V., Mishchenko, E.: *The Mathematical Theory of Optimal Processes*. Interscience Publishers, New York (1962)

21. Jirari, H., Pötz, W.: Optimal coherent control of dissipative N -level systems. Phys. Rev. A **72**(1), 013409 (2005)
22. Press, W.H., Flannery, B.P., Teukolsky, S.A., Vetterling, W.T.: Numerical Recipes in FORTRAN 77, volume 1 of Fortran Numerical Recipes: The Art of Scientific Computing. Cambridge University Press, Cambridge (1992)

Chapter 3

Various methods of optimizing
control pulses for quantum
systems with decoherence

Various methods of optimizing control pulses for quantum systems with decoherence

Lukasz Pawela¹ · Przemysław Sadowski¹

Received: 22 July 2014 / Accepted: 5 January 2016 / Published online: 25 January 2016
© The Author(s) 2016. This article is published with open access at Springerlink.com

Abstract We design control setting that allows the implementation of an approximation of an unitary operation of a quantum system under decoherence using various quantum system layouts and numerical algorithms. We focus our attention on the possibility of adding ancillary qubits which help to achieve a desired quantum map on the initial system. Furthermore, we use three methods of optimizing the control pulses: genetic optimization, approximate evolution method and approximate gradient method. To model the noise in the system we use the Lindblad equation. We obtain results showing that applying the control pulses to the ancilla allows one to successfully implement unitary operation on a target system in the presence of noise, which is not possible which control field applied to the system qubits.

Keywords Quantum information · Quantum computation · Control in mathematical physics

1 Introduction

One of the fundamental issues of quantum information science is the ability to manipulate the dynamics of a given complex quantum system. Since the beginning of quantum mechanics, controlling a quantum system has been an implicit goal of quantum physics, chemistry and implementations of quantum information processing [1].

✉ Przemysław Sadowski
psadowski@iitis.pl

Łukasz Pawela
lpawela@iitis.pl

¹ Institute of Theoretical and Applied Informatics, Polish Academy of Sciences, Baltycka 5,
44-100 Gliwice, Poland

If a given quantum system is controllable, i.e. it is possible to drive it into a previously fixed state, it is desirable to develop a control strategy to accomplish the desired control task. In the case of finite dimensional quantum systems, the criteria for controllability can be expressed in terms of Lie-algebraic concepts [2–4]. These concepts provide a mathematical tool, in the case of closed quantum systems, i.e. systems without external influences.

A widely used method for manipulating a quantum system is a coherent control strategy, where the manipulation of the quantum states is achieved by applying semi-classical potentials in a fashion that preserves quantum coherence. In the case when a system is controllable, it is a point of interest what actions must be performed to control a system most efficiently, bearing in mind limitations imposed by practical restrictions [5–9]. The always present noise in the quantum system may be considered such a constraint [10–17]. Therefore it is necessary to study methods of obtaining piecewise constant control pulses which implement the desired quantum operation on a noisy system.

It is an important question whether the system is controllable with a control applied only on a subsystem. This kind of approach is called a *local-controllability* and can be considered only in the case when the subsystems of a given system interact. Coupled spin chains or spin networks [4, 18–20] may serve as examples. Local control has a practical importance in proposed quantum computer architectures, as its implementation is simpler and the effect of decoherence is reduced by decreased number of control actuators [21, 22].

In this paper we study various methods of adding ancillary qubits to a given quantum system, in order to overcome the interaction with an external environment. This means, we wish to perform a time evolution on a greater system than the target one and discard the ancilla afterward. This scheme should implement a unitary transformation on the target subsystem.

2 Model of the quantum system

We test our approach on a toy model and implement the unitary operations $U_{\text{NOT}} = \sigma_x \otimes \mathbb{1}$ and $U_{\text{SWAP}} = \mathbb{1} \otimes \sum_{ij} |i\rangle\langle j| \otimes |j\rangle\langle i|$ on a quantum system modeled as a an isotropic Heisenberg spin-1/2 chain of a finite length N . We will study two- and three-qubit systems. The total Hamiltonian of the aforementioned quantum control system is given by

$$H(t) = H_0 + H_c(t), \quad (1)$$

where

$$H_0 = J \sum_{i=1}^{N-1} S_x^i S_x^{i+1} + S_y^i S_y^{i+1} + S_z^i S_z^{i+1} \quad (2)$$

is a drift part given by the Heisenberg Hamiltonian. The control is performed only on the i th spin and is Zeeman-like, i.e.

$$H_c(t) = h_x(t)S_x^i + h_y(t)S_y^i. \quad (3)$$

In the above S_k^i denotes k^{th} Pauli matrix acting on the spin i . Time-dependent control parameters $h_x(t)$ and $h_y(t)$ are chosen to be piecewise constant. For notational convenience, we set $\hbar = 1$ and after this rescaling frequencies and control-field amplitudes can be expressed in units of the coupling strength J , and on the other hand all times can be expressed in units of $1/J$ [23].

We model the noisy quantum system dynamics using the Markovian approximation with the master equation in the Kossakowski–Lindblad form

$$\frac{d\rho}{dt} = -i[H(t), \rho] + \sum_j \gamma_j \left(L_j \rho L_j^\dagger - \frac{1}{2} \{L_j^\dagger L_j, \rho\} \right), \quad (4)$$

where L_j are the *Lindblad* operators, representing the environment influence on the system [24] and ρ is the state of the system.

The main goal of this paper is to compare various methods for optimizing control pulses $h_x(t)$, $h_y(t)$ for the model introduced above. As we are working within the Markovian approximation of the quantum system, we need to assume the environment is fast. Strictly speaking, this means that the environment autocorrelation functions are δ -functions in time. Another way to view this approximation is that the environment has no memory.

It is a widely known fact, that coherent control in the form of pulses on the system's qubits cannot overcome decoherence. This is intuitively true, because such control results in an unitary evolution of the system and this cannot fight the non-unitary dynamics. However, if we apply the control pulses to an ancilla, we are effectively creating an additional environment and as a result produce non-unitary evolution which can be viewed as a damping on the system. This evolution smooths the effect of the piecewise constant control pulses and in turn validates the singular coupling limit on the noisy environment.

In order to show that the singular coupling limit [25, 26] is valid in the case of piecewise constant control, we calculate the derivative of the reduced state and show that it is continuous. We consider the state $\rho_S = \text{Tr}_A(\rho)$ after tracing out the ancilla

$$\begin{aligned} \frac{d\rho_S}{dt} &= \text{Tr}_A \left(-i[H(t), \rho] + \sum_j \gamma_j (L_j \rho L_j^\dagger - \frac{1}{2} \{L_j^\dagger L_j, \rho\}) \right) \\ &= \text{Tr}_A \left(-i[H_0, \rho] + \sum_j \gamma_j (L_j \rho L_j^\dagger - \frac{1}{2} \{L_j^\dagger L_j, \rho\}) \right) + \text{Tr}_A(-i[H_c(t), \rho]). \end{aligned} \quad (5)$$

Here the index A denotes the ancilla and index S denotes the system on which we have the target operation. The part corresponding to the drift Hamiltonian and environment influence is time independent. Because the control Hamiltonian is a combination of unitary operators and acts non-trivially on the ancilla only, the time-dependent term vanishes after tracing out the ancilla,

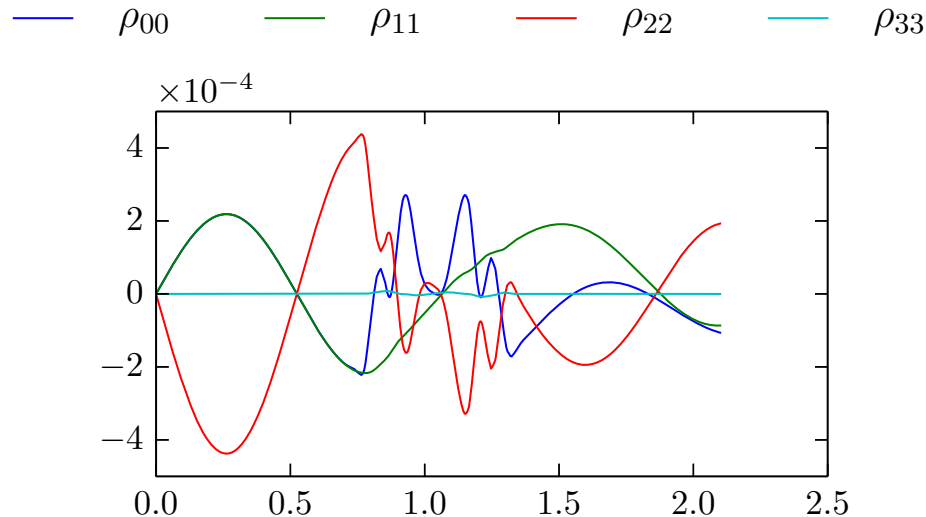


Fig. 1 An example of the derivatives of the diagonal elements of the system with the ancilla traced out

$$\begin{aligned}
 \text{Tr}_A(-i[H_c(t), \rho]) &= -i \sum_{k \in \{x, y\}} h_k(t) \text{Tr}_A([S_k^A, \rho]) \\
 &= -i \sum_{k \in \{x, y\}} h_k(t) \left(\sum_i (\langle i |_A \otimes \mathbb{1}_S) (S_k^A \otimes \mathbb{1}_S) \rho (|i\rangle_A \otimes \mathbb{1}_S) \right. \\
 &\quad \left. - \sum_i (\langle i |_A S_k^A \otimes \mathbb{1}_S) \rho (S_k^A \otimes \mathbb{1}_S) (S_k^{A\dagger} |i\rangle_A \otimes \mathbb{1}_S) \right) = 0, \quad (6)
 \end{aligned}$$

where the second equation results from the fact that the partial trace result is the same for any basis selection. Thus, provided that control is applied on the ancilla register only, evolution of the rest of the system is smooth, even in the case of non-continuous control pulse functions.

We show the derivatives of the diagonal elements of an example density matrix of the state of the system with the ancilla traced out. The derivatives for are shown in Fig. 1. They are obtained for the system (c) shown in Fig. 2. The damping parameter is $\gamma = 0.01$. This is an illustration of the result given in Eq. (5) showing that the derivative of the reduced system is continuous, despite the control pulses on the ancilla being piecewise constant.

In the next section we present three methods for the purpose of the comparison. The comparison of the control pulses obtained by different methods is done by applying these pulses into the above model and analysis of the obtained results.

3 Various approaches to fidelity maximization

In this Section, we describe three methods we used to optimize control pulses. The first method is based on an approximate method for obtaining a mapping which is close to a unitary one. In order to obtain the approximation, we expand the superoperator into the Taylor series up to a linear term. After this we calculate the exact gradient of the fidelity function with respect to the control pulses. The second one uses an exact formula for

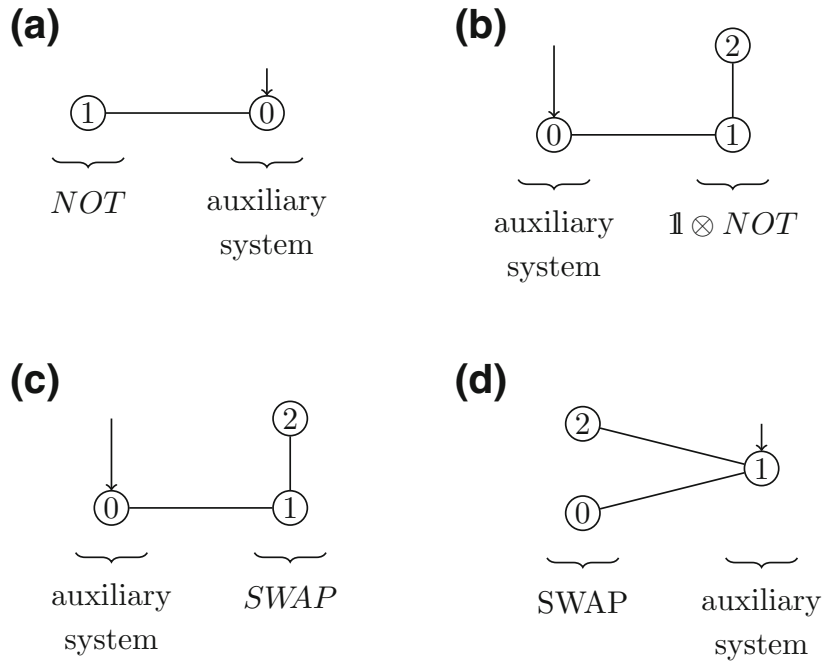


Fig. 2 Systems used for numerical simulation

the time evolution of the system, but we approximate the derivative of the mapping with respect to control pulses. In our numerical research, we perform optimization with use of the L-BFGS-B optimization algorithm [27]. Its main advantages lies in harnessing the approximation of Hessian of fitness function (we refer to the section 3 of [28] for details). Finally, we use genetic programming to optimize control pulses without the need for computing gradient of the fidelity function.

3.1 Approximate mapping method

Assuming piecewise constant control pulses the Hamiltonian in Eq. (4) becomes independent of time during the duration of the pulse. This allows us to simplify the master equation.

For notational convenience, let us write the decoherence part of the Eq. (4) in the following form [29] that allows us to act in the vectorized states space

$$-\mathcal{G} = \sum_j \gamma_j \left(L_j \otimes \overline{L_j} - \frac{1}{2} \left[\left(L_j^\dagger L_j \right) \otimes \mathbb{1} + \mathbb{1} \otimes \left(L_j^\dagger L_j \right) \right] \right), \quad (7)$$

where \overline{L}_j denotes the conjugate of L_j . The first term in Eq. 4 can be transformed into

$$-i\mathcal{H} = -i(\mathbb{1} \otimes \overline{H} - H \otimes \mathbb{1}). \quad (8)$$

These observations allow us to write a mapping representing the evolution of a system in an initial state ρ under Eq. (4) for time t as

$$\mathcal{S} = \exp(-t\mathcal{F}), \quad (9)$$

where $-\mathcal{F} = -\mathcal{G} - i\mathcal{H}$. The final state of the evolution is

$$\text{res}(\rho_f) = \mathcal{S}\text{res}(\rho), \quad (10)$$

where $\text{res}(\cdot)$ is a linear mapping defined for dyadic operators as

$$\text{res}(|\phi\rangle\langle\psi|) = |\phi\rangle\overline{|\psi\rangle}. \quad (11)$$

The extension to all other operators follows from linearity.

We can approximate the superoperator A as

$$\begin{aligned} \mathcal{S} &= \exp \left[-\frac{1}{2}t \sum_j (L_j^\dagger L_j) \otimes \mathbb{1} + \mathbb{1} \otimes (L_j^\dagger L_j) \right] \\ &\quad \times \exp \left(t \sum_j L_j \otimes \overline{L_j} \right) \times \exp(-ti\mathcal{H}) + O(t^2) \\ &= \mathcal{A}(t)\mathcal{B}(t)\mathcal{C}(t) + O(t^2). \end{aligned} \quad (12)$$

Note that, only the $\mathcal{C}(t)$ term depends on the control pulses. Assuming piecewise constant control pulses, total evolution time T and setting n as the total number of pulses, we can write the resulting approximate superoperator as

$$\tilde{\mathcal{S}} = \prod_{k=1}^n \mathcal{A}(\Delta t_k)\mathcal{B}(\Delta t_k)\mathcal{C}(\Delta t_k), \quad (13)$$

where Δt_k is the length of the k th time interval. As we assume all the control pulses are of the same length, we will write t_k instead of Δt_k .

The derivative of the superoperator with respect to a control pulse $h_j(t_l)$ is

$$\begin{aligned} \frac{\partial \tilde{\mathcal{S}}}{\partial h_j(t_l)} &= \left(\prod_{k=1}^{l-1} \mathcal{A}(t_k)\mathcal{B}(t_k)\mathcal{C}(t_k) \right) \times \left(\mathcal{A}(t_l)\mathcal{B}(t_l) \frac{\partial \mathcal{C}(t_l)}{\partial h_j(t_l)} \right) \\ &\quad \times \left(\prod_{k=l+1}^n \mathcal{A}(t_k)\mathcal{B}(t_k)\mathcal{C}(t_k) \right). \end{aligned} \quad (14)$$

We use the fidelity as the figure of merit

$$F = \frac{1}{2^{2N}} \Re(\text{Tr} \mathcal{S}_{\text{target}}^\dagger \tilde{\mathcal{S}}), \quad (15)$$

where N is the number of qubits in the system and $\mathcal{S}_{\text{target}}$ is the target superoperator. The derivative of the fidelity with respect to the control pulse in the j th direction and in the l th time interval is given by:

$$\frac{\partial F}{\partial h_j(t_l)} = \frac{1}{2^{2N}} \Re \left(\text{Tr} \left(\mathcal{S}_{\text{target}} \frac{\partial \tilde{\mathcal{S}}}{\partial h_j(t_l)} \right) \right). \quad (16)$$

3.2 Approximate gradient method

In this section we follow the results by Machnes et al. [30]. In order to introduce the approximate gradient method, we introduce the following notation

$$\hat{H}(\cdot) = [H(t), \cdot], \quad \hat{H}_i(\cdot) = [H_0 + H_i(t), \cdot], \quad \hat{L}(\cdot) = \sum_j \gamma_j (L_j \cdot L_j^\dagger - \frac{1}{2} \{L_j^\dagger L_j, \cdot\}). \quad (17)$$

This allows us to write Eq. (4) in the form

$$\frac{\partial \rho(t)}{\partial t} = -(\mathrm{i}\hat{H} + \hat{L})(\rho(t)). \quad (18)$$

The evolution of a quantum map X under this equation is given by

$$\frac{\partial X(t)}{\partial t} = -(\mathrm{i}\hat{H} + \hat{L})X(t). \quad (19)$$

In order to perform numerical simulations, Eq. (19) needs to be discretized. Given a total evolution time T , we divide it into n small intervals, each of length $\Delta t = T/n$. Hence, the quantum map in the k th time interval is given by

$$X_k = \exp \left[-\Delta t (\mathrm{i}\hat{H}(t_k) + \hat{L}(t_k)) \right]. \quad (20)$$

We utilize the trace fidelity as the figure of merit for this optimization problem

$$F = \frac{1}{2^{2N}} \Re \text{Tr} \left[X_{\text{target}}^\dagger X(T) \right] = \frac{1}{2^{2N}} \Re \text{Tr} \left[\Lambda^\dagger(t_k) X_k X(t_{k-1}) \right], \quad (21)$$

where operators $X(t_{k-1}) = X_{k-1} X_{k-2} \dots X_1 X_0$ and $\Lambda^\dagger(t_k) = X^\dagger X_n X_{n-1} \dots X_{k+2} X_{k+1}$ are introduced in order to split the time evolution at any given time k and highlight the term only depending on $h_j(t_k)$, $j \in \{x, y\}$. This allows us to write the derivative of the figure of merit with respect to the control pulses as

$$\frac{\partial F}{\partial h_j(t_k)} = \frac{1}{2^{2N}} \Re \text{Tr} \left[\Lambda^\dagger(t_k) \left(\frac{\partial X_k}{\partial h_j(t_k)} \right) X(t_{k-1}) \right]. \quad (22)$$

Since \hat{L} and $\mathrm{i}\hat{H}$ need not commute, we cannot calculate the derivative $\frac{\partial X_k}{\partial h_j(t_k)}$ using exact methods. The best approach is to use the following approximation for the gradient (see [30], section III.B)

$$\frac{\partial X_k}{\partial h_j(t_k)} \approx -\Delta t \left(i\hat{H}_i + \frac{\partial \hat{L}(h_j(t_k))}{\partial h_j(t_k)} \right) X_k. \quad (23)$$

In our test cases, the damping does not depend on the control pulses; hence, we may rewrite Eq. (23) as:

$$\frac{\partial X_k}{\partial h_j(t_k)} \approx -i\Delta t \hat{H}_i X_k. \quad (24)$$

This approximation is valid provided that

$$\Delta t \ll \frac{1}{||i\hat{H} + \hat{L}||_2}. \quad (25)$$

3.3 Genetic programming

Genetic programming (GP) is a numerical method based on the evolutionary mechanisms [31, 32]. There are two main reasons for using GP for finding optimal control pulses. First of all it enables us to perform numerical optimization in the case of a complicated fitness function. On the other hand, one should note that the values of control pulses in different time intervals can be set independently. Thus the idea of genetic code fits well as a model for a control setting. Thanks to such a representation, genetic programming enables us to exchange values of control pulses in some fixed intervals between control settings that result in most accurate approximation of the desired evolution.

Genetic programming belongs to the family of search heuristics inspired by the mechanism of natural evolution. Each element of a search space being candidate for a solution is identified with a representative of a population. Every member of a population has its unique genetic code, which is its representation in optimization algorithm. In most of the cases, genetic code is a sequence of values from a fixed set Σ of possible values of all the features that characterize a potential solution $x \in \Sigma^n$ in the search space. Searching for the optimal solution is done by the systematic modification and evaluation of genetic codes of population members due to the rules of the evolution such as mutation, selection, crossing-over and inheritance.

Mutators are functions that change single elements of a genetic code randomly. A basic example of a mutator is a function that randomly changes values of a representative x at all positions with some non-zero probability

$$M(x)_i = \begin{cases} x_i, & \text{probability } p, \\ \text{rand}(\Sigma), & \text{probability } 1 - p. \end{cases} \quad (26)$$

Crossovers implement the mechanism of inheritance. This function divides given parental genetic code and creates a new genetic code. Commonly two new codes are created at the same time from two parental codes. An example of such crossover is so-called two point cut, where both parental codes (x_i, y_i) are cut into three regions and the middle segments are interchanged

$$x'_i = \begin{cases} x_i, & i \leq c_1 \vee c_2 \leq i, \\ y_i, & c_1 < i < c_2, \end{cases} \quad y'_i = \begin{cases} x_i, & c_1 < i < c_2, \\ y_i, & i \leq c_1 \vee c_2 \leq i, \end{cases} \quad (27)$$

where $c_1 < c_2$ are randomly chosen indices. In every iteration of the algorithm, all members of the population are evaluated using fitness function $f : \Sigma^n \rightarrow \mathfrak{N}$ which enables elements ordering. Then, using a selector function, the set of the best members is obtained and used to create a new generation of the population using mutation and crossover functions. There is a number of strategies for defining selector function—from completely random choices to the deterministic choice of best representatives.

Strategy based on evolution mechanism makes genetic programming especially useful when parts of genetic code represent features of elements of a search space that can be interchanged between elements independently. In such case GA is expected to find the features that occur in well-fitted representatives and mix them in order to find the best possible combination. Pseudocode representing this approach is presented in Listing 1.

```

population = RandomPopulation()
for( generationsNumber ) {
    newPopulation = []
    for(i = 0; i<population.size()/2; i++) {
        mom = Selector(population)
        dad = Selector(population)
        (sister, brother) = CrossOver(mom, dad)
        Mutator(sister)
        Mutator(brother)
        newPopulation.append(sister)
        newPopulation.append(brother)
    }
    population = newPopulation
}

```

Listing 1: Pseudocode representing the algorithm of genetic programming. Functions `Selector`, `Mutator` and `CrossOver` work as defined in Sect. 3.3.

While the customization of population representation and fitness function unavoidably relies on the optimization problem, other parameters of genetic programming such as crossover and mutation methods are universal.

In this case the search space is the space of control pulse sequences Σ^n for n time intervals, where each control pulse has bounded absolute value $\Sigma = [-100, 100]$. In order to optimize a controlled evolution of a system governed by the Lindblad equation, we perform optimization of the average distance between target state operator and the resulting state for each basis matrix of the space of input states. For each basis matrix ρ_0^i in the space of the system joined with ancilla, we compare the reduced resulting state $\text{Tr}_A(\rho_T^i)$ with the target one $\rho_{\text{target}}^i = U_{\text{target}} \text{Tr}_A(\rho_0^i) U_{\text{target}}^\dagger$. Our fitness function is defined as

$$F = \frac{1}{2^{2N}} \sum_{i=1}^{2^{2N}} \text{Tr} \left(\rho_{\text{target}}^i \text{Tr}_A \left(\rho_T^i \right) \right), \quad (28)$$

where Tr_A denotes tracing out the ancilla and N is the total number of qubits in the system.

4 Results and discussion

Our goal in this section is to study the impact of different spin chain configurations on the final fidelity of the operation. To find the best spin chain configuration, we study the following systems:

- (a) One-qubit system with one-qubit ancilla. The control is performed on the ancillary qubit, and the target is a NOT operation on the system qubit.
- (b) Two-qubit system with one-qubit ancilla. The control is performed on the ancillary qubit, and the target is a $\mathbb{1} \otimes NOT$ operation on the system qubits
- (c) Two-qubit system with one-qubit ancilla. The control is performed on the ancillary qubit, and the target is a $SWAP$ operation on the system qubits

In all of the simulations, we set the number of control pulses to 32 for two-qubit systems and 128 for the three-qubit systems. We limit the strength of the control pulses to $h_{\max} = 100$. We set $J = 1$. In each case we split all of the qubits forming the system into two subsystems: the one that performs some fixed evolution and the auxiliary one. Each data point is the result of 72 simulations, and we chose the result with the highest fidelity. The initial control pulses were random vectors with elements sampled independently from a uniform distribution on $[-100, 100]$.

Table 1 Number of time steps and corresponding Δt for different simulation setups in the two-qubit scenario

	Genetic optimization		Approximate evolution		Approximate gradient	
	n	$\Delta t (10^{-3})$	n	$\Delta t (10^{-3})$	n	$\Delta t (10^{-3})$
Equal number of steps	32	65.625	32	65.625	32	65.625
Equal computation time	32	65.625	128	16.406	128	16.406

Table 2 Number of time steps and corresponding Δt for different simulation setups in the three-qubit scenario

	Genetic optimization		Approximate evolution		Approximate gradient	
	n	$\Delta t (10^{-3})$	n	$\Delta t (10^{-3})$	n	$\Delta t (10^{-3})$
Equal number of steps	128	16.406	128	16.406	128	16.406
Equal computation time	128	16.406	512	4.102	512	4.102

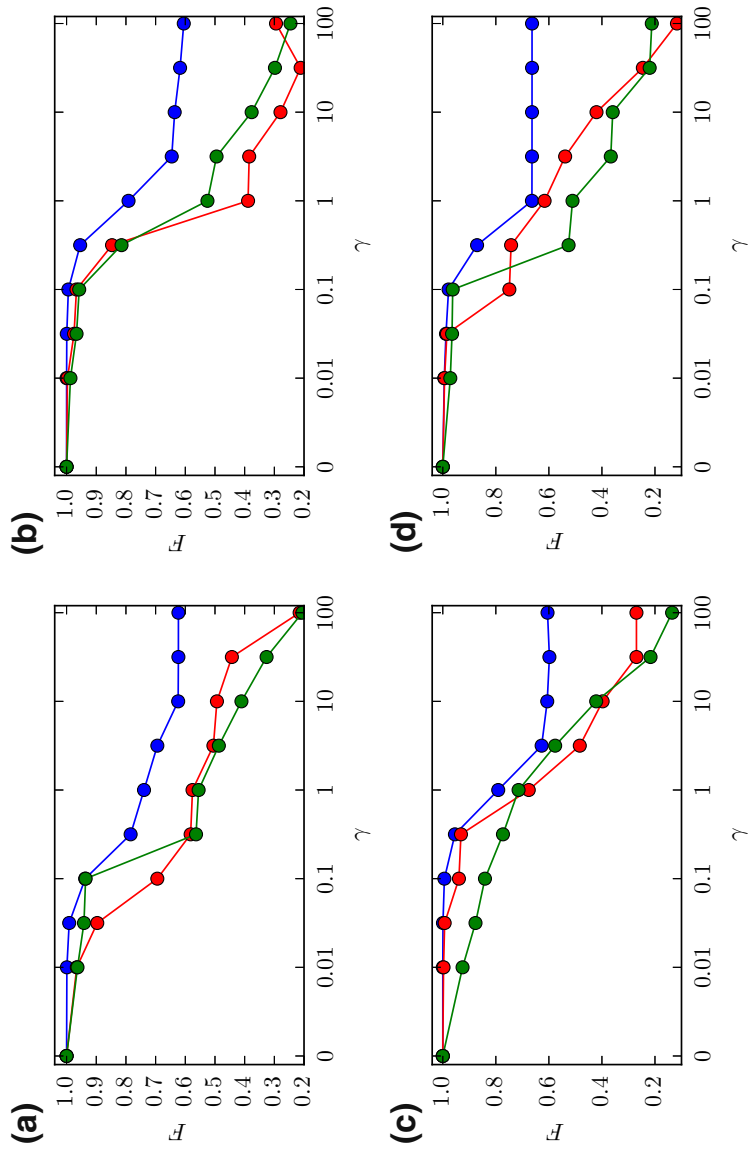


Fig. 3 Simulation results for the phase damping channel, **a** 2-qubit system, target NOT gate, **b** 3-qubit system, target $1 \otimes NOT$ gate, **c** 3-qubit, target $SWAP$ gate, **d** 3-qubit, target $SWAP$ gate between first and last qubit

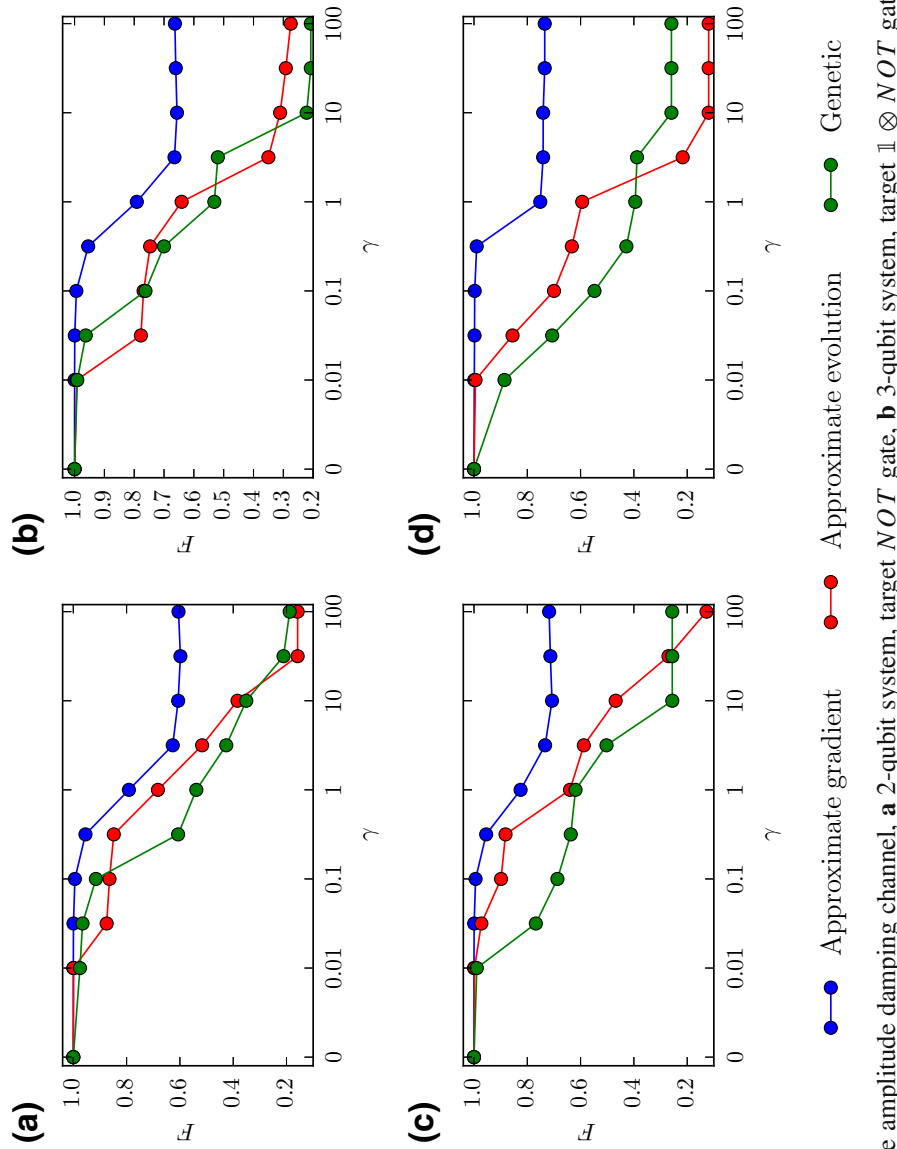


Fig. 4 Simulation results for the amplitude damping channel, **a** 2-qubit system, target NOT gate, **b** 3-qubit system, target NOT gate, **c** 3-qubit, target $SWAP$ gate, **d** 3-qubit, target $SWAP$ gate between first and last qubit

Table 3 Average computation times in seconds for different simulation setups

	Genetic optimization		Approximate evolution		Approximate gradient	
	2	3	2	3	2	3
Number of qubits	2	3	2	3	2	3
Equal number of steps	766	15741	521	1931	687	1745
Equal computation time	4248	24531	3875	21478	4026	22167

In our study we choose the phase damping and the amplitude damping channels as noise models. The former is given by the Lindblad operator $L = \sigma_z$, the latter is given by the operator $L = \sigma_- = |0\rangle\langle 1|$. In order to objectively compare the control methods, we study two setups: with equal number of steps of the algorithm and with equal computation time. The number of steps and length of these intervals are shown in Table 1 and Table 2.

Figure 3 shows the results for the phase damping channel. In the case of the NOT target gate, shown in Fig. 3a, b, we obtain the best results performing optimization with the approximate gradient method. In this setup the control is performed on the ancillary qubit, which leads to a smoother evolution of the target qubit, as the interaction between the two-qubits smooths impact of the control fields. Another feature of the result is the fact that the fidelity of the optimized operation decreases significantly when $\gamma \approx J$.

In the case of the SWAP target gate, shown in Fig. 3c, d, we get similar results. This is consistent with the results for the two qubit systems. In this case the genetic optimization and approximate evolution perform poorer compared to the approximate gradient method.

Next, in Fig. 4 we show the results for the amplitude damping channel. These results are similar to the phase damping case. Again there is a drop in the fidelity of the operations when $\gamma \approx J$.

Finally, we focus on comparing the algorithms when the computation times are on the same order of magnitude. To achieve this, we added more control pulses in the gradient-based methods. In the case of both gradient-based methods, we used 128 pulses for the two-qubit scenario and 512 for the three-qubit scenario. The computation times are summarized in Table 3. Results are presented in Figs 5 and 6. The obtained results show that using the method based on approximate gradient of the fitness function, we get control pulses providing the most accurate evolution.

5 Conclusions

We studied various methods of obtaining piecewise constant control pulses that implement an unitary evolution on a system governed by Kossakowski–Lindblad equation in the restrictive singular coupling limit. The studied methods included genetic optimization and the L-BFGS-B algorithm with the use of fidelity gradient based on an approximate evolution of the quantum system and an approximate gradient method for the exact evolution case.

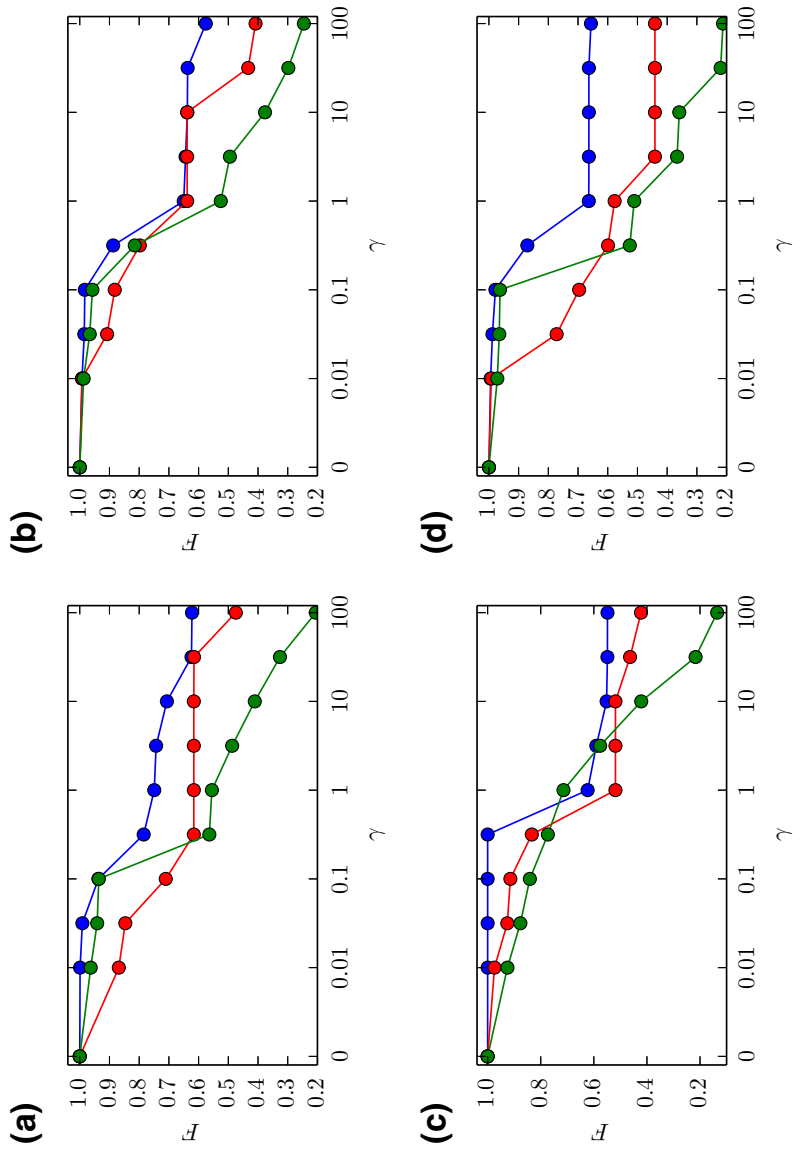


Fig. 5 Simulation results for the phase damping channel with equal computation time, **a** 2-qubit system, target NOT gate, **b** 3-qubit system, target $\mathbb{I} \otimes NOT$ gate, **c** 3-qubit target $SWAP$ gate, **d** 3-qubit, target $SWAP$ gate between first and last qubit

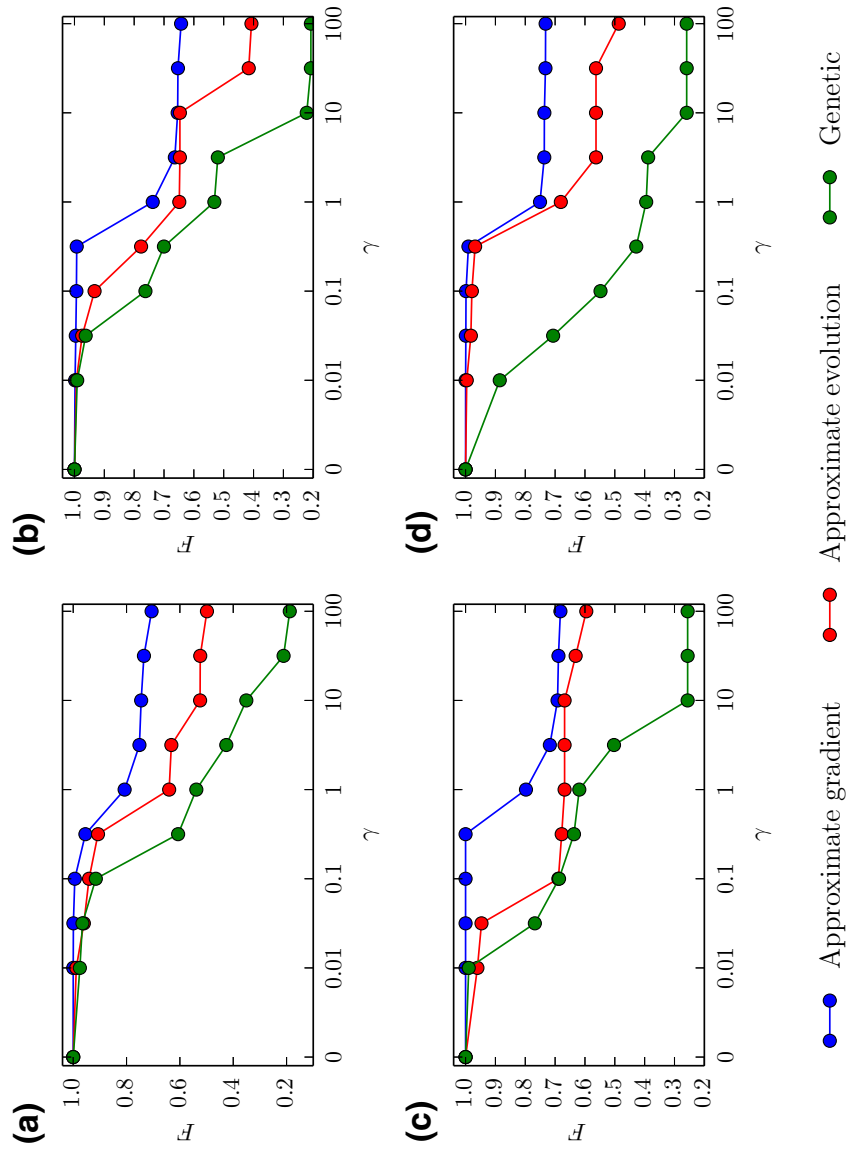


Fig. 6 Simulation results for the amplitude damping channel with equal computation time, **a** 2-qubit system, target NOT gate, **b** 3-qubit system, target $1 \otimes NOT$ gate, **c** 3-qubit, target $SWAP$ gate, **d** 3-qubit, target $SWAP$ gate between first and last qubit

Our results show that, by adding an ancilla, it is possible to implement a unitary evolution on a system under the Markovian approximation. What we have found is that it is sufficient to apply the control pulses to the ancillary qubits. This is caused by the fact that the interaction between the two qubits smooths impact of the control fields. This is limited to the case when the environment is slower than the frequency of oscillation of the qubits. In other words we require that $\gamma < J$.

The comparison of the numerical optimization methods used for control design led to the conclusion that using approximate gradient-based approach one gets the best results in terms of fidelity of the target unitary and the operator resulting from obtained control pulses.

Acknowledgments We would like to thank an anonymous reviewer for his/hers insightful comments. ŁP was supported by the Polish National Science Centre under the Grant Number DEC-2012/05/N/ST7/01105. PS was supported by the Polish National Science Centre under the Grant Number N N514 513340.

Open Access This article is distributed under the terms of the Creative Commons Attribution 4.0 International License (<http://creativecommons.org/licenses/by/4.0/>), which permits unrestricted use, distribution, and reproduction in any medium, provided you give appropriate credit to the original author(s) and the source, provide a link to the Creative Commons license, and indicate if changes were made.

References

1. Cheng, C.-J., Hwang, C.-C., Liao, T.-L., Chou, G.-L.: Optimal control of quantum systems: a projection approach. *J. Phys. A Math. Gen.* **38**, 929 (2005)
2. Albertini, F., D'Alessandro, D.: The Lie algebra structure and controllability of spin systems. *Linear Algebra Appl.* **350**, 213 (2002). ISSN 0024-3795
3. Elliott, D.: *Bilinear Control Systems: Matrices in Action*. Springer, Berlin (2009). ISBN 1402096127
4. d'Alessandro, D.: *Introduction to quantum control and dynamics*. Chapman & Hal, London (2008)
5. Morzhin, O.V.: Nonlocal improvement of controlling functions and parameters in nonlinear dynamical systems. *Autom. Remote Control* **73**, 1822 (2012)
6. Dominy, J.M., Paz-Silva, G.A., Rezakhani, A., Lidar, D.: Analysis of the quantum Zeno effect for quantum control and computation. *J. Phys. A Math. Theor.* **46**, 075306 (2013)
7. Qi, B.: A two-step strategy for stabilizing control of quantum systems with uncertainties. *Automatica* **49**, 834 (2013)
8. Pawela, Ł., Puchała, Z.: Quantum control with spectral constraints. *Quantum Inf. Process.* **13**, 227 (2014)
9. Pawela, Ł., Puchała, Z.: Quantum control robust with respect to coupling with an external environment. *Quantum Inf. Process.* **14**, 437 (2015)
10. Li, J.-S., Ruths, J., Stefanatos, D.: A pseudospectral method for optimal control of open quantum systems. *J. Chem. Phys.* **131**, 164110 (2009)
11. Khodjasteh, K., Lidar, D.A., Viola, L.: Arbitrarily accurate dynamical control in open quantum systems. *Phys. Rev. Lett.* **104**, 090501 (2010)
12. Schmidt, R., Negretti, A., Ankerhold, J., Calarco, T., Stockburger, J.T.: Optimal control of open quantum systems: cooperative effects of driving and dissipation. *Phys. Rev. Lett.* **107**, 130404 (2011)
13. Gawron, P., Kurzyk, D., Pawela, Ł.: Decoherence effects in the quantum qubit flip game using Markovian approximation. *Quantum Inf. Process.* **13**, 665 (2014)
14. Schulte-Herbrüggen, T., Spörl, A., Khaneja, N., Glaser, S.: Optimal control for generating quantum gates in open dissipative systems. *J. Phys. B At. Mol. Opt. Phys.* **44**, 154013 (2011)
15. Hwang, B., Goan, H.-S.: Optimal control for non-Markovian open quantum systems. *Phys. Rev. A* **85**, 032321 (2012)
16. Clausen, J., Bensky, G., Kurizki, G.: Task-optimized control of open quantum systems. *Phys. Rev. A* **85**, 052105 (2012)

17. Floether, F.F., de Fouquieres, P., Schirmer, S.G.: Robust quantum gates for open systems via optimal control: Markovian versus non-Markovian dynamics. *New J. Phys.* **14**, 073023 (2012)
18. Burgarth, D., Giovannetti, V.: Full control by locally induced relaxation. *Phys. Rev. Lett.* **99**, 100501 (2007)
19. Burgarth, D., Bose, S., Bruder, C., Giovannetti, V.: Local controllability of quantum networks. *Phys. Rev. A* **79**, 60305 (2009). ISSN 1094–1622
20. Puchała, Z.: Local controllability of quantum systems. *Quantum Inf. Process.* **12**, 459 (2013)
21. Montangero, S., Calarco, T., Fazio, R.: Robust optimal quantum gates for Josephson charge qubits. *Phys. Rev. Lett.* **99**, 170501 (2007)
22. Fisher, R., Helmer, F., Glaser, S.J., Marquardt, F., Schulte-Herbrüggen, T.: Optimal control of circuit quantum electrodynamics in one and two dimensions. *Phys. Rev. B* **81**, 085328 (2010)
23. Heule, R., Bruder, C., Burgarth, D., Stojanović, V.M.: Local quantum control of Heisenberg spin chains. *Phys. Rev. A* **82**, 052333 (2010)
24. Nielsen, M.A., Chuang, I.L.: *Quantum Computation and Quantum Information*. Cambridge University Press, Cambridge (2000). ISBN 9780521635035
25. Davies, E.B.: Markovian master equations. *Commun. Math. Phys.* **39**, 91 (1974)
26. DAlessandro, D., Jonckheere, E., Romano, R.: in 21st International Symposium on the Mathematical Theory of Networks and Systems (MTNS) (2014), pp. 1677–1684
27. Zhu, C., Byrd, R.H., Lu, P., Nocedal, J., Trans, A.C.M.: Algorithm 778: L-BFGS-B: fortran subroutines for large-scale bound-constrained optimization. *Math. Softw.* **23**, 550 (1997). ISSN 0098–3500
28. Byrd, R.H., Lu, P., Nocedal, J., Zhu, C.: A limited memory algorithm for bound constrained optimization. *SIAM J. Sci. Comput.* **16**, 1190 (1995)
29. Havel, T.F.: Robust procedures for converting among Lindblad, Kraus and matrix representations of quantum dynamical semigroups. *J. Math. Phys.* **44**, 534 (2003)
30. Machnes, S., Sander, U., Glaser, S.J., de Fouquieres, P., Gruslys, A., Schirmer, S., Schulte-Herbrüggen, T.: Comparing, optimizing, and benchmarking quantum-control algorithms in a unifying programming framework. *Phys. Rev. A* **84**, 022305 (2011)
31. Spector, L.: *Automatic Quantum Computer Programming: A Genetic Programming Approach*. Springer, Berlin (2004)
32. Gepp, A., Stocks, P.: A review of procedures to evolve quantum algorithms. *Genet. Program. Evol. Mach.* **10**, 181–228 (2009)

Chapter 4

Quantum control with spectral constraints

Quantum control with spectral constraints

Łukasz Pawela · Zbigniew Puchała

Received: 1 May 2012 / Accepted: 18 September 2013 / Published online: 6 October 2013
© The Author(s) 2013. This article is published with open access at Springerlink.com

Abstract Various constraints concerning control fields can be imposed in the realistic implementations of quantum control systems. One of the most important is the restriction on the frequency spectrum of acceptable control parameters. It is important to consider the limitations of experimental equipment when trying to find appropriate control parameters. Therefore, in this paper, we present a general method of obtaining a piecewise-constant controls, which are robust with respect to spectral constraints. We consider here a Heisenberg spin chain; however, the method can be applied to a system with more general interactions. To model experimental restrictions, we apply an ideal low-pass filter to numerically obtained control pulses. The usage of the proposed method has negligible impact on the control quality as opposed to the standard approach, which does not take into account spectral limitations.

Keywords Quantum information · Quantum computation · Control in mathematical physics

1 Introduction

One of the fundamental issues of the quantum information science is the ability to manipulate the dynamics of a given complex quantum system. Since the beginning of quantum mechanics, controlling a quantum system has been an implicit

Ł. Pawela (✉) · Z. Puchała
Institute of Theoretical and Applied Informatics, Polish Academy of Sciences,
Bałycka 5, 44-100 Gliwice, Poland
e-mail: lukasz.pawela@gmail.com

Z. Puchała
e-mail: z.puchala@iitis.pl

goal of quantum physics, chemistry, and implementations of quantum information processing.

If a given quantum system is controllable, i.e., it is possible to drive it into a previously fixed state, it is desirable to develop a control strategy to accomplish the required control task. In the case of finite dimensional quantum systems, the criteria for controllability can be expressed in terms of Lie-algebraic concepts [1–3]. These concepts provide a mathematical tool, in the case of closed quantum systems, i.e., systems without external influences.

It is an important question whether the system is controllable when the control is performed only on a subsystem. This kind of approach is called a *local-controllability* and can be considered only in the case when the subsystems of a given system interact. As examples may serve coupled spin chains or spin networks [2,4–6]. Local-control has a practical importance in proposed quantum computer architectures, as its implementation is simpler and the effect of decoherence is reduced by decreased number of control actuators [7,8].

A widely used method for manipulating a quantum system is a coherent control strategy, where the manipulation of the quantum states is achieved by applying semi-classical potentials in a fashion that preserves quantum coherence. In the case when a system is controllable, it is a point of interest what actions must be performed to control a system most efficiently, bearing in mind limitations imposed by practical restrictions. Various constraints concerning control fields can be imposed in the realistic implementations of quantum control systems. One of the most important is the restriction on the frequency spectrum of acceptable control parameters. Such restrictions come into play, for example, in an experimental setup that utilizes an external magnetic field [9]. In the case of such systems, due to various limitations, the application of piecewise-constant controls is not accurate. The real realization of controls is somehow smoothed by some filter induced by an experimental limitations. Thus, it is reasonable to seek control parameters in the domain imposed by the experimental restrictions.

In article [10], there has been discussed how the low-pass filtering, i.e., eliminating high-frequency components in a Fourier spectra, on a numerically obtained optimal control pulses affects a quality of performed control. This approach makes a contact with experimental realizations, since it implements the limitations of real quantum control systems.

In this paper, we present a general method of obtaining a piecewise-constant controls, which is robust with respect to low-pass filtering. The above means that elimination of high frequencies in a Fourier spectra reduces the fidelity only by a small amount. We utilize this approach to obtain numerically control pulses on a Heisenberg spin chain [10–12]; however, it can be applied to a quantum system with more general interactions.

This paper is organized as follows. In Sect. 2, we provide a general description of a quantum mechanical control system. In Sect. 3, we provide the description of the simulation setup used to test our model. Section 4 contains results obtained from numerical simulations and their discussion. In Sect. 5, we provide a summary of the presented work and give some concluding remarks.

2 Our model

To demonstrate a method of obtaining piecewise-constant controls, which are robust with respect to low-pass filtering, we will consider an isotropic Heisenberg spin-1/2 chain of a finite length N . The control will be performed on the first spin only. The total Hamiltonian of the aforementioned quantum control system is given by

$$H(t) = H_0 + H_c(t), \quad (1)$$

where

$$H_0 = J \sum_{i=1}^{N-1} S_x^i S_x^{i+1} + S_y^i S_y^{i+1} + S_z^i S_z^{i+1}, \quad (2)$$

is a drift part given by the Heisenberg Hamiltonian. The control is performed only on a first spin and is Zeeman-like, i.e.,

$$H_c(t) = h_x(t) S_x^1 + h_y(t) S_y^1. \quad (3)$$

In the above, S_k^i denotes k^{th} Pauli matrix acting on the spin i . Time-dependent control parameters $h_x(t)$ and $h_y(t)$ are chosen to be piecewise constant. We will refer to the values of the control pulses in the i^{th} time interval as $h_{x,i}$ and $h_{y,i}$. When we reference a general control pulse without specifying the direction, we will write h_l and the corresponding control Hamiltonian will be denoted H_l . Furthermore, as opposed to [10], we do not restrict the control fields to be alternating with x and y , i.e., they can be applied simultaneously (see e.g. [13] for similar approach). For notational convenience, we set $\hbar = 1$, and after this, rescaling frequencies and control field amplitudes can be expressed in units of the coupling strength J , and on the other hand, all times can be expressed in units of $1/J$ [10].

The system described above is operator controllable, as it was shown in [5] and follows from a controllability condition using a graph infection property introduced in the same article. The controllability of the described system can be also deduced from a more general condition utilizing the notion of hypergraphs [6].

Since the interest here is focused on operator control, a quality of a control will be measured with the use of gate fidelity,

$$F = \frac{1}{2^N} |\text{Tr}(U_T^\dagger U(h))|, \quad (4)$$

where U_T is the target quantum operation and $U(h)$ is an operation achieved by control parameters h . We choose gate fidelity as it neglects global phases.

To obtain piecewise-constant controls, which are robust with respect to low-pass filtering we will minimize the power in the high frequency part of a controls Fourier spectrum. We will do so by minimizing the following functional

$$G = (1 - \mu)P - \mu F, \quad (5)$$

where F is the gate fidelity described above, μ is a weight assigned to fidelity and P is a contribution of high frequencies in the total power of the control parameters. The above can be stated as, if y is a vector of Fourier coefficients for a control parameters h of length n , i.e.

$$y = Qh, \text{ where } Q = n^{-1/2} \{e^{2\pi i k l / n}\}_{k,l=0}^{n-1}, \quad (6)$$

then P is given by

$$P = \frac{\sum_{i=\frac{n}{2}-\Delta}^{\frac{n}{2}+\Delta} |y_i|^2}{|y|^2}, \quad (7)$$

for some Δ related to the cutoff frequency of low-pass filter.

3 Simulation setup

To demonstrate the beneficialness of our approach, we study three- and four-qubit spin chains. The control field is applied to the first qubit only. Our target gates are:

$$\text{NOT}_N = \mathbb{1}^{\otimes N-1} \otimes \sigma_x, \quad (8)$$

the negation of the last qubit of the chain, and

$$\text{SWAP}_N = \mathbb{1}^{\otimes N-2} \otimes \text{SWAP}, \quad (9)$$

swapping the states between the last two qubits.

For each of these cases, we find two sets of control parameters. One with frequency constraints and one without. Next, we calculate an appropriate filter and using these filtered values of control parameters, we calculate the fidelity of the quantum operation. In each case, 120 independent sets of control parameters were found.

We provide an explicit example in which we set the duration of the control pulse to $\Delta t = 0.2$ and the total number of pulses in each direction to $n = 128$ for the three-qubit chain and $n = 512$ in the four-qubit case, although the presented method may be applied for arbitrary values of Δt and n . The weight of fidelity in Eq. (5) is set to $\mu = 1$ in the unconstrained case and to $\mu = 0.05$ in the constrained case. Although the weight of the fidelity is small, the optimization still yields high fidelity values while maintaining low contribution of high frequencies in the power spectrum. We set the cutoff frequency in Eq. (7) to $\Delta = \frac{n}{4}$.

The applied filter is a frequency filter with the cutoff frequency equal to the frequency discriminated by the functional (5). As an example, we consider this filter

to be an ideal low-pass filter, which was previously studied, e.g., in [11]. Obviously, one can use other filters. A more general discussion of spectral filtering is presented in [14]. The ideal low-pass filter leaves the frequencies only in the interval $[-\omega_0, \omega_0] : f(\omega) = \Theta(\omega + \omega_0) - \Theta(\omega - \omega_0)$, where Θ is the Heaviside step function. We obtain the following expressions for the filtered control parameters [11]:

$$\hat{h}_k(t) = \frac{1}{\pi} \sum_{i=1}^n h_{k,i} [a_{i+1}(t) - a_i(t)], \quad (10)$$

where $k \in \{x, y\}$ and t denotes time. In other words, $\hat{h}_k(t)$ is a filtered version of the control fields h_k at the time moment t .

$$a_n(t) = \text{Si} [\omega_0(n\Delta t - t)], \quad (11)$$

$$\text{Si}(x) = \int_0^x (\sin t/t) dt. \quad (12)$$

The calculation of the gradient of the fidelity function can be found in the work by Machnes et al. [15]. Here, we only show the final result of the calculation

$$\frac{\partial F(U_k)}{\partial h_l} = \frac{1}{N} \Re \text{Tr} \left\{ e^{-i\phi} U_T^\dagger U_n \dots U_{k+1} \frac{\partial U_K}{\partial h_l} U_{k-1} U_1 \right\}, \quad (13)$$

where

$$e^{-i\phi} = \frac{\overline{\text{Tr}(U_T^\dagger U(h))}}{F},$$

and $\frac{\partial U_K}{\partial h_l}$ may be computed using the following formula [15, Equation (24)]

$$\langle \lambda_k | \frac{\partial U}{\partial h_l} | \lambda_m \rangle = \begin{cases} -i\Delta t \langle \lambda_k | H_l | \lambda_m \rangle e^{-i\Delta t \lambda_k} & \text{if } \lambda_k = \lambda_m \\ \langle \lambda_k | H_l | \lambda_m \rangle \frac{e^{-i\Delta t \lambda_k} - e^{-i\Delta t \lambda_m}}{(\lambda_k - \lambda_m)} & \text{if } \lambda_k \neq \lambda_m \end{cases}, \quad (14)$$

where U is the unitary gate implemented by the control pulses

$$U = \exp(-i\Delta t H) = \exp \left(-i\Delta t \left(H_0 + \sum_l h_l H_l \right) \right). \quad (15)$$

In this case, H_l is the control Hamiltonian corresponding to the control pulse h_l . $|\lambda\rangle$ and λ are the eigenvectors and eigenvalues of the total Hamiltonian of the system.

We conduct our simulations using the Broyden–Fletcher–Goldfarb–Shanno (BFGS) method [16]. This method is commonly used in quantum control theory for optimization of control pulses [10, 11, 17]. We first choose an initial guess for the

control field vectors. The algorithm then generates iteratively new control field vectors such that at each iteration point, the fidelity is increased. The algorithm terminates after a desired accuracy is reached. This procedure ensures convergence to a local maximum, but does not guarantee the convergence to a globally optimal sequence. Hence, we perform a number of simulations, using different initial conditions.

To calculate the gradient of P , one should note an elementary fact concerning differentiation of vector valued functions. For a real vector h , we define $y = Ah$ for some fixed matrix A . Straightforward calculations give us

$$\frac{\partial |y_k|^2}{\partial h_l} = 2\Re(\overline{A}_{kl}y_k). \quad (16)$$

In the case when matrix is a quantum Fourier transform gate $A = Q$ defined in Eq. (6), we obtain that

$$\frac{\partial |y_k|^2}{\partial h_l} = 2\Re(\overline{Q}_{kl}y_k) = \frac{2}{\sqrt{n}}\Re(e^{-2\pi i k l / n} y_k). \quad (17)$$

This calculation is used to find the gradient of the contribution of high frequencies in the total power given by Eq. (7).

4 Results

Figure 1a shows a plot of the control parameters for the target gate $U_T = \text{NOT}_3$ before and after applying the frequency filter. These parameters were found using with the value of the weight $\mu = 1$, resulting in no penalty for high-frequency terms. Clearly, the signal after filtering differs from the original values. This is reflected in the values of the fidelity of the operation. Before filtering, the fidelity is $F > 1 - 10^{-12}$; however, after filtering, the value drops to $F = 0.85$.

Next, in Fig. 1b, we show the plot of the control parameters for the target gate $U_T = \text{NOT}_3$, before and after applying the frequency filter. Only this time, the controls were found using the value of the weight $\mu = 0.05$ resulting in a penalty for high-frequency terms. A short glance reveals that the filtered parameters are almost the same as the original ones. This is reflected by the fidelity of the operation. Before filtering, the fidelity is $F > 1 - 10^{-9}$, and after filtering, it drops only to $F > 1 - 10^{-2}$, which is still a satisfactory value. Hence, these sets of control parameters are well-suited for use in computations.

Figure 2a, b shows analogical results for the target gate $U_T = \text{SWAP}_3$. The qualitative results in this case are the same as for the NOT_3 target gate discussed earlier. Fidelity values before and after filtering are the same order as for the NOT_3 gate. Again, we reach a conclusion that these sets of control parameters are well suited for use in computations.

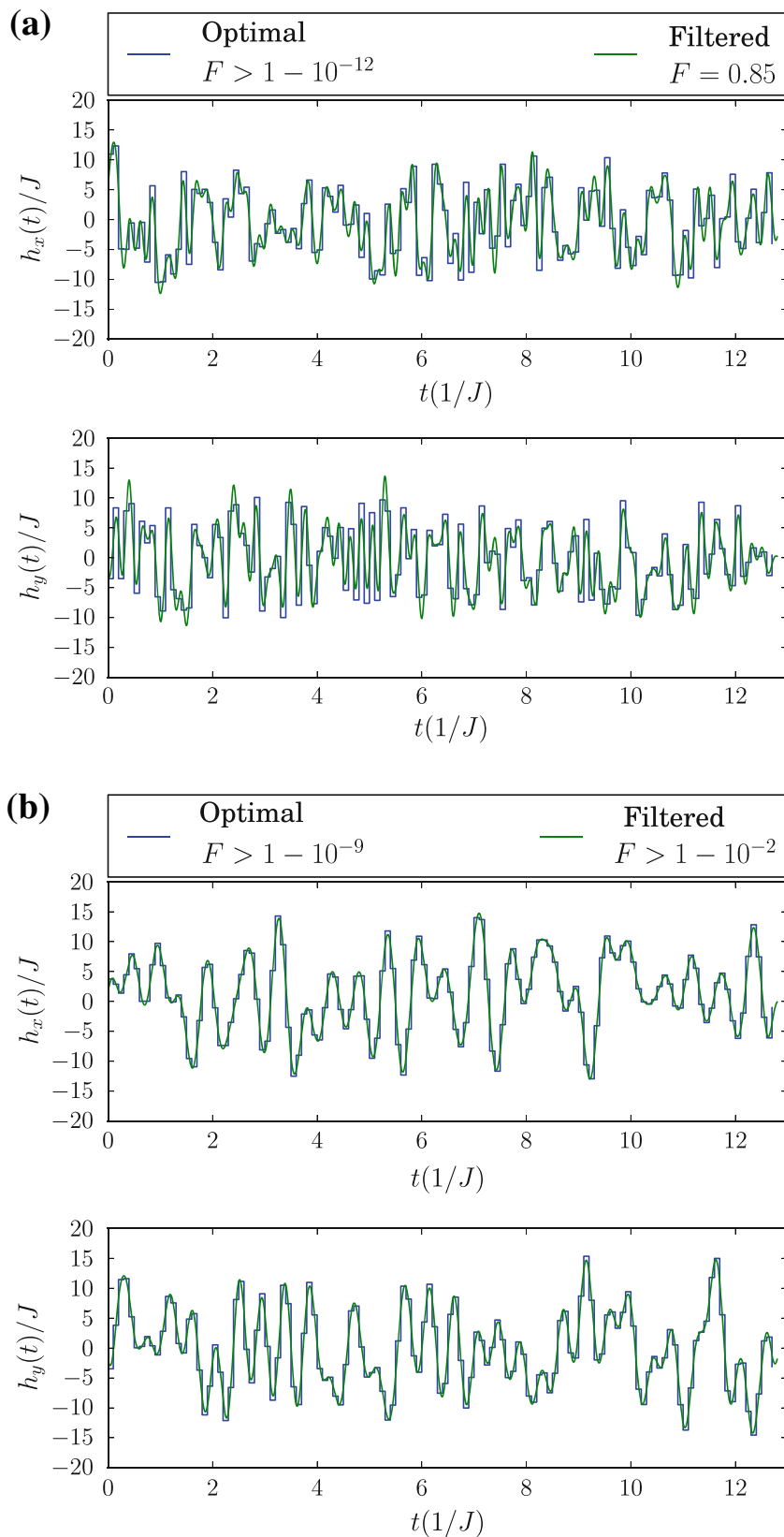


Fig. 1 x and y components of the control field for target gate $U_T = \text{NOT}_3$. **a** Unconstrained case. **b** Constrained case

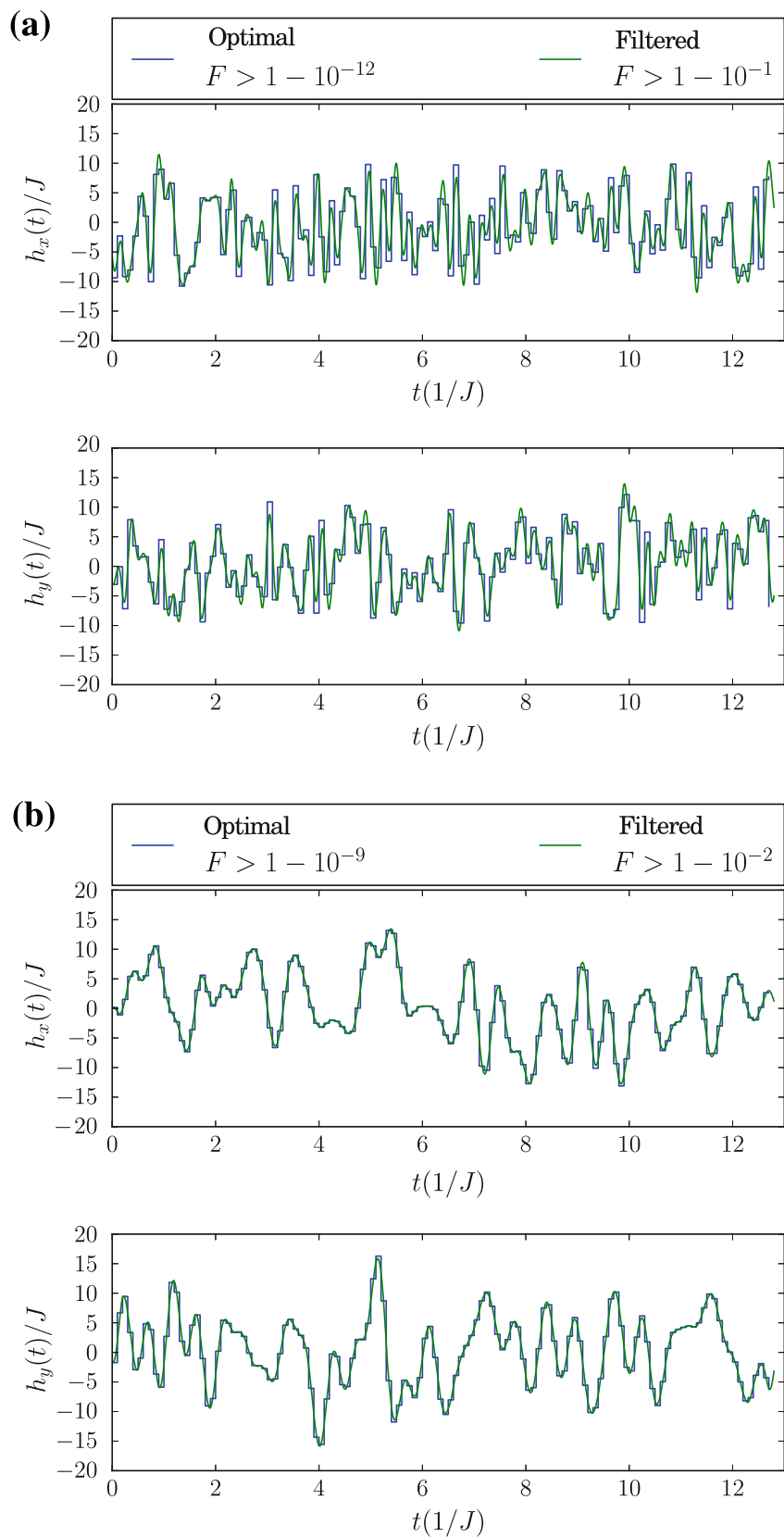


Fig. 2 x and y components of the control field for target gate $U_T = \text{SWAP}_3$. **a** Unconstrained case. **b** Constrained case

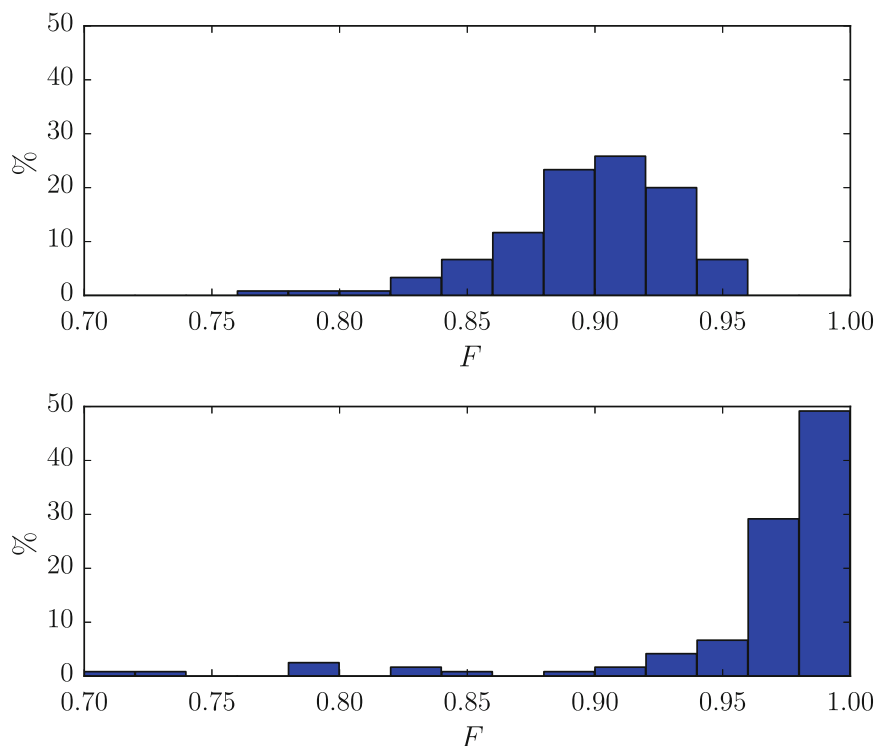


Fig. 3 A histogram of the fidelities after filtering. *Top* without considering spectral constraints, *bottom* with spectral constraints considered. Target gate $U_T = \text{NOT}_3$

Results obtained for the four-qubit chain (not shown here) qualitatively resemble the results for the three-qubit chain. In this case, a penalty for high-frequency terms of the control parameters also leads to higher fidelities after filtering.

Figure 3 depicts the histograms of fidelities of filtered control parameters for the NOT_3 gate for different initial vectors of control fields. These vectors are drawn at random; coordinates are stochastically independent and have a uniform distribution on an interval $[-10, 10]$. The top plot shows the histograms for control parameters found without spectral constraints and the bottom one shows what happens when one takes spectral constraints into consideration. Clearly, a typical set of control parameters has a higher fidelity of operation when one considers spectral constraints in the optimization phase. Strictly speaking, around 80 % of the control parameter sets have a fidelity greater than 0.96, whereas in the unconstrained case, there are no control parameter sets that have such high fidelities. These facts lead to a conclusion that optimization with spectral constraints will lead to high fidelity of experimental realizations of the NOT_3 gate.

Analogical results for the SWAP_3 are shown in Fig. 4. The top plot shows the histograms for control parameters found without spectral constraints, and the bottom one shows what happens when one takes spectral constraints into consideration. In this case, around 75 % of all constrained control parameter sets have a fidelity higher than 0.96 after filtering. Also, there are no unconstrained control parameter sets with fidelities in this range. Hence, spectral constraints imposed during the optimization step have led to control parameters far less sensitive to experimental equipment limitations.

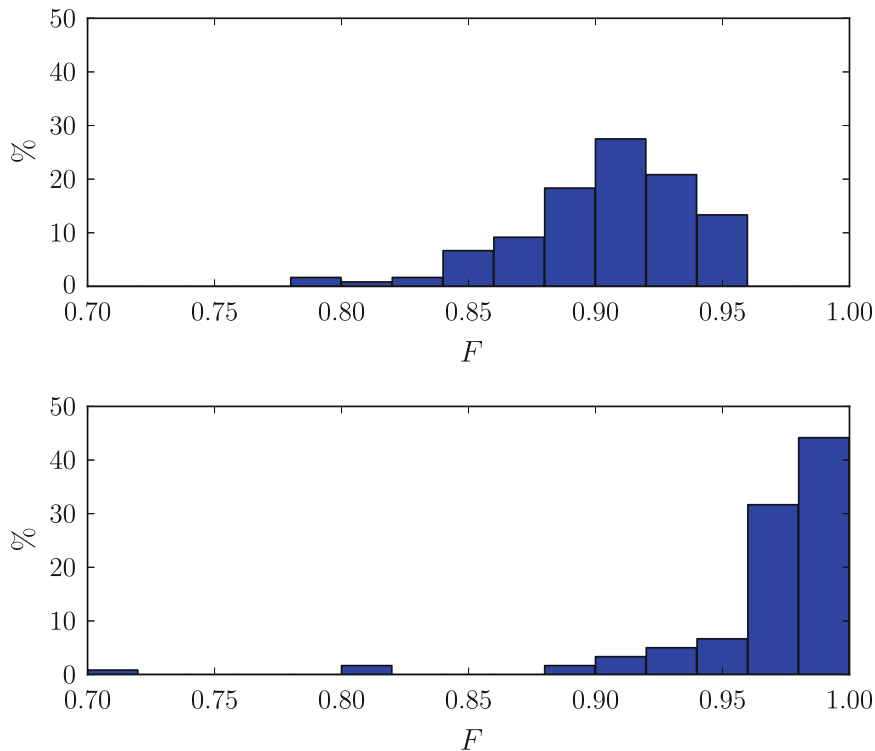


Fig. 4 A histogram of the fidelities after filtering. *Top* without considering spectral constraints, *bottom* with spectral constraints considered. Target gate $U_T = \text{SWAP}_3$

5 Conclusions

We investigated the impact of spectral constraints imposed on the control parameters of a quantum operation on the fidelity of the quantum operation which they implement. In order to compare our approach with the unconstrained case, we apply an ideal low-pass filter to the control parameters.

We have shown that imposing spectral constraints on the control parameters leads to higher average fidelity of the quantum operation after appropriate filtering, than in the unconstrained case. These results are independent of the type of quantum operation and the number of qubits in the system under consideration.

Furthermore, the requirement for smooth control parameters does not result in the increase in time necessary to conduct a quantum operation. Comparing with other research in the field [11], our times are on the same order.

Further work on this subject might take into account more subtle parameters of the experimental setup than the frequency cutoff of signal sources. For instance, one could wish to find control parameters that are far from transient characteristics of the experimental setup. This may lead to an enhancement of fidelities of operations achieved experimentally by eliminating unwanted signal roughness.

Acknowledgments Work by Ł. Pawela was partially supported by the Polish National Science Centre under the Grant Number N N514 513340. Z. Puchała was partially supported by the Polish Ministry of Science and Higher Education under the project number IP2011 044271. The development of numerical methods was supported by the Grant N N514 513340. Analytical studies were supported by the project IP2011 044271. Numerical simulations presented in this work were performed on the “Leming” and “Świstak” computing systems of The Institute of Theoretical and Applied Informatics, Polish Academy of Sciences.

Open Access This article is distributed under the terms of the Creative Commons Attribution License which permits any use, distribution, and reproduction in any medium, provided the original author(s) and the source are credited.

References

1. Albertini, F., D'Alessandro, D.: The Lie algebra structure and controllability of spin systems. *Linear Algebra Its Appl.* **350**, 213 (2002). ISSN 0024-3795, <http://www.sciencedirect.com/science/article/pii/S0024379502002902>
2. d'Alessandro, D.: *Introduction to Quantum Control and Dynamics*. Chapman & Hall, London (2008)
3. Elliott, D.: *Bilinear Control Systems: Matrices in Action*. Springer, Berlin (2009). ISBN 1402096127
4. Burgarth, D., Giovannetti, V.: Full control by locally induced relaxation. *Phys. Rev. Lett.* **99**, 100501 (2007). doi:[10.1103/PhysRevLett.99.100501](https://doi.org/10.1103/PhysRevLett.99.100501)
5. Burgarth, D., Bose, S., Bruder, C., Giovannetti, V.: Local controllability of quantum networks. *Phys. Rev. A* **79**, 60305 (2009). ISSN 1094-1622, doi:[10.1103/PhysRevA.79.060305](https://doi.org/10.1103/PhysRevA.79.060305)
6. Puchała, Z.: Local controllability of quantum systems. *Quantum Inf. Process.* (2012). doi:[10.1007/s11128-012-0391-x](https://doi.org/10.1007/s11128-012-0391-x)
7. Montangero, S., Calarco, T., Fazio, R.: Robust optimal quantum gates for Josephson charge qubits. *Phys. Rev. Lett.* **99**, 170501 (2007). doi:[10.1103/PhysRevLett.99.170501](https://doi.org/10.1103/PhysRevLett.99.170501)
8. Fisher, R., Helmer, F., Glaser, S.J., Marquardt, F., Schulte-Herbrüggen, T.: Optimal control of circuit quantum electrodynamics in one and two dimensions. *Phys. Rev. B* **81**, 085328 (2010). doi:[10.1103/PhysRevB.81.085328](https://doi.org/10.1103/PhysRevB.81.085328)
9. Chaudhury, S., Merkel, S., Herr, T., Silberfarb, A., Deutsch, I., Jessen, P.: Quantum control of the hyperfine spin of a Cs atom ensemble. *Phys. Rev. Lett.* **99**, 163002 (2007). doi:[10.1103/PhysRevLett.99.163002](https://doi.org/10.1103/PhysRevLett.99.163002)
10. Heule, R., Bruder, C., Burgarth, D., Stojanović, V. M.: Local quantum control of Heisenberg spin chains. *Phys. Rev. A* **82**, 052333 (2010). doi:[10.1103/PhysRevA.82.052333](https://doi.org/10.1103/PhysRevA.82.052333)
11. Heule, R., Bruder, C., Burgarth, D., Stojanović, V.M.: Controlling qubit arrays with anisotropic XXZ Heisenberg interaction by acting on a single qubit. *Eur. Phys. J. D* **63**, 41 (2011), ISSN 1434-6060, 1434-6079, <http://www.springerlink.com/content/b4rr1wg3400442lv/>
12. Miszczak, J., Gawron, P., Puchała, Z.: Qubit flip game on a Heisenberg spin chain. *Quantum Inf. Process.* (2012). doi:[10.1007/s11128-011-0322-2](https://doi.org/10.1007/s11128-011-0322-2)
13. Khaneja, N., Reiss, T., Kehlet, C., Schulte-Herbrüggen, T., Glaser, S.J.: Optimal control of coupled spin dynamics: design of NMR pulse sequences by gradient ascent algorithms. *J. Magn. Reson.* **172**, 296 (2005), ISSN 1090-7807, <http://www.sciencedirect.com/science/article/pii/S1090780704003696>
14. Werschnik, J., Gross, E.: Quantum optimal control theory. *J. Phys. B: Atom. Molecul. Opt. Phys.* **40**, R175 (2007)
15. Machnes, S., Sander, U., Glaser, S.J., de Fouquières, P., Gruslys, A., Schirmer, S., Schulte-Herbrüggen, T.: Comparing, optimizing, and benchmarking quantum-control algorithms in a unifying programming framework. *Phys. Rev. A* **84**, 022305 (2011). doi:[10.1103/PhysRevA.84.022305](https://doi.org/10.1103/PhysRevA.84.022305)
16. Press, W., Flannery, B., Teukolsky, S., Vetterling, W.: *Numerical Recipes in FORTRAN 77: Volume 1 of Fortran Numerical Recipes: The Art of Scientific Computing*, vol. 1. Cambridge University Press, Cambridge (1992)
17. Burgarth, D., Maruyama, K., Murphy, M., Montangero, S., Calarco, T., Nori, F., Plenio, M.B.: arXiv:0905.3373 (2009), *Phys. Rev. A* **81**, 040303(R) (2010), <http://arxiv.org/abs/0905.3373>

Chapter 5

Quantum control robust with
respect to coupling with an
external environment

Quantum control robust with respect to coupling with an external environment

Lukasz Pawela · Zbigniew Puchała

Received: 8 October 2013 / Accepted: 4 November 2014 / Published online: 27 November 2014
© The Author(s) 2014. This article is published with open access at Springerlink.com

Abstract We study coherent quantum control strategy that is robust with respect to coupling with an external environment. We model this interaction by appending an additional subsystem to the initial system and we choose the strength of the coupling to be proportional to the magnitude of the control pulses. Therefore, to minimize the interaction, we impose L_1 norm restrictions on the control pulses. In order to efficiently solve this optimization problem, we employ the BFGS algorithm. We use three different functions as the derivative of the L_1 norm of control pulses: the signum function, a fractional derivative $\frac{d^\alpha |x|}{dx^\alpha}$, where $0 < \alpha < 1$, and the Fermi–Dirac distribution. We show that our method allows to efficiently obtain the control pulses which neglect the coupling with an external environment.

Keywords Quantum information · Quantum computation · Control in mathematical physics

1 Introduction

The ability to manipulate the dynamics of a given complex quantum system is one of the fundamental issues of the quantum information science. It has been an implicit goal in many fields of science such as quantum physics, chemistry, or implementations

L. Pawela (✉) · Z. Puchała

Institute of Theoretical and Applied Informatics, Polish Academy of Sciences,
Bałycka 5, 44-100 Gliwice, Poland
e-mail: lpawela@iitis.pl

Z. Puchała
Institute of Physics, Jagiellonian University,
Reymonta 4, 30-059 Kraków, Poland
e-mail: z.puchala@iitis.pl

of quantum information processing [1–3]. The usage of experimentally controllable quantum systems to perform computational task is a very promising perspective. Such usage is possible only if a system is controllable. Thus, the controllability of a given quantum system is an important issue of the quantum information science, since it concerns whether it is possible to drive a quantum system into a previously fixed state.

When manipulating quantum systems, a coherent control strategy is a widely used method. In this case, the application of semiclassical potentials, in a fashion that preserves quantum coherence, is used to manipulate quantum states. If a given system is controllable, it is interesting to obtain control sequence that drives a system to a desired state and simultaneously minimize the value of the disturbance caused by imperfections of practical implementation. In the realistic implementations of quantum control systems, there can be various factors which disturb the evolution [4]. One of the main issues in this context is *decoherence*—the fact that the systems are very sensitive to the presence of the environment, which often destroys the main feature of the quantum dynamics. Other disturbance can be a result of the restriction on the frequency spectrum of acceptable control parameters [5]. In the case of such systems, it is not accurate to apply piecewise-constant controls. In an experimental setup that utilizes an external magnetic field [6,7], such restrictions come into play and cannot be neglected.

In many situations, the interaction with the control fields causes an undesirable coupling with the environment, which can lead to a destruction of the interesting features of the system [8]. In such situations, it is reasonable to seek a control field with minimal total influence on a system. Depending on a type of interaction with an environment, the influence differs. In this article, we consider an interaction that is proportional to the magnitude of a control field. To minimize the influence of an environment in such case, when the control field performs the desired evolution, the L_1 norm should be minimized.

A different dynamical method for beating decoherence in open quantum systems is dynamical decoupling [9–12]. In this case, additional perturbation on a system is added, which protects the evolution against the effects of the environment influence at the same time driving the system to the desired state. In our case, the interaction with the environment is in strict relation to the control strategy, since it emerges only if the control pulses are applied. On the other hand, in a typical dynamical decoupling scheme, the coupling to the environment is constant, given by some Hamiltonian H_{SE} acting on the system and environment. Another approach to robust quantum control is quantum sliding mode control [13]. This model combines unitary control and periodic projective measurements. First, the initial state is driven into a *sliding mode* and then a periodic projective measurement is performed. Finally, there is risk-sensitive quantum control [14,15] that is a robust control method with a feedback loop.

The paper is organized as follows. In Sect. 2, we introduce the model used for simulations. Section 3 describes the simulation setup. In Sect. 4, we show results of numerical simulations, and in Sect. 5, we draw the final conclusions.

2 Our model

To demonstrate a method of obtaining piecewise-constant controls, which have minimal energy, we will consider an isotropic Heisenberg spin-1/2 chain of a finite length N . The control will be performed on the first spin only. The total Hamiltonian of the aforementioned quantum control system is given by

$$H(t) = H_0 + H_c(t), \quad (1)$$

where

$$H_0 = J \sum_{i=1}^{N-1} \left(S_x^i S_x^{i+1} + S_y^i S_y^{i+1} + S_z^i S_z^{i+1} \right), \quad (2)$$

is a drift part given by the Heisenberg Hamiltonian. The control is performed only on a first spin and is Zeeman like, i.e.,

$$H_c(t) = h_x(t) S_x^1 + h_y(t) S_y^1. \quad (3)$$

In the above, S_k^i denotes k^{th} Pauli matrix which acts on the spin i . Time dependent control parameters $h_x(t)$ and $h_y(t)$ are chosen to be piecewise constant. Furthermore, as opposed to [16], we do not restrict the control fields to be alternating with x and y , i.e., they can be applied simultaneously (see e.g., [17] for similar approach). For notational convenience, we set $\hbar = 1$; and after this, rescaling frequencies and control field amplitudes can be expressed in units of the coupling strength J ; and on the other hand, all times can be expressed in units of $1/J$ [16].

The system described above is operator controllable, as it was shown in [18] and follows from a controllability condition using a graph infection property introduced in the same article. The controllability of the described system can be also deduced from a more general condition utilizing the notion of hypergraphs [19].

Since the interest here is focused on operator control sequence, a quality of a control will be measured with the use of gate fidelity,

$$F = \frac{1}{2^N} \left| \text{Tr}(U_T^\dagger U(h)) \right|, \quad (4)$$

where U_T is the target quantum operation, and $U(h)$ is an operation achieved by control parameters h . We choose gate fidelity as it neglects global phases.

In the case of disturbed system, we will measure the quality of the control by a trace distance between Choi–Jamiołkowski states, which gives an estimation of a diamond norm.

In many situations, the interaction with the control fields causes an undesirable coupling with the environment, which can lead to a destruction of the interesting features of the system. We will consider a general model described by

$$H(t) = H_0 + H_c(t) + \gamma(|h_x| + |h_y|) H_1, \quad (5)$$

where H_1 denotes a general Hamiltonian responsible for a coupling with an environment, and the interaction is proportional to the magnitude of a control field. To minimize the influence of an environment in this model, we introduce an additional constrain on the control pulses, namely we wish to minimize the L_1 norm of control pulses

$$\|h_k\|_1 = \sum_{i=1}^n |h_k^i|, \quad (6)$$

where $k \in \{x, y\}$ and n are the total number of control pulses. In order to make this quantity comparable with fidelity, we impose bounds on the maximal amplitude of the control pulses. To accommodate this, we introduce the following penalty

$$P = \frac{\sum_{i=1}^n |h_k^i|}{nb}, \quad (7)$$

where b is the bound on the control pulse amplitude. This leads to the following functional we wish to minimize

$$G = (1 - \mu)P - \mu F, \quad (8)$$

where μ is a weight assigned to fidelity.

To optimize the control pulses, we utilize the BFGS algorithm [20]. In order to use this method effectively, we need to calculate the explicit form of derivatives of Eq. (6). We propose the following functions to be used as the derivative of the absolute value:

- The *signum* function:

$$\frac{d|x|}{dx} = \text{sgn}(x). \quad (9)$$

- A fractional derivative:

$$\frac{d^\alpha|x|}{dx^\alpha} = \pm \frac{\Gamma(2)}{\Gamma(2 - \alpha)} x^{1-\alpha}, \quad (10)$$

where $\Gamma(x) = (x - 1)!$ and we set $\alpha = 0.99$.

- Rescaled Fermi–Dirac distribution

$$\frac{d|x|}{dx} \approx 2 \left(\frac{-1}{\exp(\frac{x}{kT}) + 1} + 0.5 \right), \quad (11)$$

where we set $kT = 0.01$.

The signum function is the natural conclusion when one thinks about the derivative of the L_1 norm as it penalizes any nonzero control pulses in the control scheme. To further out studies, we introduce two approximations of the derivative of the L_1 norm. The first one utilizes the idea of fractional derivatives [21]. This allows us to achieve a continuous function, which quickly increases from 0 to 1 for positive values of the argument and decreases from 0 to -1 for negative values. Although continuous, the

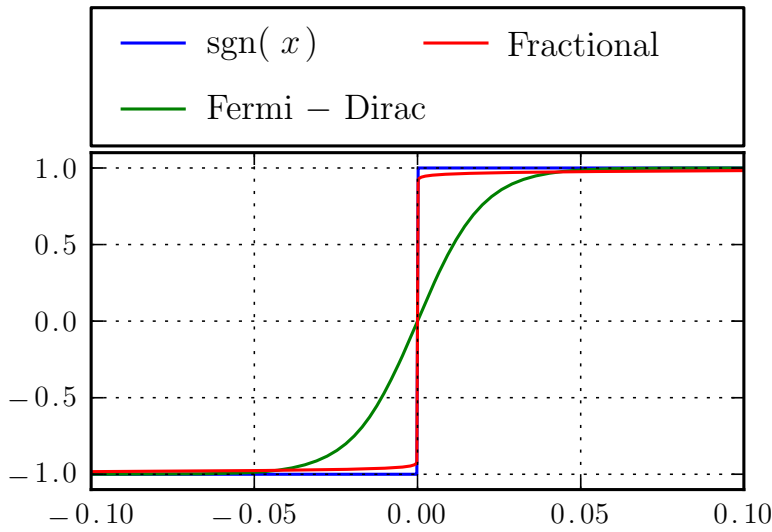


Fig. 1 Comparison of different derivative approximations

function has the drawback that control pulses with lower magnitude are less penalized. The penalty can be adjusted by using the parameter α

The last proposed approximation is a rescaled Fermi–Dirac distribution [22]. The distribution is given by

$$f(x) = \frac{1}{\exp\left(\frac{x-E_f}{kT}\right) + 1}, \quad (12)$$

where E_f is the Fermi energy level. The usage is justified, as for $T = 0$ the function is given as

$$f(E) = \begin{cases} 1 & \text{if } E < E_f, \\ 0 & \text{if } E > E_f, \end{cases} \quad (13)$$

We rescale this function in the following manner: First, we set $E_f = 0$. Next, in order to obtain behavior similar to the signum function, we translate and rescale the function, so that $f(x) = -1$ for $x \ll 0$ and $f(x) = 1$ for $x \gg 0$. After these operations we obtain

$$f(x) = 2\left(\frac{-1}{\exp\left(\frac{x}{kT}\right) + 1} + 0.5\right), \quad (14)$$

From our point of view, the function has properties similar to the fractional derivative and the penalty for low magnitude pulses can be adjusted by using the “temperature” T . A comparison of these approximations is shown in Fig. 1.

3 Simulation setup

To demonstrate the beneficialness of our approach, we study three- and four-qubit spin chains. The control field is applied to the first qubit only. Our target gates are:

$$\text{NOT}_N = \mathbb{1}^{\otimes N-1} \otimes \sigma_x, \quad (15)$$

the negation of the last qubit of the chain, and

$$\text{SWAP}_N = \mathbb{1}^{\otimes N-2} \otimes \text{SWAP}, \quad (16)$$

swapping the states between the last two qubits. This set of gates is universal in quantum computation.

We provide an explicit example in which we set the duration of the control pulse to $\Delta t = 0.2$ and the total number of pulses in each direction to $n = 64$ for the three-qubit chain and $n = 256$ in the four-qubit case, although the presented method may be applied for arbitrary values of Δt and n . The weight of fidelity in Eq. (8) is set to $\mu = 0.2$ in the three-qubit scenario and to $\mu = 0.4$ in the four-qubit scenario.

4 Results

We show examples of control sequences obtained by using our method in Figs. 2 and 3. They depict results obtained for the three-qubit NOT gate optimization and four-qubit SWAP gate optimization, respectively. In the three-qubit scenario, we find, as expected, a control sequence that equal to zero most of the time with irregular, high amplitude pulses. A similar case can be made for the swap gate in the four-qubit scenario. The main difference is that in this case, the high amplitude pulses are surrounded by groups of weaker pulses. The results shown here are for the fractional derivative approximation. Simulations for other approximation yield nearly identical results.

The fidelity obtained in both cases is $F > 0.99$, and the value of P has the order of 10^{-2} .

Finally, we show the evolution of each qubit's state. Let the qubits be in the state $|\psi\rangle_0 = |000\rangle$ in the case of the three-qubit scenario. Figure 4 shows the time evolution of the target qubit in this setup. The final state of the chain is $\psi_f = |001\rangle$. Note that the evolution is smooth, no signs of control pulses are visible in the qubit's trajectory. In the four-qubit scenario the time evolution of the target qubits is shown in Figs. 5

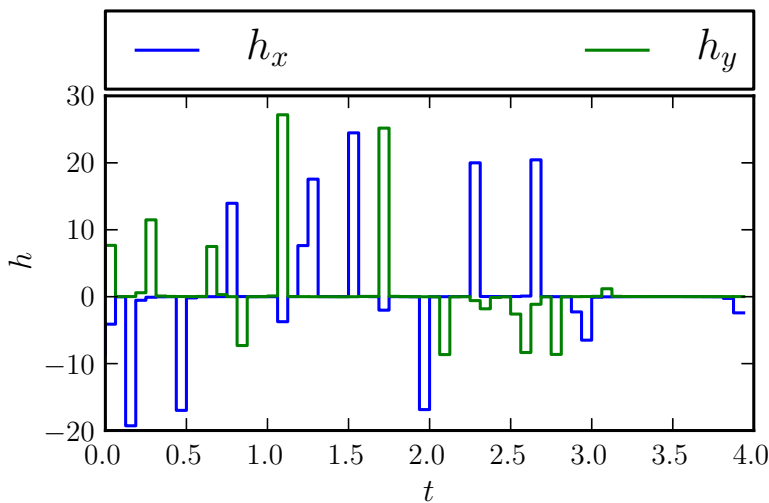


Fig. 2 Example control sequences h_x and h_y for the NOT gate in the three-qubit scenario

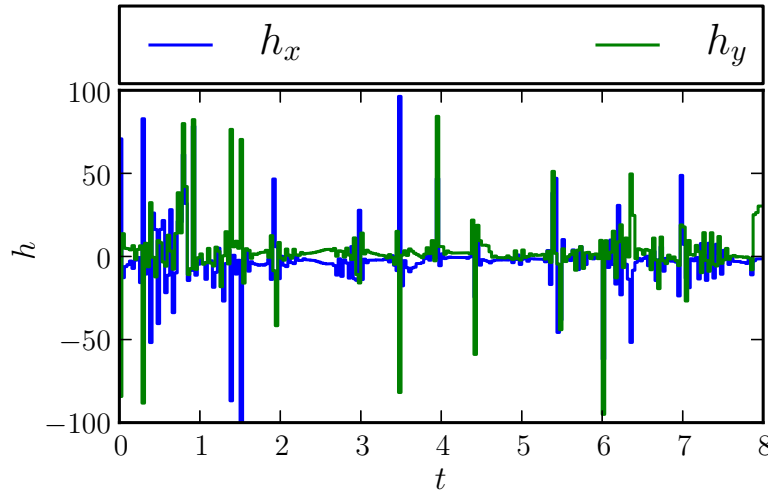
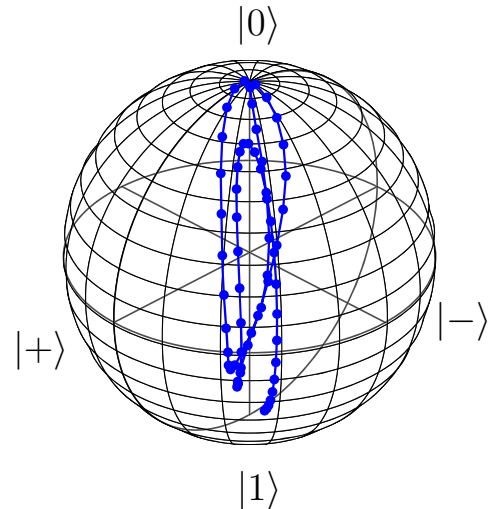


Fig. 3 Example control sequences h_x and h_y for the SWAP gate in the four-qubit scenario

Fig. 4 Time evolution of the target qubit of a three-qubit chain from the state $|000\rangle$ to the state $|001\rangle$ under the operator $\mathbb{1} \otimes \mathbb{1} \otimes \sigma_x$ implemented by optimized control sequences



and 6. Let the initial state of the chain be equal to $|\phi_0\rangle = |0010\rangle$. The final state of the chain is $|\phi\rangle = |0001\rangle$. In this case, the figures show that the transition is performed along the shortest path possible. Also, note that the evolution is quite smooth, and the application of each control pulse is not visible in these figures.

In order to demonstrate the advantages of our approach, we perform additional simulations, where we put $\mu = 1$ in Eq. (8). This is the unconstrained problem of finding optimal control pulses. Next, we introduce an interaction with an environment, proportional to $|h_x| + |h_y|$. We model the interaction with the environment by adding a qubit to the chain. The Hamiltonian for this case is

$$\begin{aligned} H_{\text{graph}}(t) &= H_0 + H_c(t) + \gamma(|h_x| + |h_y|) \\ &\times \sum_{i=1}^N \left(S_x^i S_x^{N+1} + S_y^i S_y^{N+1} + S_z^i S_z^{N+1} \right). \end{aligned} \quad (17)$$

Fig. 5 Time evolution of the third qubit of a four-qubit chain from the state $|0010\rangle$ to the state $|0001\rangle$ under the operator $\mathbb{1} \otimes \mathbb{1} \otimes \text{SWAP}$ implemented by optimized control sequences

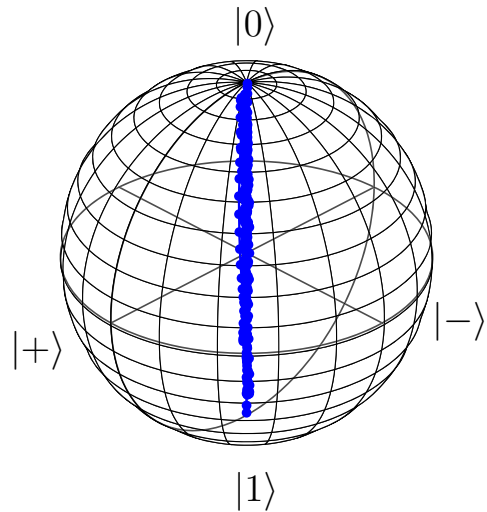
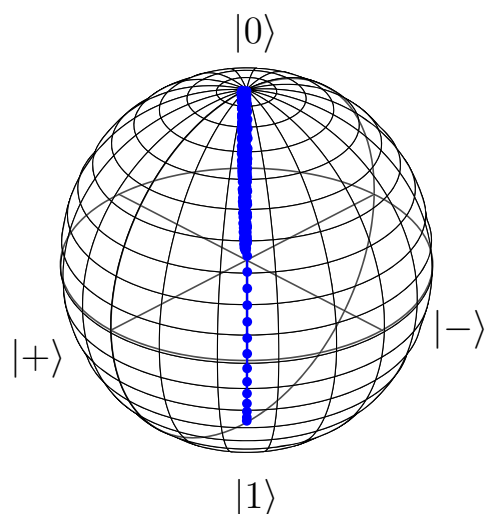


Fig. 6 Time evolution of the fourth qubit of a four-qubit chain from the state $|0010\rangle$ to the state $|0001\rangle$ under the operator $\mathbb{1} \otimes \mathbb{1} \otimes \text{SWAP}$ implemented by optimized control sequences



In order to compare the evolution with the additional qubit with a given U_T , we use the following scheme. For a quantum channel Φ , let us write $J(\Phi)$ to denote the associated state:

$$J(\Phi) = \frac{1}{n} \sum_{1 \leq i, j \leq n} \Phi(|i\rangle\langle j|) \otimes |i\rangle\langle j|. \quad (18)$$

Here, we are assuming that the channel maps $n \times n$ complex matrices into $m \times m$ complex matrices. The matrix $J(\Phi)$ is sometimes called the Choi–Jamiołkowski representation of Φ . For quantum channels Φ_0 and Φ_1 , we may define the “diamond norm distance” between them as

$$\|\Phi_0 - \Phi_1\|_\diamond = \sup_{k, \rho} \|(\Phi_0 \otimes \mathbb{1}_k)(\rho) - (\Phi_1 \otimes \mathbb{1}_k)(\rho)\|_1 \quad (19)$$

where $\mathbb{1}_k$ denotes the identity channel from the set of $k \times k$ complex matrices to itself; $\|\cdot\|_1$ denotes the trace norm; and the supremum is taken over all $k \geq 1$ and all density matrices ρ from the set of $nk \times nk$ complex matrices. The supremum always happens

Table 1 Summary of the value of Eq. (20) for the studied cases

	Without additional qubit		With additional qubit	
	$\mu = 1$	$\mu < 1$	$\mu = 1$	$\mu < 1$
NOT ₃	0.0000	0.0000	0.0975	0.0086
NOT ₄	0.0000	0.004	0.9788	0.0142
SWAP ₃	0.0000	0.0001	0.0135	0.0133
SWAP ₄	0.0000	0.0020	0.0843	0.0064

For $\mu = 1$ we have a control optimization without regarding the L_1 norm of control pulses

to be achieved for some choice of $k \leq n$ and some rank 1 density matrix ρ . A coarse bound for the diamond norm defined in Eq. (19) is known [23]

$$\frac{1}{n} \|\Phi_0 - \Phi_1\|_{\diamond} \leq \|J(\Phi_0) - J(\Phi_1)\|_1 \leq \|\Phi_0 - \Phi_1\|_{\diamond}. \quad (20)$$

Therefore, to compare the target operations with and without the additional qubit, we study the L_1 of the difference of the Jamiołkowski matrices of the respective quantum channels $\|J(\Phi_0) - J(\Phi_1)\|_1$. The results for different target operations are summarized in Table 1. We show results obtained for Fermi–Dirac approximation of the derivative. As stated in the table, the bigger the system under consideration is the greater is the gain from using our method.

5 Conclusions

In this work, we introduced a method of obtaining a piecewise-constant control field for a quantum system with an additional constrain of minimizing the L_1 norm. To demonstrate the beneficialness of our approach, we have shown results obtained for a spin chain, on which we implemented two quantum operations: negation of the last qubit of the chain and swapping the states of the two last qubits of the chain. Our results show that it is possible to obtain control fields which have minimal energy and still give a high fidelity of the quantum operation. Our method may be used in situations where the interaction with the control field causes additional coupling to the environment. As our method allows one to minimize the number of control pulses, it also minimizes the amount of coupling to the environment. It is important to note that our model differs from known in the literature dynamical decoupling, in which additional perturbation on a system is added, which protects the evolution against the effects of the environment influence. In our case the interaction with the environment is related to the control strategy, and it emerges only if the control is applied. Our model allows to optimize high fidelity control pulses for the cases with and without external environment, as shown in Table 1 as long as the coupling is induced by the control pulses themselves. Other possible usage of our method includes systems, in which it is possible to use rare, but high value of control pulses, for example, superconducting magnets with high impulse current.

Acknowledgments Ł. Pawela was supported by the Polish National Science Centre under the Grant Number N N514 513340. Z. Puchała was supported by the Polish Ministry of Science and Higher Education under the Project Number IP2011 044271.

Open Access This article is distributed under the terms of the Creative Commons Attribution License which permits any use, distribution, and reproduction in any medium, provided the original author(s) and the source are credited.

References

1. d'Alessandro, D.: Introduction to Quantum Control and Dynamics. Chapman & Hall, London (2008)
2. Albertini, F., D'Alessandro, D.: The Lie algebra structure and controllability of spin systems. *Linear Algebra Appl.* **350**(1), 213–235. <http://www.sciencedirect.com/science/article/pii/S0024379502002902> (2002)
3. Werschnik, J., Gross, E.: Quantum optimal control theory. *J. Phys. B At. Mol. Opt. Phys.* **40**, R175–R211 (2007)
4. Pawela, Ł., Sadowski, P.: arXiv preprint [arXiv:1310.2109](https://arxiv.org/abs/1310.2109) (2013) (under review)
5. Pawela, Ł., Puchała, Z.: Quantum control with spectral constraints. *Quantum Inf. Process.* **13**, 227–237 (2014)
6. Chaudhury, S., Merkel, S., Herr, T., Silberfarb, A., Deutsch, I.H., Jessen, P.S.: Quantum control of the hyperfine spin of a Cs atom ensemble. *Phys. Rev. Lett.* **99**, 163002 (2007). doi:[10.1103/PhysRevLett.99.163002](https://doi.org/10.1103/PhysRevLett.99.163002)
7. Jami, S., Amerian, Z., Ahmadi, F., Motevalizadeh, L.: Effects of external magnetic field on thermal entanglement in a spin-one chain with three particles. *Indian J. Phys.* **87**(4), 367–372 (2013)
8. Zhang, S., Jie, Q., Wang, Q.: Revival and decay of entanglement in a two-qubit system coupled to a kicked top. *Indian J. Phys.* **86**(5), 387–393 (2012)
9. Viola, L., Knill, E., Lloyd, S.: Dynamical decoupling of open quantum systems. *Phys. Rev. Lett.* **82**, 2417 (1999a)
10. Viola, L., Lloyd, S., Knill, E.: Universal control of decoupled quantum systems. *Phys. Rev. Lett.* **83**, 4888 (1999b)
11. Viola, L., Knill, E.: Robust dynamical decoupling of quantum systems with bounded controls. *Phys. Rev. Lett.* **90**, 037901 (2003)
12. Dahleh, M., Peirce, A., Rabitz, H.: Optimal control of uncertain quantum systems. *Phys. Rev. A* **42**, 1065 (1990)
13. Dong, D., Petersen, I.R.: Sliding mode control of quantum systems. *New J. Phys.* **11**, 105033 (2009)
14. James, M.: Risk-sensitive optimal control of quantum systems. *Phys. Rev. A* **69**, 032108 (2004)
15. D'Helon, C., Doherty, A., James, M., Wilson, S.: In: 2006 45th IEEE Conference on Decision and Control (IEEE, 2006), pp. 3132–3137 (2006)
16. Heule, R., Bruder, C., Burgarth, D., Stojanović, V.M.: Local quantum control of Heisenberg spin chains. *Phys. Rev. A* **82**, 052333 (2010). doi:[10.1103/PhysRevA.82.052333](https://doi.org/10.1103/PhysRevA.82.052333)
17. Khaneja, N., Reiss, T., Kehlet, C., Schulte-Herbrüggen, T., Glaser, S.J.: Optimal control of coupled spin dynamics: design of NMR pulse sequences by gradient ascent algorithms. *J. Magn. Reson.* **172**, 296–305. <http://www.sciencedirect.com/science/article/pii/S1090780704003696> (2005)
18. Burgarth, D., Bose, S., Bruder, C., Giovannetti, V.: Local controllability of quantum networks. *Phys. Rev. A* **79**, 060305 (2009). doi:[10.1103/PhysRevA.79.060305](https://doi.org/10.1103/PhysRevA.79.060305)
19. Puchała, Z.: Local controllability of quantum systems. *Quantum Inf. Process.* **12**, 459–466 (2013). doi:[10.1007/s11128-012-0391-x](https://doi.org/10.1007/s11128-012-0391-x)
20. Press, W., Flannery, B., Teukolsky, S., Vetterling, W.: Numerical Recipes in FORTRAN 77: Volume 1, Volume 1 of Fortran Numerical Recipes: The Art of Scientific Computing, vol. 1. Cambridge university press, Cambridge (1992)
21. Miller, K.S., Ross, B.: An Introduction to the Fractional Calculus and Fractional Differential Equations. Wiley, New York (1993)
22. Smirnov, B.M.: Fermi–Dirac Distribution, pp. 57–73. Wiley-VCH Verlag GmbH & Co. KGaA (2007). doi:[10.1002/9783527608089.ch4](https://doi.org/10.1002/9783527608089.ch4)
23. Kitaev, A.Y., Shen, A.H., Vyalyi, M.N.: Classical and Quantum Computation, vol. 47 of Graduate Studies in Mathematics. American Mathematical Society, Providence (2002)

Chapter 6

Quantifying channels output
similarity with applications to
quantum control

Quantifying channels output similarity with applications to quantum control

Łukasz Pawela¹ · Zbigniew Puchała^{1,2}

Received: 25 February 2015 / Accepted: 29 December 2015 / Published online: 12 January 2016
© The Author(s) 2016. This article is published with open access at Springerlink.com

Abstract In this work, we aim at quantifying quantum channel output similarity. In order to achieve this, we introduce the notion of quantum channel superfidelity, which gives us an upper bound on the quantum channel fidelity. This quantity is expressed in a clear form using the Kraus representation of a quantum channel. As examples, we show potential applications of this quantity in the quantum control field.

Keywords Quantum control · Fidelity · Superfidelity

1 Introduction

Recent applications of quantum mechanics are based on processing and transferring information encoded in quantum states. The full description of quantum information processing procedures is given in terms of quantum channels, i.e. completely positive, trace- preserving maps on the set of quantum states.

In many areas of quantum information processing, one needs to quantify the difference between ideal quantum procedure and the procedure which is performed in the laboratory. This is especially true in the situation when one deals with imperfections during the realization of experiments. These imperfections can be countered,

✉ Łukasz Pawela
lpawela@iitis.pl

Zbigniew Puchała
z.puchala@iitis.pl

¹ Institute of Theoretical and Applied Informatics, Polish Academy of Sciences, Bałycka 5,
44-100 Gliwice, Poland

² Institute of Physics, Jagiellonian University, ulica prof. Stanisława Łojasiewicza 11,
30-348 Kraków, Poland

in a quantum control setup, using various techniques, such us dynamical decoupling [1–4], sliding mode control [5] and risk sensitive quantum control [6, 7]. A different approach is to model the particular setup and optimize control pulses for a specific task in a specific setup [8–11]. In particular, the problem of quantifying the distance between quantum channels was studied in the context of channel distinguishability.

One possible approach to quantifying the distance between two quantum channels is to consider the fidelity between Choi–Jamiołkowski states corresponding to quantum channels [12]. Another approach could involve the diamond norm [13] of quantum channels. We propose an approach which focuses on the outputs of quantum channels.

The main aim of this paper is to provide a succinct expression for the channel output similarity. As a measure of similarity, we will consider the superfidelity function and define channel superfidelity. Then we will show examples of application of our results to various pairs of quantum channels. In the final part of the paper, we will study the impact of Hamiltonian errors on the channel superfidelity. First, we will consider a single qubit at a finite temperature, and next we will move to an extended quantum control example.

2 Preliminaries

Henceforth, we will denote the set of linear operators, transforming vectors from a finite-dimensional Hilbert space \mathcal{X} to another finite-dimensional Hilbert space \mathcal{Y} by $\mathcal{L}(\mathcal{X}, \mathcal{Y})$. We put $\mathcal{L}(\mathcal{X}) = \mathcal{L}(\mathcal{X}, \mathcal{X})$. By $\mathcal{U}(\mathcal{X})$, we will denote the set of unitary operators on \mathcal{X} . Given an operator $A \in \mathcal{L}(\mathcal{X}, \mathcal{Y})$, we denote by $\|A\|_p$ its Schatten p-norm. By \bar{A} , we will denote the element-wise complex conjugation of A .

2.1 Quantum states and channels

First, we introduce two basic notions: density operators and superoperators:

Definition 1 We call an operator $\rho \in \mathcal{L}(\mathcal{X})$ a density operator iff $\rho \geq 0$ and $\text{Tr}\rho = 1$. We denote the set of all density operators on \mathcal{X} by $\mathcal{D}(\mathcal{X})$.

From this follows that ρ is in the form $\rho = \sum_j \lambda_j |\lambda_j\rangle\langle\lambda_j|$, where λ_j and $|\lambda_j\rangle$ denote the j th eigenvalue and eigenvector of ρ , respectively.

Definition 2 A superoperator is a linear mapping acting on linear operators $\mathcal{L}(\mathcal{X})$ on a finite-dimensional Hilbert space \mathcal{X} and transforming them into operators on another finite-dimensional Hilbert space \mathcal{Y} . Thus

$$\Phi : \mathcal{L}(\mathcal{X}) \rightarrow \mathcal{L}(\mathcal{Y}). \quad (1)$$

Now we define the tensor product of superoperators

Definition 3 Given superoperators

$$\Phi_1 : \mathcal{L}(\mathcal{X}_1) \rightarrow \mathcal{L}(\mathcal{Y}_1), \Phi_2 : \mathcal{L}(\mathcal{X}_2) \rightarrow \mathcal{L}(\mathcal{Y}_2), \quad (2)$$

we define the product superoperator

$$\Phi_1 \otimes \Phi_2 : \mathcal{L}(\mathcal{X}_1 \otimes \mathcal{X}_2) \rightarrow \mathcal{L}(\mathcal{Y}_1 \otimes \mathcal{Y}_2), \quad (3)$$

to be the unique linear mapping that satisfies the equation

$$(\Phi_1 \otimes \Phi_2)(A_1 \otimes A_2) = \Phi_1(A_1) \otimes \Phi_2(A_2), \quad (4)$$

for all operators $A_1 \in \mathcal{L}(\mathcal{X}_1)$, $A_2 \in \mathcal{L}(\mathcal{X}_2)$.

In the most general case, the evolution of a quantum system can be described using the notion of a *quantum channel* [14–16].

Definition 4 A quantum channel is a superoperator Φ that satisfies the following restrictions:

1. Φ is trace preserving, i.e. $\forall A \in \mathcal{L}(\mathcal{X}) \quad \text{Tr}(\Phi(A)) = \text{Tr}(A)$,
2. Φ is completely positive, that is for every finite-dimensional Hilbert space \mathcal{Z} the product of Φ and identity mapping on $\mathcal{L}(\mathcal{Z})$ is a non-negativity-preserving operation, i.e.

$$\forall \mathcal{Z} \forall A \in \mathcal{L}(\mathcal{X} \otimes \mathcal{Z}) \quad A \geq 0 \Rightarrow \Phi \otimes \mathbb{1}_{\mathcal{L}(\mathcal{Z})}(A) \geq 0. \quad (5)$$

Many different representations of quantum channels can be chosen, depending on the application. In this paper, we will use only the Kraus representation.

Definition 5 The Kraus representation of a completely positive superoperator (Def. 4(2)) is given by a set of operators $K_i \in \mathcal{L}(\mathcal{X}, \mathcal{Y})$. The action of the superoperator Φ is given by:

$$\Phi(\rho) = \sum_i K_i \rho K_i^\dagger, \quad (6)$$

This form ensures that the superoperator is completely positive. For it to be also trace preserving, we need to impose the following constraint on the Kraus operators

$$\sum_i K_i^\dagger K_i = \mathbb{1}_{\mathcal{X}}, \quad (7)$$

where $\mathbb{1}_{\mathcal{X}}$ denotes the identity operator acting on the Hilbert space \mathcal{X} .

2.2 Superfidelity

In this section, we introduce the *superfidelity*, along with its properties

Definition 6 Superfidelity of two density operators $\rho, \sigma \in \mathcal{D}(\mathcal{X})$ is given by

$$G(\rho, \sigma) = \text{Tr}(\rho\sigma) + \sqrt{1 - \text{Tr}\rho^2}\sqrt{1 - \text{Tr}\sigma^2}. \quad (8)$$

The superfidelity is an upper bound for the fidelity function [14, 17].

Properties of the superfidelity [17] ($\rho_1, \rho_2, \rho_3, \rho_4 \in \mathcal{D}(\mathcal{X})$):

1. Bounds: $0 \leq G(\rho_1, \rho_2) \leq 1$.
2. Symmetry: $G(\rho_1, \rho_2) = G(\rho_2, \rho_1)$.
3. Unitary invariance: $G(\rho_1, \rho_2) = G(U\rho_1 U^\dagger, U\rho_2 U^\dagger)$, where $U \in \mathcal{U}(\mathcal{X})$.
4. Joint concavity [18]:

$$G(p\rho_1 + (1-p)\rho_2, p\rho_3 + (1-p)\rho_4) \leq pG(\rho_1, \rho_3) + (1-p)G(\rho_2, \rho_4) \quad (9)$$

for $p \in [0, 1]$.

5. Supermultiplicativity:

$$G(\rho_1 \otimes \rho_2, \rho_3 \otimes \rho_4) \geq G(\rho_1, \rho_3)G(\rho_2, \rho_4). \quad (10)$$

6. Bound for trace distance [19]

$$\frac{1}{2}\|\rho_1 - \rho_2\|_1 \geq 1 - G(\rho_1, \rho_2). \quad (11)$$

2.3 Supporting definitions

In this section, we define additional operations used in our proof. We begin with the *partial trace*

Definition 7 For all operators A, B the partial trace is a linear mapping defined as:

$$\text{Tr}_{\mathcal{Y}} A \otimes B = A \text{Tr} B. \quad (12)$$

The extension to operators not in the tensor product form follows from linearity.

We will also need the notion of conjugate superoperator

Definition 8 Given a quantum channel $\Phi : \mathcal{L}(\mathcal{X}) \rightarrow \mathcal{L}(\mathcal{Y})$, for every operator $A \in \mathcal{L}(\mathcal{X}), B \in \mathcal{L}(\mathcal{Y})$, we define the conjugate superoperator $\Phi^\dagger : \mathcal{L}(\mathcal{Y}) \rightarrow \mathcal{L}(\mathcal{X})$ as the mapping satisfying

$$\text{Tr}(\Phi(A)B) = \text{Tr}(A\Phi^\dagger(B)). \quad (13)$$

Note that the conjugate to completely positive superoperator is completely positive, but is not necessarily trace preserving

Next, we will define a reshaping operation, which preserves the lexicographical order and its inverse.

Definition 9 We define the linear mapping

$$\text{res} : \mathcal{L}(\mathcal{X}, \mathcal{Y}) \rightarrow \mathcal{Y} \otimes \mathcal{X}, \quad (14)$$

for dyadic operators as

$$\text{res}(|\psi\rangle\langle\phi|) = |\psi\rangle\overline{|\phi\rangle}, \quad (15)$$

for $|\psi\rangle \in \mathcal{Y}$ and $|\phi\rangle \in \mathcal{X}$ and uniquely extended by linearity.

We introduce the inverse of the $\text{res}(\cdot)$

Definition 10 We define the linear mapping

$$\text{unres} : \mathcal{Y} \otimes \mathcal{X} \rightarrow \mathcal{L}(\mathcal{X}, \mathcal{Y}) \quad (16)$$

such that

$$\forall X \in \mathcal{L}(\mathcal{X}, \mathcal{Y}) \quad \text{unres}(\text{res}(X)) = X. \quad (17)$$

Remark 1 For every choice of Hilbert spaces $\mathcal{X}_1, \mathcal{X}_2, \mathcal{Y}_1$ and \mathcal{Y}_2 and every choice of operators $A \in \mathcal{L}(\mathcal{X}_1, \mathcal{Y}_1)$, $B \in \mathcal{L}(\mathcal{X}_2, \mathcal{Y}_2)$ and $X \in \mathcal{L}(\mathcal{X}_2, \mathcal{X}_1)$, it holds that:

$$(A \otimes B)\text{res}(X) = \text{res}(AXB^T) \quad (18)$$

Remark 2 For any choice of Hilbert spaces \mathcal{X} and \mathcal{Y} and any choice of $|\zeta\rangle \in \mathcal{X} \otimes \mathcal{Y}$ and $A \in \mathcal{L}(\mathcal{Y}, \mathcal{X})$ such that $|\zeta\rangle = \text{res}(A)$ it holds that

$$\text{Tr}_{\mathcal{Y}} |\zeta\rangle \langle \zeta| = \text{Tr}_{\mathcal{Y}} (\text{res}(A)\text{res}(A)^\dagger) = AA^\dagger. \quad (19)$$

Next, we introduce the *purification* of quantum states:

Definition 11 Given Hilbert spaces \mathcal{X} and \mathcal{Y} , we will call $|\zeta\rangle \in \mathcal{X} \otimes \mathcal{Y}$ a purification of $\rho \in \mathcal{D}(\mathcal{X})$ if

$$\text{Tr}_{\mathcal{Y}} |\zeta\rangle \langle \zeta| = \rho. \quad (20)$$

Theorem 1 For every choice of Hilbert spaces \mathcal{X} and \mathcal{Y} and let $|\phi\rangle, |\psi\rangle \in \mathcal{X} \otimes \mathcal{Y}$ satisfy

$$\text{Tr}_{\mathcal{Y}} (|\phi\rangle \langle \phi|) = \text{Tr}_{\mathcal{Y}} (|\psi\rangle \langle \psi|). \quad (21)$$

Then there exists a unitary operator $U \in \mathcal{U}(\mathcal{X})$ such that $|\psi\rangle = (\mathbb{1}_{\mathcal{X}} \otimes U)|\phi\rangle$

From Definition 11, Theorem 1 and Remark 2 we get that given a state $\rho \in \mathcal{D}(\mathcal{X})$ its purification $|\zeta\rangle \in \mathcal{X} \otimes \mathcal{X}$ is given by:

$$|\zeta\rangle = (\mathbb{1}_{\mathcal{X}} \otimes U)\text{res}(\sqrt{\rho}). \quad (22)$$

Verification of this equation is straightforward. First, we note that we may omit the term $(\mathbb{1}_{\mathcal{X}} \otimes U)$. Next we apply Remark 2 which allows us to show that for this choice of $|\zeta\rangle$ we get:

$$\text{Tr}_{\mathcal{Y}} |\zeta\rangle \langle \zeta| = \sqrt{\rho} (\sqrt{\rho})^\dagger = \rho. \quad (23)$$

2.4 Quantum channel fidelity

First, we introduce the *fidelity* and *channel fidelity* [12]

Definition 12 Given two density operators ρ, σ we define the fidelity between ρ and σ as:

$$F(\rho, \sigma) = \|\sqrt{\rho}\sqrt{\sigma}\|_1^2 = \left(\text{Tr} \sqrt{\sqrt{\rho}\sigma\sqrt{\rho}} \right)^2 \quad (24)$$

Definition 13 Quantum channel fidelity of a channel $\Phi : \mathcal{L}(\mathcal{X}) \rightarrow \mathcal{L}(\mathcal{X})$ for some σ is defined as:

$$F_{\text{ch}}(\Phi; \sigma) = \inf F(\xi, (\Phi \otimes \mathbb{1}_{\mathcal{L}(\mathcal{Z})})(\xi)), \quad (25)$$

where the infimum is over all Hilbert spaces \mathcal{Z} and all $\xi \in \mathcal{D}(\mathcal{X} \otimes \mathcal{Z})$ such that $\text{Tr}_{\mathcal{Z}} \xi = \sigma$

It can be shown [20] that this infimum is independent of ξ and is given by

$$F_{\text{ch}}(\Phi; \sigma) = \sum_i |\text{Tr}(\sigma K_i)|^2, \quad (26)$$

where K_i form the Kraus representation of Φ .

3 Our results

In this section, we present our main theorem and its proof. In the second subsection, we present a quantum circuit that allows one to measure the quantum channel superfidelity without performing full state tomography.

3.1 Theorem and proof

Definition 14 Consider two quantum channels $\Phi, \Psi : \mathcal{L}(\mathcal{X}) \rightarrow \mathcal{L}(\mathcal{X})$ and a density operator $\sigma \in \mathcal{D}(\mathcal{X})$. We define the quantum channel superfidelity to be:

$$G_{\text{ch}}(\Phi, \Psi; \sigma) = \inf G((\Phi \otimes \mathbb{1}_{\mathcal{L}(\mathcal{Z})})(\xi), (\Psi \otimes \mathbb{1}_{\mathcal{L}(\mathcal{Z})})(\xi)), \quad (27)$$

where the infimum is over all Hilbert spaces \mathcal{Z} and over all purifications $\xi = |\zeta\rangle\langle\zeta| \in \mathcal{D}(\mathcal{X} \otimes \mathcal{Z})$ of σ .

The channel superfidelity $G_{\text{ch}}(\Phi, \Psi; \sigma)$ places a lower bound on the output superfidelity of two quantum channels in the case of the same input states. Henceforth, where unambiguous, we will write the channel superfidelity as G_{ch} .

Theorem 2 Given quantum channels $\Phi, \Psi : \mathcal{L}(\mathcal{X}) \rightarrow \mathcal{L}(\mathcal{X})$ with Kraus forms given by the sets $\{K_i\}_i$ and $\{L_j\}_j$, respectively, the quantum channel superfidelity is given by:

$$\begin{aligned} G_{\text{ch}} &= \sum_{i,j} |\text{Tr}\sigma K_i^\dagger L_j|^2 + \sqrt{1 - \sum_{i,j} |\text{Tr}\sigma K_i^\dagger K_j|^2} \\ &\times \sqrt{1 - \sum_{i,j} |\text{Tr}\sigma L_i^\dagger L_j|^2}. \end{aligned} \quad (28)$$

Proof As we limit ourselves only to pure states ξ , in order to calculate the superfidelity, we need to compute the following quantities:

$$\begin{aligned} & \text{Tr} (\Phi \otimes \mathbb{1}_{\mathcal{L}(\mathcal{Z})}) (|\xi\rangle\langle\xi|) (\Psi \otimes \mathbb{1}_{\mathcal{L}(\mathcal{Z})}) (|\xi\rangle\langle\xi|), \\ & \text{Tr} [(\Phi \otimes \mathbb{1}_{\mathcal{L}(\mathcal{Z})}) (|\xi\rangle\langle\xi|)]^2, \\ & \text{Tr} [(\Psi \otimes \mathbb{1}_{\mathcal{L}(\mathcal{Z})}) (|\xi\rangle\langle\xi|)]^2. \end{aligned} \quad (29)$$

As the general idea is shared between all of these quantities, we will show here the calculation for the first one. We get

$$\begin{aligned} & \text{Tr} (\Phi \otimes \mathbb{1}_{\mathcal{L}(\mathcal{Z})}) (|\xi\rangle\langle\xi|) (\Psi \otimes \mathbb{1}_{\mathcal{L}(\mathcal{Z})}) (|\xi\rangle\langle\xi|) = \\ & \text{Tr} |\xi\rangle\langle\xi| (\Phi^\dagger \circ \Psi \otimes \mathbb{1}_{\mathcal{L}(\mathcal{Z})}) (|\xi\rangle\langle\xi|) = \\ & \langle\xi| (\Phi^\dagger \circ \Psi \otimes \mathbb{1}_{\mathcal{L}(\mathcal{Z})}) (|\xi\rangle\langle\xi|) |\xi\rangle, \end{aligned} \quad (30)$$

where the first equality follows from the definition of the conjugate superoperator. The Kraus form of the superoperator $\Phi^\dagger \circ \Psi$ is given by the set $\{K_i^\dagger L_j\}_{i,j}$. Now, we may write $|\xi\rangle$ as

$$|\xi\rangle = \text{res}(\sqrt{\sigma} U), \quad (31)$$

for some $U \in \mathcal{L}(\mathcal{Z}, \mathcal{X})$ such that UU^\dagger is a projector on the image of σ . We obtain:

$$\begin{aligned} \langle\xi| (\Phi^\dagger \circ \Psi \otimes \mathbb{1}_{\mathcal{L}(\mathcal{Z})}) (|\xi\rangle\langle\xi|) |\xi\rangle &= \sum_{i,j} |\langle\xi| (K_i^\dagger L_j) \otimes \mathbb{1}_{\mathcal{Z}} |\xi\rangle|^2 = \\ \sum_{i,j} |\text{res}(\sqrt{\sigma} U)^\dagger ((K_i^\dagger L_j) \otimes \mathbb{1}_{\mathcal{Z}}) \text{res}(\sqrt{\sigma} U)|^2 &= \\ \sum_{i,j} |\text{Tr} U^\dagger \sqrt{\sigma} K_i^\dagger L_j \sqrt{\sigma} U|^2 &= \sum_{i,j} |\text{Tr} \sigma K_i^\dagger L_j|^2. \end{aligned} \quad (32)$$

This quantity is independent of the particular purification of σ . Following the same path for the other two quantities shown in Eq. (29), we recover the expression for the channel superfidelity from Eq. (28). \square

Since the superfidelity is an upper bound for the fidelity function, we obtain, the following inequality:

$$G_{\text{ch}}(\Phi, \Psi; \sigma) \geq F(\Phi, \Psi; \sigma), \quad (33)$$

where $F(\Phi, \Psi; \sigma) = \inf_{\mathcal{Z}, \xi} F((\Phi \otimes \mathbb{1}_{\mathcal{L}(\mathcal{Z})})(\xi), (\Psi \otimes \mathbb{1}_{\mathcal{L}(\mathcal{Z})})(\xi))$ and the infimum is over all Hilbert spaces \mathcal{Z} and all $\xi \in \mathcal{D}(\mathcal{X} \otimes \mathcal{Z})$ such that $\text{Tr}_{\mathcal{Z}} \xi = \sigma$.

The following simple corollaries are easily derived from Theorem 2.

Corollary 1 *Given a quantum channel Φ , the superfidelity between its input and output reduces to the channel fidelity of Φ :*

$$G_{\text{ch}}(\Phi, \mathbb{1}; \sigma) = F_{\text{ch}}(\Phi; \sigma) \quad (34)$$

Proof Assume Φ has the Kraus form $\{K_i\}_i$. Substituting the identity for L_j in Eq. (27), we recover Eq. (25) which completes the proof. \square

Corollary 2 *If Φ is a unitary channel i. e. $\Phi(\rho) = U\rho U^\dagger$ for any $U \in \mathcal{U}(\mathcal{X})$ and $\Psi' : \rho \mapsto U^\dagger \Psi(\rho)U$, where Ψ is an arbitrary quantum channel then*

$$G_{\text{ch}}(\Phi, \Psi; \sigma) = F_{\text{ch}}(\Psi'; \sigma). \quad (35)$$

Proof If Φ is a unitary channel, then the second term in Eq. (28) vanishes. Let us assume that Ψ has a Kraus form $\{L_j\}_j$. We get $G_{\text{ch}} = \sum_j |\text{Tr}\sigma U^\dagger L_j|^2$.

The Kraus form of the channel Ψ' is given by the set $\{U^\dagger L_j : K_j \in \mathcal{L}(\mathcal{X})\}$. Using this in Eq. (25), we get $F_{\text{ch}}(\Psi'; \sigma) = \sum_j |\text{Tr}\sigma U^\dagger L_j|^2$. This completes the proof. \square

Corollary 3 *If $\sigma \in \mathcal{D}(\mathcal{X})$ is a pure state, i.e. $\sigma = |\psi\rangle\langle\psi|$, then*

$$G_{\text{ch}}(\Phi, \Psi; \sigma) = G(\Phi(\sigma), \Psi(\sigma)). \quad (36)$$

Proof Let us only focus on the first terms in Eqs. (8) and (28). We will denote these terms T and T_{ch} , respectively. Let us assume that channels Φ and Ψ have Kraus forms $\{K_i\}_i$ and $\{L_j\}_j$, respectively. We get:

$$\begin{aligned} T &= \text{Tr} \sum_{ij} K_i |\psi\rangle\langle\psi| K_i^\dagger L_j |\psi\rangle\langle\psi| L_j^\dagger \\ &= \sum_{ij} \langle\psi| K_i^\dagger L_j |\psi\rangle \langle\psi| L_j^\dagger K_i |\psi\rangle = \sum_{ij} |\langle\psi| K_i^\dagger L_j |\psi\rangle|^2 = T_{\text{ch}}. \end{aligned} \quad (37)$$

Performing similar calculations for other terms, we recover Eq. (36) \square

3.2 Quantum circuit for measuring channel superfidelity

Using the quantum circuit shown in Fig. 1, we can measure the quantum channel superfidelity in an experimental setup. This setup allows us to estimate the $\text{Tr}(\Phi \otimes \mathbb{1}_{\mathcal{L}(\mathcal{Z})})(|\zeta\rangle\langle\zeta|)(\Psi \otimes \mathbb{1}_{\mathcal{L}(\mathcal{Z})})(|\zeta\rangle\langle\zeta|) = 2p_0 - 1$, where p_0 is the probability of finding the top qubit in the state $|0\rangle$. Modifying the circuit appropriately, we can measure all the quantities shown in Eq. (29).

Note that this approach is far simpler, compared to estimating the channel fidelity which would require us to perform full state tomography. Furthermore, analytical calculations involving fidelity get cumbersome quickly, as it requires calculating expressions of the form $\|\sqrt{\Phi(\sigma)}\sqrt{\Psi(\sigma)}\|_1$.

4 Simple examples

In this section, we provide a number of examples of the application of Theorem 2.

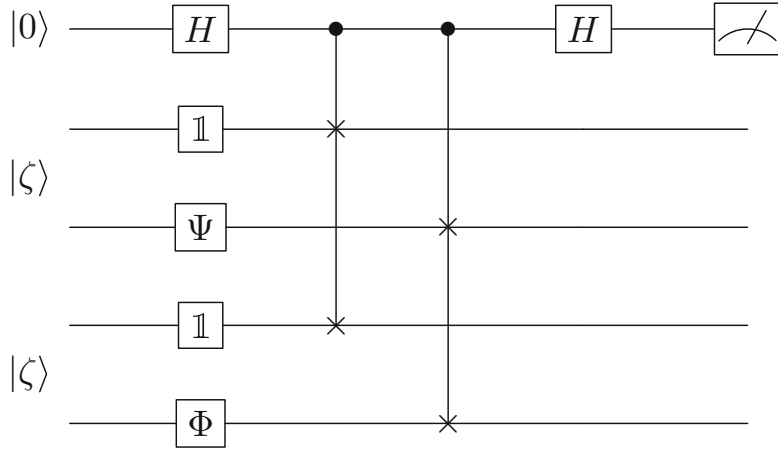


Fig. 1 Quantum circuit for measuring $\text{Tr}(\Phi \otimes 1_{\mathcal{L}(Z)})(|\zeta\rangle\langle\zeta|)(\Psi \otimes 1_{\mathcal{L}(Z)})(|\zeta\rangle\langle\zeta|) = 2p_0 - 1$, where p_0 is the probability of finding the top qubit in state $|0\rangle$ [21]. This allows direct estimation of the channel superfidelity

4.1 Erasure channel

Definition 15 Given a quantum state $\xi \in \mathcal{D}(\mathcal{X})$, the erasure channel is given by:

$$\Phi(A) = \xi, \quad (38)$$

for any A in $\mathcal{L}(\mathcal{X})$. The Kraus form of this channel is given by the set $\{K_{ij} : K_{ij} = \sqrt{\lambda_i} |\lambda_i\rangle\langle j|\}_{ij}$, λ_i and $|\lambda_i\rangle$ denote the i th eigenvalue and the corresponding eigenvector of ξ .

Let us consider the superfidelity between the erasure channel Φ and a unitary channel $\Psi : \sigma \mapsto U\sigma U^\dagger$ for some $U \in \mathcal{U}(\mathcal{X})$. We note that the second term in Eq. (28) vanishes. What remains is:

$$\begin{aligned} G_{\text{ch}} &= \sum_{ij} \lambda_i |\langle j | \sigma U^\dagger | \lambda_i \rangle|^2 = \sum_j \langle j | \sigma U^\dagger \left(\sum_i \lambda_i |\lambda_i\rangle\langle\lambda_i| \right) U \sigma |j\rangle \\ &= \text{Tr} \sigma^2 \Psi^\dagger(\xi) \leq \sum_i \lambda_i^\downarrow \mu_i^\downarrow, \end{aligned} \quad (39)$$

where μ_i^\downarrow and λ_i^\downarrow denote the eigenvalues of σ and ξ , respectively, sorted in a descending order. The last inequality follows from von Neumann's trace inequality [22].

4.2 Sensitivity to channel error

Consider a quantum channel Φ with the Kraus form $\{K_i\}$ and a quantum channel $\Psi : \rho \mapsto U_\epsilon \Phi(\rho) U_\epsilon^\dagger$, where $U_\epsilon = \exp(-i\epsilon H) \in \mathcal{U}(\mathcal{X})$. We get:

$$G_{\text{ch}}(\Phi, \Psi; \sigma) = 1 + \sum_{ij} |\text{Tr} \sigma K_i^\dagger U_\epsilon K_j|^2 - \sum_{ij} |\text{Tr} \sigma K_i^\dagger K_j|^2. \quad (40)$$

Now, we concentrate on the change of the quantum channel superfidelity under the change of ϵ . As we are interested only in small values of ϵ , we expand Eq. (40) up to the linear term in the Taylor series. For small values of ϵ , we get:

$$G_{\text{ch}} \approx 1 - 2\epsilon \sum_{ij} \Im \text{Tr} \sigma K_i^\dagger H K_j \overline{\text{Tr} \sigma K_i^\dagger K_j}. \quad (41)$$

Note that this depends on the value of the observable H of the operator $K_j \sigma K_i^\dagger$.

5 Sensitivity to Hamiltonian parameters

In this section, we will show how the channel superfidelity is affected by errors in the system Hamiltonian parameters. First, we will show analytical results for a single qubit system at a finite temperature. Next, we show numerical results for a simple, three-qubit spin chain.

5.1 Single qubit at a finite temperature

A single qubit at a finite temperature is described by the master equation

$$\begin{aligned} \dot{\rho}(t) = & -i\frac{\Omega + \epsilon}{2}[\sigma_z, \rho(t)] + \gamma_+ \left(\sigma_- \rho(t) \sigma_+ - \frac{1}{2}\{\sigma_+ \sigma_-, \rho(t)\} \right) \\ & + \gamma_- \left(\sigma_+ \rho(t) \sigma_- - \frac{1}{2}\{\sigma_- \sigma_+, \rho(t)\} \right), \end{aligned} \quad (42)$$

where $\sigma_+ = |1\rangle \langle 0|$, $\sigma_- = \sigma_+^\dagger$ and ϵ is the error in Ω . Our goal is to calculate the quantum channel superfidelity between the case when there is no error in Ω , i.e. $\epsilon = 0$ and the case with error in Ω . Henceforth, we will assume $\gamma_- = \gamma_+ = 1$ for clarity.

For a given time T , Eq. (42) may be rewritten as

$$\rho(T) = \Phi_T^\epsilon(\rho(0)), \quad (43)$$

where Φ_T^ϵ is a quantum channel in the quantum dynamical semigroup. A natural representation $M_{\Phi_T^\epsilon}$ for the channel Φ_T^ϵ may be found as [23]:

$$M_{\Phi_T^\epsilon} = e^{-FT}, \quad (44)$$

where

$$\begin{aligned} F = & -i\frac{\Omega + \epsilon}{2}(\mathbb{1} \otimes \sigma_z - \sigma_z \otimes \mathbb{1}) - \sigma_- \otimes \sigma_- - \sigma_+ \otimes \sigma_+ + \\ & + \frac{1}{2}(\sigma_+ \sigma_- \otimes \mathbb{1} + \sigma_- \sigma_+ \otimes \mathbb{1} + \mathbb{1} \otimes \sigma_+ \sigma_- + \mathbb{1} \otimes \sigma_- \sigma_+). \end{aligned} \quad (45)$$

In this representation, we may rewrite Eq. (43) as

$$\text{res}(\rho(T)) = M_{\Phi_T^\epsilon} \text{res}(\rho(0)). \quad (46)$$

The Choi–Jamiołkowski representation of the channel Φ_T is given by $D_{\Phi_T^\epsilon} = (M_{\Phi_T^\epsilon})^R$. Here, M^R denotes the *reshuffle* operation on matrix M [14]. Now, it is simple to find the Kraus form of the channel Φ_T^ϵ . The Kraus operators are related to the eigenvalues λ_i and eigenvectors $|\lambda_i\rangle$ of $D_{\Phi_T^\epsilon}$ in the following manner:

$$K_i^{\Phi_T^\epsilon} = \sqrt{\lambda_i} \text{unres}(|\lambda_i\rangle). \quad (47)$$

Inserting these Kraus operators into Eq. (28), we get

$$G_{\text{ch}}(\Phi_T^0, \Phi_T^\epsilon; \rho) = 1 - 2e^{-2T}(1 - \cos \epsilon T)\rho_{00}(0)\rho_{11}(0), \quad (48)$$

where $\rho_{ii}(0) = \langle i | \rho(0) | i \rangle$. Note that we get $G_{\text{ch}} = 1$ in two cases. First, for large T and second when $\epsilon T = \frac{\pi}{2}$. As we are mainly interested in small values of ϵ , we expand $\cos \epsilon T$ up to the second term in the Taylor series. We get:

$$G_{\text{ch}}(\Phi_T^0, \Phi_T^\epsilon; \rho) \approx 1 - \epsilon^2 T^2 e^{-2T} \rho_{00}(0)\rho_{11}(0). \quad (49)$$

In this setup, the channel superfidelity has a quadratic dependence on the error parameter ϵ . This should be compared with the results in Sect. 4.2.

5.2 Quantum control example

In this section, we consider a three-qubit spin chain with dephasing interactions with the environment. We will consider piecewise constant control pulses. The time evolution of the system is governed by the equation:

$$\dot{\rho}(t) = -i[H, \rho(t)] + \gamma(\sigma_z \rho(t) \sigma_z - \rho(t)), \quad (50)$$

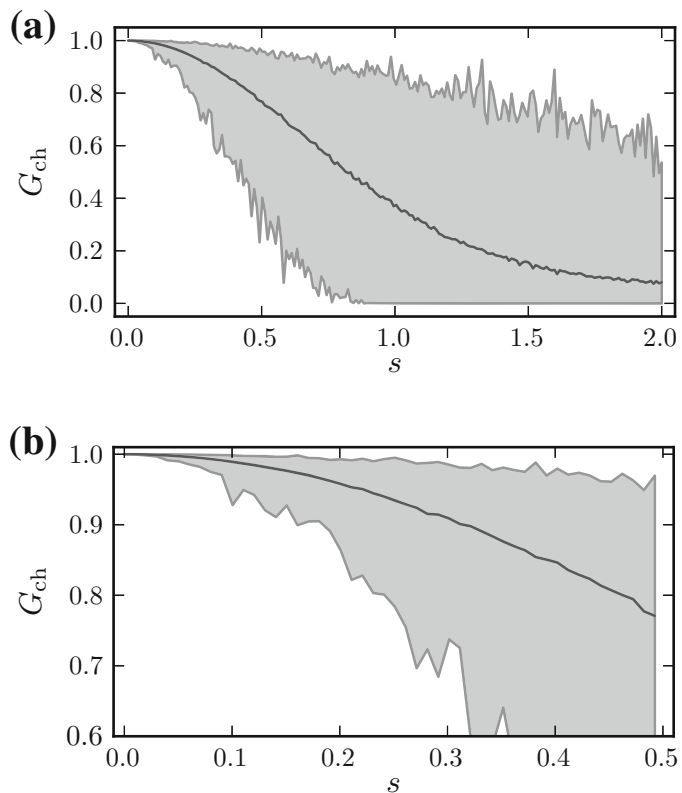
where $H = H_d + H_c$. Here H_d is the drift term of the Hamiltonian given by

$$H_d = J \sum_{i=1}^2 \sum_{\alpha \in \{x, y, z\}} \sigma_\alpha^i \sigma_\alpha^{i+1}, \quad (51)$$

where σ_α^i denotes σ_α acting on site i . We set the control Hamiltonian H_c to:

$$H_c = \sum_i^N h_x(t_i) \sigma_x^1 + h_y(t_i) \sigma_y^1, \quad (52)$$

Fig. 2 Quantum channel superfidelity as a function of noise in the system's control pulses. The *shaded area* represents the range of the achieved channel superfidelity, and the *black line* is the average channel superfidelity



where $h_x(t_i)$ and $h_y(t_i)$ denote the control pulses in the time interval t_i . We set the target to be

$$U_T = \mathbb{1} \otimes \mathbb{1} \otimes \sigma_x, \quad (53)$$

i.e. a NOT gate on the third qubit. We fixed the number of time intervals $N = 64$, the total evolution time $T = 6.1$ and the maximum amplitude of a single control pulse $\forall k \in x, y \max(|h_k|) = 10$.

First, we optimize control pulses for the system, such that we achieve a high fidelity of the gate U_T . Next, to each control pulse we add a noise term h_ϵ which has a normal distribution, $h_\epsilon = N(0, s)$. Figure 2 shows the change of G_{ch} as a function of the standard deviation s . We have conducted 100 simulations for each value of s . As expected, the quantum channel superfidelity decreases slowly for low values of s . After a certain value, the decrease becomes rapid. As values of s increase, the minimum and maximum achieved fidelity diverge rapidly. This is represented by the shaded area in Fig. 2. We can approximate the average value of the channel fidelity as $\langle G_{\text{ch}} \rangle \approx 1 - cs^2$. Fitting this function to the curve shown in Fig. 2b gives a relative error which is less than 0.5 %.

6 Conclusions

We have studied the superfidelity of a quantum channel. This quantity allows us to provide an upper bound on the fidelity of the output of two quantum channels. We shown an example of application of this quantity to a unitary and an erasure

channel. The obtained superfidelity can be easily limited from above by the product w eigenvalues of the input state σ and the result of the erasure channel ξ .

Furthermore, as shown in our examples, the quantum channel superfidelity may have potential applications in quantum control theory as an easy to compute figure of merit of quantum operations. In a simple setup, where the desired quantum channel is changed by a unitary transformation $U_\epsilon = \exp(-i\epsilon H)$ we get a linear of the decrease of channel superfidelity on the noise parameter ϵ . On the other hand, when we introduce the noise as a control error in a single qubit quantum control setup, we get a quadratic dependence on the noise parameter.

Finally, we shown numerical results for a more complicated system. We calculated the quantum channel superfidelity for a three-qubit quantum control setup. First, we found control pulses which achieve a high fidelity of the desired quantum operation, next we introduced Gaussian noise in the control pulses. Our results show that the quantum channel superfidelity stayed high for a wide range of the noise strength.

Acknowledgments We would like to thank Piotr Gawron for inspiring discussions. ŁP was supported by the Polish National Science Centre under decision number DEC-2012/05/N/ST7/01105. ZP supported by the Polish National Science Centre under the post-doc programme, decision number DEC-2012/04/S/ST6/00400.

Open Access This article is distributed under the terms of the Creative Commons Attribution 4.0 International License (<http://creativecommons.org/licenses/by/4.0/>), which permits unrestricted use, distribution, and reproduction in any medium, provided you give appropriate credit to the original author(s) and the source, provide a link to the Creative Commons license, and indicate if changes were made.

References

1. Viola, L., Knill, E., Lloyd, S.: Dynamical decoupling of open quantum systems. *Phys. Rev. Lett.* **82**(12), 2417 (1999)
2. Viola, L., Lloyd, S., Knill, E.: Universal control of decoupled quantum systems. *Phys. Rev. Lett.* **83**(23), 4888 (1999)
3. Viola, L., Knill, E.: Robust dynamical decoupling of quantum systems with bounded controls. *Phys. Rev. Lett.* **90**(3), 037901 (2003)
4. Dahleh, M., Peirce, A., Rabitz, H.: Optimal control of uncertain quantum systems. *Phys. Rev. A* **42**(3), 1065 (1990)
5. Dong, D., Petersen, I.R.: Sliding mode control of quantum systems. *New J. Phys.* **11**(10), 105033 (2009)
6. James, M.: Risk-sensitive optimal control of quantum systems. *Phys. Rev. A* **69**(3), 032108 (2004)
7. D'Helon, C., Doherty, A., James, M., Wilson, S.: Quantum risk-sensitive control. In : 45th IEEE Conference on Decision and Control, 2006, pp. 3132–3137. IEEE (2006)
8. Pawela, Ł., Sadowski, P.: Various Methods of Optimizing Control Pulses for Quantum Systems with Decoherence. arXiv preprint [arXiv:1310.2109](https://arxiv.org/abs/1310.2109), (2013)
9. Pawela, Ł., Puchała, Z.: Quantum control robust with respect to coupling with an external environment. *Quantum Inf. Process.* **14**(2), 437–446 (2015)
10. Gawron, P., Kurzyk, D., Pawela, Ł.: Decoherence effects in the quantum qubit flip game using markovian approximation. *Quantum Inf. Process.* **13**, 665–682 (2014)
11. Pawela, Ł., Puchała, Z.: Quantum control with spectral constraints. *Quantum Inf. Process.* **13**, 227–237 (2014)
12. Raginsky, M.: A fidelity measure for quantum channels. *Phys. Lett. A* **290**(1), 11–18 (2001)
13. Piani, M., Watrous, J.: All entangled states are useful for channel discrimination. *Phys. Rev. Lett.* **102**(25), 250501 (2009)

14. Bengtsson, I., Życzkowski, K.: Geometry of Quantum States: An Introduction to Quantum Entanglement. Cambridge University Press, Cambridge, UK (2006)
15. Nielsen, M.A., Chuang, I.L.: Quantum Computation and Quantum Information. Cambridge University Press, Cambridge (2000)
16. Puchała, Z., Miszczak, J.A., Gawron, P., Gardas, B.: Experimentally feasible measures of distance between quantum operations. *Quantum Inf. Process.* **10**(1), 1–12 (2011)
17. Miszczak, J.A., Puchała, Z., Horodecki, P., Uhlmann, A., Życzkowski, K.: Sub- and super-fidelity as bounds for quantum fidelity. *Quantum Inf. Comput.* **9**(1), 103–130 (2009)
18. Mendonça, P.E., Napolitano, RdJ, Marchiolli, M.A., Foster, C.J., Liang, Y.-C.: Alternative fidelity measure between quantum states. *Phys. Rev. A* **78**(5), 052330 (2008)
19. Puchała, Z., Miszczak, J.A.: Bound on trace distance based on superfidelity. *Phys. Rev. A* **79**(2), 024302 (2009)
20. Watrous, J.: Theory of Quantum Information. <https://cs.uwaterloo.ca/~watrous/CS766/LectureNotes/all.pdf> (2011)
21. Ekert, A.K., Alves, C.M., Oi, D.K.L., Horodecki, M., Horodecki, P., Kwek, L.C.: Direct estimations of linear and nonlinear functionals of a quantum state. *Phys. Rev. Lett.* **88**(21), 217901 (2002)
22. Horn, R., Johnson, C.: Topics in Matrix Analysis. Cambridge University Press, Cambridge (1991)
23. Havel, T.F.: Robust procedures for converting among Lindblad, Kraus and Matrix representations of quantum dynamical semigroups. *J. Math. Phys.* **44**(2), 534–557 (2003)

Oświadczenie współautorów
publikacji naukowych, określające
indywidualny wkład każdego
z nich w jej powstanie

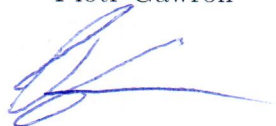
Gliwice, 23.01.2017

Piotr Gawron
Instytut Informatyki Teoretycznej i Stosowanej PAN
ul. Bałycka 5,
44-100 Gliwice

Oświadczenie współautorstwa

Oświadczam, że w pracy
Decoherence effects in the quantum qubit flip game using Markovian approximation
mój udział polegał na: postawieniu problemu badawczego, zaproponowania modelu gry oraz dekoherencji oraz wspólnej redakcji tekstu.

Piotr Gawron



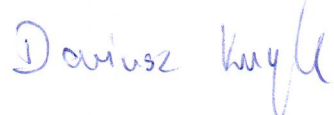
Gliwice, 23.01.2017

Dariusz Kurzyk
Instytut Informatyki Teoretycznej i Stosowanej PAN
ul. Bałtycka 5,
44-100 Gliwice

Oświadczenie współautorstwa

Oświadczam, że w pracy
Decoherence effects in the quantum qubit flip game using Markovian approximation
mój udział polegał na analitycznych rozważaniach ilustrujących wpływ dekoherencji na wynik gry.

Dariusz Kurzyk



Gliwice, 23.01.2017

Przemysław Sadowski
Instytut Informatyki Teoretycznej i Stosowanej PAN
ul. Bałycka 5,
44-100 Gliwice

Oświadczenie współautorstwa

Oświadczam, że w pracy
Various methods of optimizing control pulses for quantum systems with decoherence
mój udział polegał na uzasadnieniu poprawności stosowania modelu singular coupling limit w optymalizacji opartej o okresowo stały, nieciągły sygnał kontroli; opracowanie optymalizacji za pomocą algorytmów genetycznych; współudział w pisaniu manuskryptu.



Przemysław Sadowski

Gliwice, 23.01.2017

Zbigniew Puchała
Instytut Informatyki Teoretycznej i Stosowanej PAN
ul. Bałtycka 5,
44-100 Gliwice

Oświadczenie współautorstwa

Oświadczam, że w pracy
Quantum control with spectral constraints
mój udział polegał na

- zaproponowaniu problemu badawczego,
- współudziale w redakcji tekstu publikacji.



Zbigniew Puchała

Gliwice, 23.01.2017

Zbigniew Puchała
Instytut Informatyki Teoretycznej i Stosowanej PAN
ul. Bałtycka 5,
44-100 Gliwice

Oświadczenie współautorstwa

Oświadczam, że w pracy
Quantum control robust with respect to coupling with an external environment
mój udział polegał na

- zaproponowaniu problemu badawczego,
- współudziale w redakcji tekstu publikacji.



Zbigniew Puchała

Gliwice, 23.01.2017

Zbigniew Puchała
Instytut Informatyki Teoretycznej i Stosowanej PAN
ul. Bałtycka 5,
44-100 Gliwice

Oświadczenie współautorstwa

Oświadczam, że w pracy
Quantifying channels output similarity with applications to quantum control
mój udział polegał na

- zaproponowaniu problemu badawczego,
- dowodzi twierdzenia 2,
- współudziałie w redakcji tekstu publikacji.



Zbigniew Puchała

**Declarations of co-authorship,
detailing each co-authors
individual contribution to each
work**

Piotr Gawron
Institute of Theoretical and Applied Informatics PAS
Bałycka 5,
44-100 Gliwice

Gliwice, 23.01.2017

Declaration of co-autorship

I hereby declare that my individual contribution to the work
Decoherence effects in the quantum qubit flip game using Markovian approximation
involved proposing the research problem, proposing the game and dechorence
model and co-authoring the paper.



Piotr Gawron

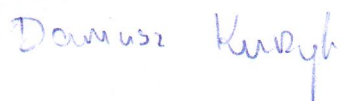
Dariusz Kurzyk
Institute of Theoretical and Applied Informatics PAS
Bałycka 5,
44-100 Gliwice

Gliwice, 23.01.2017

Declaration of co-autorship

I hereby declare that my individual contribution to the work
Decoherence effects in the quantum qubit flip game using Markovian approximation
involved with an analytical investigation which shows the influence of decoherence on the game result.

Dariusz Kurzyk

Dariusz Kurzyk

Przemysław Sadowski
Institute of Theoretical and Applied Informatics PAS
Bałycka 5,
44-100 Gliwice

Gliwice, 23.01.2017

Declaration of co-autorship

I hereby declare that my individual contribution to the work
Various methods of optimizing control pulses for quantum systems with decoherence
involved justification of correctness of applying singular coupling limit model
in the case of piecewise constant, non-continuous control pulses; developing
optimization methods based on genetic algorithms; co-writing the manuscript.



Przemysław Sadowski

Zbigniew Puchała
Institute of Theoretical and Applied Informatics PAS
Bałycka 5,
44-100 Gliwice

Gliwice, 23.01.2017

Declaration of co-autorship

I hereby declare that my individual contribution to the work
Quantum control with spectral constraints
involved

- proposing a research problem,
- participation in editing the publication.



Zbigniew Puchała

Zbigniew Puchała
Institute of Theoretical and Applied Informatics PAS
Bałycka 5,
44-100 Gliwice

Gliwice, 23.01.2017

Declaration of co-autorship

I hereby declare that my individual contribution to the work
Quantum control robust with respect to coupling with an external environment
involved

- proposing a research problem,
- participation in editing the publication.



Zbigniew Puchała

Zbigniew Puchała
Institute of Theoretical and Applied Informatics PAS
Bałycka 5,
44-100 Gliwice

Gliwice, 23.01.2017

Declaration of co-autorship

I hereby declare that my individual contribution to the work
Quantifying channels output similarity with applications to quantum control
involved

- proposing a research problem,
- proof of theorem 2,
- participation in editing the publication.

A handwritten signature in black ink, appearing to read "Zbigniew Puchała".

Zbigniew Puchała